Anionic Lipid Distribution in Membranes

by

Elaine L. Bearer

DISSERTATION

Submitted in partial satisfaction of the requirements for the degree of

DOCTOR OF PHILOSOPHY

in

Experimental Pathology

in the

GRADUATE DIVISION

of the

UNIVERSITY OF CALIFORNIA

San Francisco

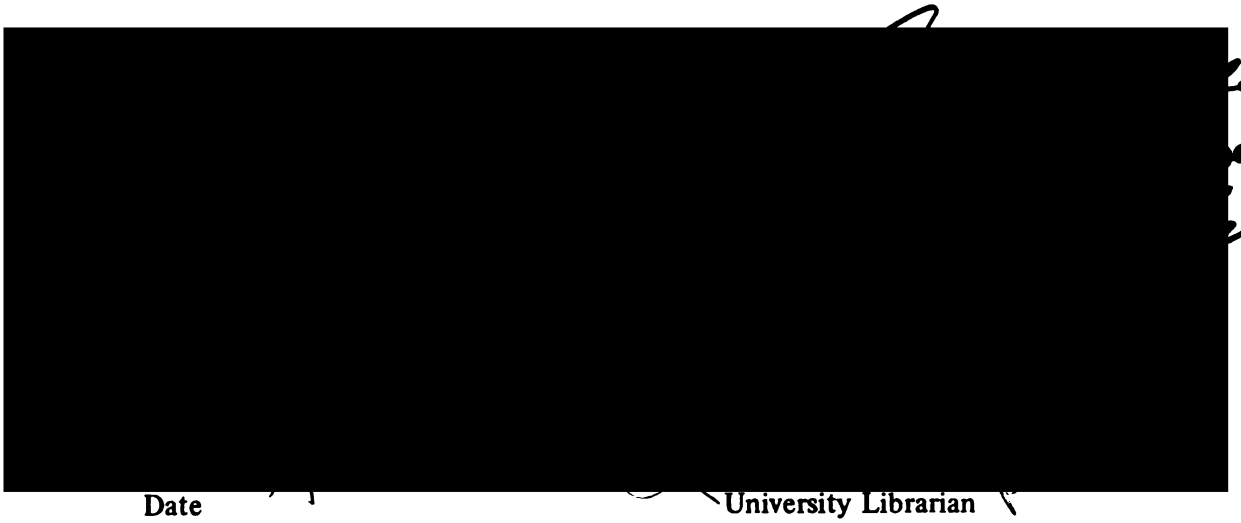

Date University Librarian

Degree Conferred: MAR 28 1982

Table of Contents

Abstract: Anionic Lipid Distribution in Membranes

E. Bearer

The cell membrane is a tapestry of regionally differing protein and lipid compositions. In this dissertation, I have ultrastructurally explored the redistribution of anionic lipids (necessary for calcium-stimulated fusion in model systems), in three cell-types, using two anionic-lipid-binding antiobiotics -- polymyxin B (PXB), which induces visible perturbation of membrane contours, and adriamycin (ADR), which fluoresces and also reduces osmium when bound to this class of lipid.

Liposome experiments demonstrated the specificity of both probes for acidic lipids. The human erythrocyte bound ADR but not PXB, confirming that the latter compound only binds available acidic lipids in either leaflet. Finally, two secretory cells, the guinea-pig spermatozoan and the human blood platelet, were used to explore whether anionic-lipid domains exist in fusional membrane and whether their presence correlates with secretory activity.

The well-established diverse functional regions of the sperm plasmalemma differed in anionic-lipid content as determined by these probes. Congruent with preparation for acrosomal-granule exocytosis, anionic-lipid concentration increased in the outer lamella of the fusional membrane. In addition to having the ability to undergo modification, domains of acidic lipids in the outer lamella are well-circumscribed, occupying only the fusigenic acrosomalcap portion of the membrane. Platelets also display a modifiable labeling with polymyxin B: In the resting

Acknowledgements

I would like to express my deepest appreciation to Dr. Daniel S. Friend for his supervision, guidance, and support throughout my research experience.

I would also like to thank Irene Rudolph, and Ivy Hsieh for their generous help in teaching me technical skills, and Rosamond Michael for teaching me how to write creative scientific prose. I also wish to thank both Dr. Demetrios Paphadjopoulos and Dr. Edward A. Smuckler for their enthusiastic and enlightening discussions. Finally, I wish to thank Susan Turner, whose effort in the office finalized this manuscript.

state, they resisted PXB, but became PXB-susceptible within 1 sec of thrombin stimulation. Three mechanisms by which sperm could maintain contiguous domains varying in lipid constitution are: 1) by extracellular interactions of protruding membrane components; 2) by differences in membrane fluidity; and 3) by anchoring to cytoplasmic structures. Brief digestion with protease, ineffectual in removing the sperm surface coat, accelerated increases in acrosomal cap anionic lipid, but did not affect the PXB-resistance of the post-acrosomal segment. Second, a low degree of fluidity in the PXB-resistant post-acrosomal segment was suggested by the lack of merocyanin S 540 binding in this area. Third, in sperm, cytoplasmic densities seen as periodic rods in quick-frozen, deep-etched cells, lined the PXB-resistant, ADR-sensitive membrane. No such structures lay beneath PXB-sensitive membrane. In platelets, morphological changes in the cytoplasmic coating accompanied the appearance of acidic lipids in the plasma membrane's external leaflet.

In conclusion, PXB and ADR were proved to be useful cytochemical tools for the determination of acidic lipid distribution, both in the plane of the outer leaflet and across the bilayer in mammalian-cell membranes. Employing them, we found that outer lamellar acidic-lipid domains and bilayer lipid asymmetry are not maintained by either hydrolyzable surface components or by degrees of membrane fluidity. However, cytoplasmic peripheral proteins are circumstantially linked to the maintenance of membrane lipid asymmetry as well as its modification which results in the emergence of acidic lipids in the outer leaflet of the plasma membrane accompanying membrane fusion.

Preface

The thesis is organized into an introduction and four chapters. The introduction presents the hypothesis that initiated this investigation and its significance with relation to cells and how they function. Furthermore, the introduction provides some of the rationale underlying the use of cytochemical probes for the study of anionic lipids in cell membranes, the structures and possible functions of these lipids, and suggested mechanisms by which the probes bind them. Each of the chapters was written for a specific journal, in the format required by that journal.

The first chapter "Fusion of phasphatidylcholine:cardiolipin vesicles arrested by quick-freezing: a re-examination of lipidic particles" was written for Nature. This chapter presents evidence that anionic-lipid-containing vesicles fuse within seconds of calcium injection, demonstrating one possible function these lipids could perform in cell membranes.

The second chapter, "Anionic lipid domains: Correlation with functional topography in a mammalian cell membrane", has been published in Proceedings of the National Academy of Science. This paper presents the evidence supporting polymyxin's (PXB's) usefulness as a cytochemical probe for anionic lipid through its ability to crenulate liposome and Drosophila larval cell membranes containing these lipids. It proceeds to demonstrate that the highly specialized gamete, the guinea-pig spermatozoan, displays regions of PXB-resistant as well as PXB-susceptible

membrane, and that susceptible domains are specialized for exocytosis (membrane fusion). Finally, this paper supports bacterial studies which proposed a direct correlation between PXB-binding and membrane protrusions, as a dansylated PXB derivative caused the sperm membrane to fluoresce only in regions which also displayed crenulations.

The third chapter, "Modifications of anionic lipid domains preceding membrane fusion in guinea-pig sperm", describes the increase of PXB susceptibility in fusional regions of the plasma membrane as the sperm progresses through capacitation to the attainment of fusional competence, culminating in the acrosome reaction. A crude trypsin extract was used to ascertain whether or not surface components played a role in this increase. In addition, radioactively labeled inorganic phosphate incorporation during capacitation was monitored to test whether lipid synthesis contributed to the increase. Synthesis could not be found to explain the increase. In addition, the hydrolysis of surface components had no effect on the PXB-resistance of the non-fusional membrane regions, although such digestion did increase the PXB susceptibility of fusional membrane, and also enhanced the incidence of acrosome reactions following calcium stimulation.

The final chapter, "Maintenance of anionic lipid domains in plasma membrane", addresses the question of what structural components of the cell could regulate the distribution of anionic lipid in the plasma membrane. By employing another anionic lipid binding probe, adriamycin (ADR), which can be observed directly in fluorescence microscopy, and

THESIS INTRODUCTION

The thrust of this thesis research has been to define by the ultrastructural localization of acidic phospholipids in cell membranes, and to demonstrate correlation between high concentrations of these lipids and the function of that region of membrane. What are anionic lipids and why are they worthy of such an investigation?

Anionic phospholipids are any phospholipid carrying a negative charge at neutral pH. Phosphotidic acid is the simplest of these, and its molecular formula is:

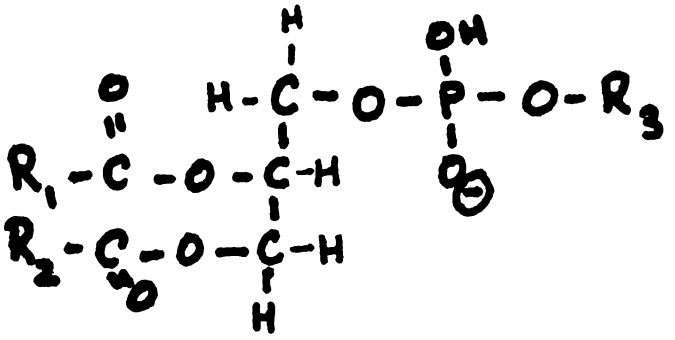

where R_1 and R_2 are acyl chains, and R_3 is a hydrogen ion. Phospholidylserine has a serine moiety at R_3; phosphatidylinositol, inositol; phosphatidylglycerol, glycerol; and phosphatidylethanolamine, ethanolamine. Cardiolipin (diphosphatidylglycerol) is more complicated, and R_3 is a phosphatidylglycerol. Thus, cardiolipin has two phosphate groups, and four acyl chains, and hence carries a double negative charge. Sphingomyelin and phosphatidylcholine (PC) are zwitterionic, and have no net charge at neutral pH.

Anionic lipids are ubiquitous in cell membranes. Bacterial membranes are entirely composed of them, having no PC at all. Mammalian cells can be composed of 70% anionic lipids. Different classes of anionic lipids are found in varing concentrations in subcellular organelles: while mitochondrial membranes are rich in cardiolipin, the cell plasma membrane is not. This suggests a function of cardiolipin related to energy metabolism. Indeed, this lipid affects the activity of mitochondrial proteins cytochrome c and cytochrome c oxidase, which in turn affects the phase behavior of the lipid.

Besides influencing proteins in their vicinity, anionic lipids may perform other functions. They appear necessary for the induction of vesicle-vesicle, Ca^{++}dependent, fusion in model membrane systems. By nature of their negative charge, they bind cations such as Ca^{++}, Mg^{++}, as well as H^{+}. The negative charge in turn can be conceptualized as a handle, by which other cell components might move these lipids around in the membrane. Furthermore, the charge may facilitate stickiness of the membrane as a whole. Finally, anionic lipids have differing phase transition behavior. Some of them can be induced by cation stimulation to leave the bilayer conformation altogether and assume the rod-like hexagonal phase at room temperature. This transition could allow them to change the fluid-gel properties of the other lipids and proteins in the membrane.

That it might be possible to develop cytohemical probes with which

to attack the problem of localization of these lipids was suggested by the work of Elias, Goerke, and Friend, who showed in 1979 that cholesterol could be localized *in situ* by filipin-binding and freeze-fracture cytochemistry. It should not seem surprising to discover that the ubiquitous molecule, cholesterol, should display such uniquely uneven distribution, as proteins and other membrane constituents have been proven to be concentrated in specific regions of cell membranes. Additionally, asymmetrical distribution of all lipids across the bilayer has been biochemically demonstrated for many cell types, including bacteria, red blood cells, platelets, and leukocytes. Most frequently, acidic lipids are concentrated in the inner, cytoplasmic leaflet, while PC and sphingomyelin occur in higher quantities in the external leaflet.

The two cytochemical reagents used in this investigation are polymyxin B (PXB) and adriamycin (ADR). Polymyxin B is a cyclic polypeptide with the following molecular structure:

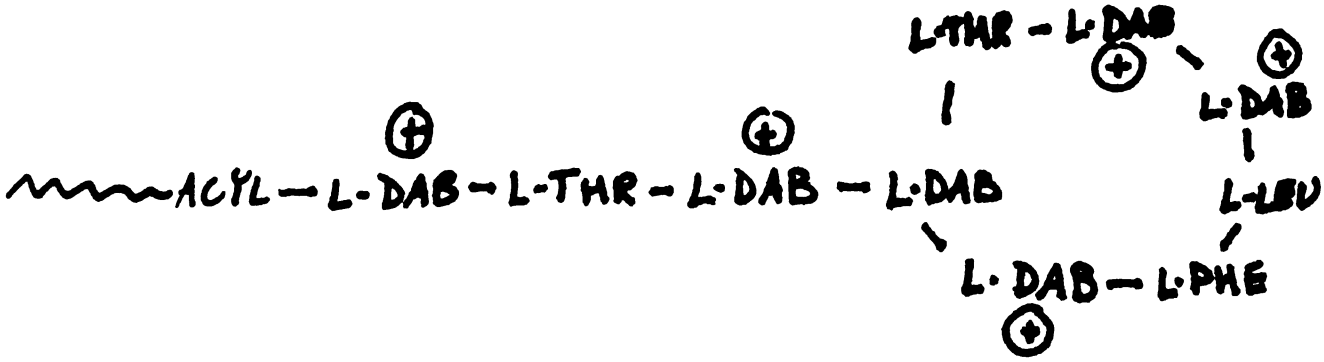

Its biochemical interaction with acidic lipids has been thoroughly characterized, and reviewed in Storm, Rosenthal, and Swanson's (1977) article. The proposed mechanism of binding involves charge-charge atttraction between the positive DAB residues in the polymyxin molecules and the negative phospholipid, followed by a stabilization of the attraction through insertion of the fatty acid tail of the antibiotic into the bilayer. The subsequent slight disruption of the intermolecular forces maintaining the lipid:lipid continuity of the bilayer enhances the probability of another PXB molecule inserting in that immediate vicinity. Thus each crenulation or protrusion results from the accumulation of PXB molecules, inserting into and expanding the membrane and causing contour deviations.

Adriamycin, on the other hand, is an anthracyclic sugar, with the following molecular structure:

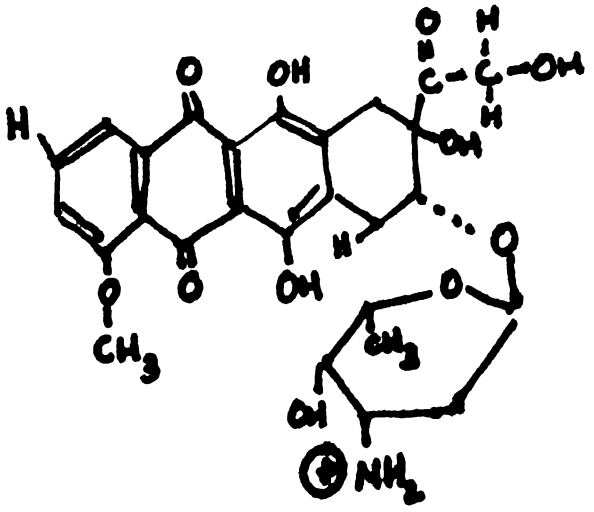

Its interaction with acidic phospholipids has been only recently described by Ruyschaert and co-workers. Some investigators suspect its

lipophilic properties to play a more important role in its anti-mitotic activity than its DNA binding. Again, it appears to be initially attracted to the membrane by a charge:charge interaction between its amino sugar and the negative lipid, followed by insertion into the membrane of the anthracyclic hydrophobic moiety. It passes easily through the membrane, perhaps by an energy-dependent or protein-mediated transport mechanism: fixed cells do not display nuclear staining. Its fluorescent properties change (emission peak shifts to the blue) when bound to the membrane, suggesting that the resonance of the multiple double bonds in the anthracyclic compound is affected by hydrophobic environment. Because of its fluorescence and its reduction of osmium, it can be observed in both living and fixed cells, and at both light and electron-microscopic magnifications.

As previous experiments by others had so clearly demonstrated the ability of these two probes to bind acidic lipids, I concentrated on ascertaining their cytochemical specificity for these lipids in model membrane systems. It was not feasible to test every conveivable cross-reactive non-lipid molecule found in cells. However, digestion of cellular surface components by proteases and saccharidases did not change the binding distribution of PXB. Both PXB and ADR were completely unable to bind to membrane deficient in acidic phospholipids, as judged by the fluorescence, or the ultrastructural cytochemistry. Threshold concentrations of acidic lipid necessary to produce binding were not determined.

The hypothesis which the results of these experiments fostered is presented in full in the discussion in the fourth chapter. Briefly, it proposes that:

1) Cells are capable of maintaining in the outer leaflet of the plasma membrane discreet domains richer in anionic lipids than neighboring regions.

2) PXB and ADR are useful cytochemical tools for the exploration of such domains and for the investigation of the presence of anionic lipid transbilayer asymmetry.

3) Acidic phospholipids appear in the outer leaflet of fusigenic membrane during preparation for fusion with internal granules.

4) Rods lying just beneath the cytoplasmic surface of the membrane are present and joined to the membrane in regions where anionic lipids are concentrated in the inner leaflet and absent or detached from the membrane which displays acidic lipids in the outer leaflet.

5) Stimulation of cells to secrete induces detachment of these rods, which lose their ability to act as an anionic lipid sink, and consequently permit these lipids to appear in the outer leaflet.

These five points are supported by the evidence which follows.

Chapter 1

Calcium-mediated fusion of cardiolipin/phosphatidylcholine vesicles arrested by quick-freezing: Re-examination of lipidic particles

ABSTRACT

Cardiolipin (CL) has been known for some years to undergo a phase transition from liquid crystalline to hexagonal II (H_{II}). This latter phase has been hypothesized to represent a destabilizing center which may initiate fusion between two lipid bilayers. Examined by electron microscopy, frozen samples of glycerinated vesicles reveal large particles ("lipidic particles") under experimental conditions which elicit both H_{II} phase transition and fusion. Hence these particles have been considered indicative of the H_{II} phase and involved in the mechanism of fusion. To eliminate the necessity of using glycerol for the cryoprotection of frozen samples, we employed the quick-freeze device of Heuser, Reese, and Landis[1] to prepare vesicles with and without glycerol. In this way, the contribution of glycerol to the production of these particles could be assessed. Furthermore, quick-freezing permitted the capture of vesicles within seconds of calcium injection, arresting fusion in various stages. By quick-freezing CL:phosphatidylcholine (PC) vesicles with and without glycerol, and with either short (sec) or long (hr) calcium treatments, the effects of time and glycerol on fusion and lipidic particle formation could be examined. We found that, in the absence of glycerol, no lipidic particles formed during the first few seconds following calcium injection, the period of maximum fusional

in osmium incubated specimens prepared for electron microscopy of thin sections, and comparing its labeling patterns with PXB distributions, it could be shown that PXB domains were only in the outer leaflet of the membrane. In contrast, (ADR) penetrated the cells and labeled both sides of the membrane. In the sperm, anionic lipid only appeared in the outer lamella when cytoplasmic elements were either missing or morphologically altered. A comparison of cytoplasmic elements underlying PXB-resistant membrane versus those under susceptible membrane in the human blood platelet revealed that these elements underwent a metamorphosis concommitant with the development of PXB-susceptibility. Thus circumstantial evidence linked cytoplasmic structures with the maintenance of asymmetry, while PXB-susceptible membrane was free of such constraints.

activity. That the height of fusional activity occurred within seconds of calcium injection was established by observing the time-course of fluorescence emission produced by the intermixing of the aqueous contents of two different CL:PC vesicle populations which accompanies calcium-induced fusion. In contrast to the rapid initiation of fusion, particles were only prevalent following 1-2 h incubations in calcium or in glycerol and calcium combined. These results intimate that fusion can be detected within 1 sec of calcium injection and does not require the production of lipidic particles.

In a 1968 article, Luzzatti et al. described X-ray crystallography of various phases of anhydrous lecithin.[2,3] Other investigators later proposed that hydrated phosphatidic acid (PA), cardiolipin (CL), phosphatidylethanolamine, and CL:PC vesicles undergo a phase transition from liquid-crystalline to H_{II} in the presence of divalent cations or at a temperature only slightly above that at which transition from the gel to liquid-crystalline state occurs.[4-8] Deamer et al. revealed the ultrastructure of this phase in platinum-carbon replicas of anhydrous cardiolipin.[6] More recently, lipids known to exist in the H_{II} phase, a rod-like structure in which head-groups line the inside of the rod, and acyl tails radiate outward, have been claimed to participate both in the fusion of model membranes[7-10] and in the formation of lipidic particles[11-14] in glycerinated freeze-fracture preparations. In contrast, we have already demonstrated that fusion can be induced under conditions which do not result in the formation of the H_{II} phase or lipidic particles. For example, vesicles composed of phosphatidylserine (PS) do not undergo H_{II} phase transitions but fuse extensively in the presence

of Ca^{++} [6,13,14]. Furthermore, PS/phosphatidylethanolamine (PE) (transesterified from egg PC) vesicles undergo Ca^{2+} -induced fusion at temperatures well below the lamellar to H_{II} transition temperature.[17] These vesicles, or PS/egg PE vesicles, also fuse in the presence of Mg^{2+} (N.D., unpublished observations), which does not induce the H_{II} phase formation.[18,19] We have also shown that membranes made of a mixture of phosphatidylinositol and dimyristoylphosphatidyl ethanolamine, which do not transform into the H_{II} phase in the physiologic temperature range, can undergo Ca^{2+}-induced fusion as long as the membrane is above the gel to liquid-crystalline transition temperature[20]. Therefore, we are suspicious of the need for H_{II} phase or lipidic particle participation in fusion, even in those systems where such transitions are possible.

Here, we report our observation that although large unilamellar vesicles composed of these lipids did indeed fuse within seconds of calcium stimulation, no lipidic particles were present in these vesicles in the absence of glycerol. However, lipidic particles only emerged after long incubations (1-2 h) in calcium or calcium and glycerol.

Unilamellar vesicles made from CL:PC (in a ratio of 1:1) or egg PE: bovine brain PS (also 1:1) according to the reverse-phase evaporation technique of Szoka and Papahadjopoulos[21] were diluted to 10 μmol/ml in histidine-Tes buffer (pH 7.4) and sized by passage through a 0.2 μm millipore filter.[22] Vesicles from any given preparation were divided into separate test tubes and prepared in the following manner: 10-λ droplets of untreated liposomes were mounted directly on filter paper glued to an aluminun platform of a quick-freeze device and frozen on

a liquid-helium-cooled copper block (according to the procedure of Heuser et al. (1)). For observing fusion, we injected 8λ droplets with 2λ of a 25-mM Ca^{2+}-buffered solution 1-2 sec before freezing. Liposomes from the same initial batch were incubated for 1 h in either 5 mM calcium alone, or in calcium and 25% glycerol, and frozen in a similar manner. Except for the use of quick-freezing, these latter preparations duplicated previously reported experiments[9,11,12,14] and displayed the lipidic particles which have been described. To determine whether these lipidic particles were a product of long incubations or could appear during fusion in the presence of glycerol, glycerinated vesicles were also treated exactly like untreated vesicles and stimulated with calcium 1 sec before freezing. We then fractured and replicated all samples at -115°C in a Balzers freeze-fracture device, cleaned the replicas, and examined them in a Siemens 101 electron microscope. Fusion of CL:PC vesicles was studied independently by assaying the intermixture of aqueous contents from two populations of vesicles, using the fluorescence technique developed by Wilschut et al.[23]

The CL:PC vesicles not stimulated with calcium remained smooth-surfaced with a 0.2 μm diameter after quick-freezing (Fig. 1A). Within 1 sec of injection, calcium triggered dumbbell- and egg-shapes as well as larger, round vesicles in the process of merging with smaller ones, such as those in Fig. 1B. The merging of two or more vesicles could clearly be discerned, although no easily identified structure, such as lipidic particles, graced their smooth membrane faces. Large unilamellar egg PE:PS vesicles also underwent fusion within a sec of calcium

injection. The "zippering" of two membrane faces (Fig. 1C) was captured in these fusing vesicles and could be seen in CL:PC vesicles as well. No gross morphological differences were apparent in the two types of vesicles. When CL:PC liposomes were treated for 1 min with calcium (5 mM) and then incubated for 1-2 h in glycerol, many large vesicles emerged 10-20% of which were embossed with 9-10-nm particles (Fig. 1D). Some of the particles described circles about .2 μ in diameter, evidently delineating the margins of fused vesicles (Fig. 1E). Barren circles like these are reminiscent of the "clearings" of intramembranous particles (IMP) observed in glycerinated eukaryotic cells such as β-islet cells[24] and guinea-pig sperm (Fig. 2A & B)[25], in which the larger IMP also measure 9 nm. Such clearings, common in stimulated, glycerinated mast cells, no longer appear when the cells have been quick-frozen in the absence of glycerol.[26] We found that long incubation of CL:PC vesicles in calcium alone resulted in far fewer larger vesicles or lipidic-particle-embellished vesicles (1-5%) than incubation in glycerol and calcium although some clustered particles did materialize (Fig. 1F). Suspensions incubated in glycerol for 2 h first and then injected with calcium within seconds of freezing revealed more extensive fusion than nonglycerinated calcium-injected specimens. Liposomes in various stages of fusion could be seen within microns of each other (Fig. 1G) but only very few of all glycerinated calcium injected vesicles exhibited structures resembling particles (Fig. 1H) at points between the vesicles where the two bilayers were not yet confluent. That this was so rare during initial fusion even in the presence of glycerol but proliferate as the suspension attains equilibrium suggests that these are stable structures and not destabilizing centers. The requirement for glycerol in eliciting

lipidic particles during the rapid initial phase of fusion intimates that glycerol contributes to their formation and stabilization.

Measurements of the time-course following calcium injection of fluorescence emission created by the intermixing of aqueous contents (dipicolinic acid encapsulated in one population of vesicles and terbium in another) confirmed that maximal fusion occurred in seconds. The technical limitations of these two methods, quick-freeze and fluorescent emission, necessitated the use of two different concentrations of vesicles: in the fluorescence assay, the vesicle suspension was considerably more dilute (0.05 μmol lipid/cc). However, since the rate of fusion increases with vesicle concentration[23] the quick-frozen vesicles would be expected to undergo fusion even faster than the more dilute preparation. As vesicles were sized to 0.2 μm before calcium stimulation, the presence of vesicles larger than 0.2 μm in the freeze-fracture replicas further confirmed that fusion had indeed occurred during the 1 sec of stimulation.

Thus, calcium-induced fusion of large unilamellar vesicles can be captured by quick-freezing within seconds of stimulation. Lipidic particles, on the other hand, take much longer incubations to appear. We conclude that lipidic particles, or the H_{II} phase they are purported to represent, are not involved as an intermediate in the stages of fusion, even in membrane types which prominently display these structures after long calcium incubations or in the presence of both calcium and glycerol. Finally, we propose that the same morphological sequence of events occurs in fusing vesicles whether they are composed of egg PE:PS or CL:PC.

REFERENCES

1. Heuser, J. E., Reese, T. S. & Landis, D. M. Cold Spring Harbor Symp. Quant. Biol. 40, 17-24 (1976).
2. Luzzati, V., Gulik-Krzywicki, T. & Tardieu, A. Nature 218, 1031-1034 (1968).
3. Luzzati, V. & Tardieu, A. Annu. Rev. Phys. Chem. 25, 79-94 (1974).
4. Rand, R. P. & Sengupta, S. Biochim. Biophys. Acta. 255, 484-492 (1972).
5. Papahadjopoulos, D., Vail, W. J., Pangborn, W. A. & Poste, G. Biochim. Biophys. Acta. 448, 265-283 (1976).
6. Deamer, D. W., Leonard, R., Tardieu, A. & Branton, D. Biochim. Biophys. Acta. 219, 47-60 (1970).
7. Cullis, P. R. & de Kruijff, B. Biochim. Biophys. Acta. 513, 31-42 (1978).
8. Cullis, P. R., Verkleij, A. J. & Ververgaert, P. H. J. Th. Biochim. Biophys. Acta. 513, 11-20 (1978).
9. Verkleij, A. J., Mombers, C., Leunissen-Bijvelt, J. & Ververgaert, P. H. J. Th. Nature 279, 162-163 (1979).
10. Cullis, P. R. & Hope, M. J. Nature 271, 672-674 (1978).
11. Cullis, P. R. & de Kruijff, B. Biochim. Biophys. Acta. 559, 399-420 (1979).
12. Van Venetie, R. & Verkleij, A. J. Biochim. Biophys. Acta. 645, 262-269 (1981).
13. Vail, W. J. & Stollery, J. G. Biochim. Biophys. Acta. 551, 74-84 (1979).
14. de Kruijff, B., Verkleij, A. J., Van Echteld, C. J. A., Gerritsen, W. J., Mombers, C., Noordam, P. C. & de Gier, J. Biochim. Biophys. Acta. 200-209 (1979).

15. Papahadjopoulos, D., Vail, W. J., Jacobson, K. & Poste, G. Biochim. Biophys. Acta. 394, 483-491 (1975).

16. Papahadjopoulos, D., Vail, W. J., Newton, C., Hir, S., Jacobson, K., Poste, G., & Lazo, R. Biochim. Biophys. Acta. 465, 579-598 (1977).

17. Duzgunes, N., Wilschut, J., Fraley, R., & Papahadjopoulos, D. Biochim. Biophys. Acta. 642, 182-195 (1981).

18. Cullis, P. R. & Verkleij, A. J. Biochim. Biophys. Acta. 552, 546-551 (1979).

19. Tilcock, C. P. S. & Cullis, P. R. Biochim. Biophys. Acta. 641, 189- (1981).

20. Sundler, R., Duzgunes, N., & Papahadjopoulos, D. Biochim. Biophys. Acta. 649, in press.

21. Szoka, F., Jr., & Papahadjopoulos, D. Ann. Rev. Biophys. Bioeng. 9, 467-508 (1980).

22. Olson, F., Hunt, C. A., Szoka, F. C., Vail, W. J., & Papahadjopoulos, D. Biochim. Biophys. Acta. 557, 9-23 (1979).

23. Wilschut, J., Duzgunes, N., Fraley, R. & Papahadjopoulos, D. Biochemistry 19, 6011-6021 (1980).

24. Orci, L., Perrelet, A. & Friend, D. S. J. Cell Biol. 75, 23-30 (1977).

25. Friend, D. S., Orci, L., Perrelet, A. & Yanagimachi, R. J. Cell Biol. 74, 561-577 (1977).

26. Chandler, D. E. & Heuser, J. J. Cell Biol. 86, 666-674 (1980).

FIGURE LEGENDS

Figure 1 Quick-frozen vesicles. X 60,000. Bar - 0.2 μm.

Figure 1A A 0.2 μm vesicle, quick-frozen.

Figure 1B Several PC:CL vesicles fusing after being injected with 5 mM $CaCl_2$ 1 sec prior to quick-freezing.

Figure 1C Two large PS:egg PE vesicles captured by quick-freeze in the act of merging. A wave (arrow) advances along the fusion front.

Figure 1D Lipidic particles decorate this PC:CL vesicle incubated for 2 h in calcium and glyerol.

Figure 1E The particles apparent following calcium-glycerol 2 h incubations outline a cleared circle the same size (0.2 μm) as unfused vesicles.

Figure 1F A few clustered particles adorn PC:CL vesicles after a 2 h incubation in calcium alone.

Figure 1G The sequence of fusion events in the outer leaflet of PC:CL vesicles injected with calcium 1 sec prior to freezing. Two vesicles on the bottom right have aggregated. At the top left, three fused vesicles remain separated by narrow necks, which widen in the adjacent vesicle.

Figure 1H PC:CL vesicles incubated for 2 h in glycerol alone and then injected with calcium 1 sec before quick-freezing, fuse, displaying a few particles in the region of confluence. These particles embellish both P (arrow) and E face, and thus probably are created by points of incomplete fusion.

Figure 2 Comparison of lipidic particles and the intramembranous particles of cells. X 60,000.

2A A guinea-pig sperm, fixed, cryoprotected with 25% glycerol for 2 h quenched in liquid Freon 22 and frozen in liquid N_2, as described.[25] Both large and small (arrows) clearings occupy the site of future sperm-egg fusion. The size of the larger IMP ringing the clearings as well as the size of the smaller clearings is similar to the particles and clearings seen in glycerinated, calcium incubated PC:CL liposomes (2B).

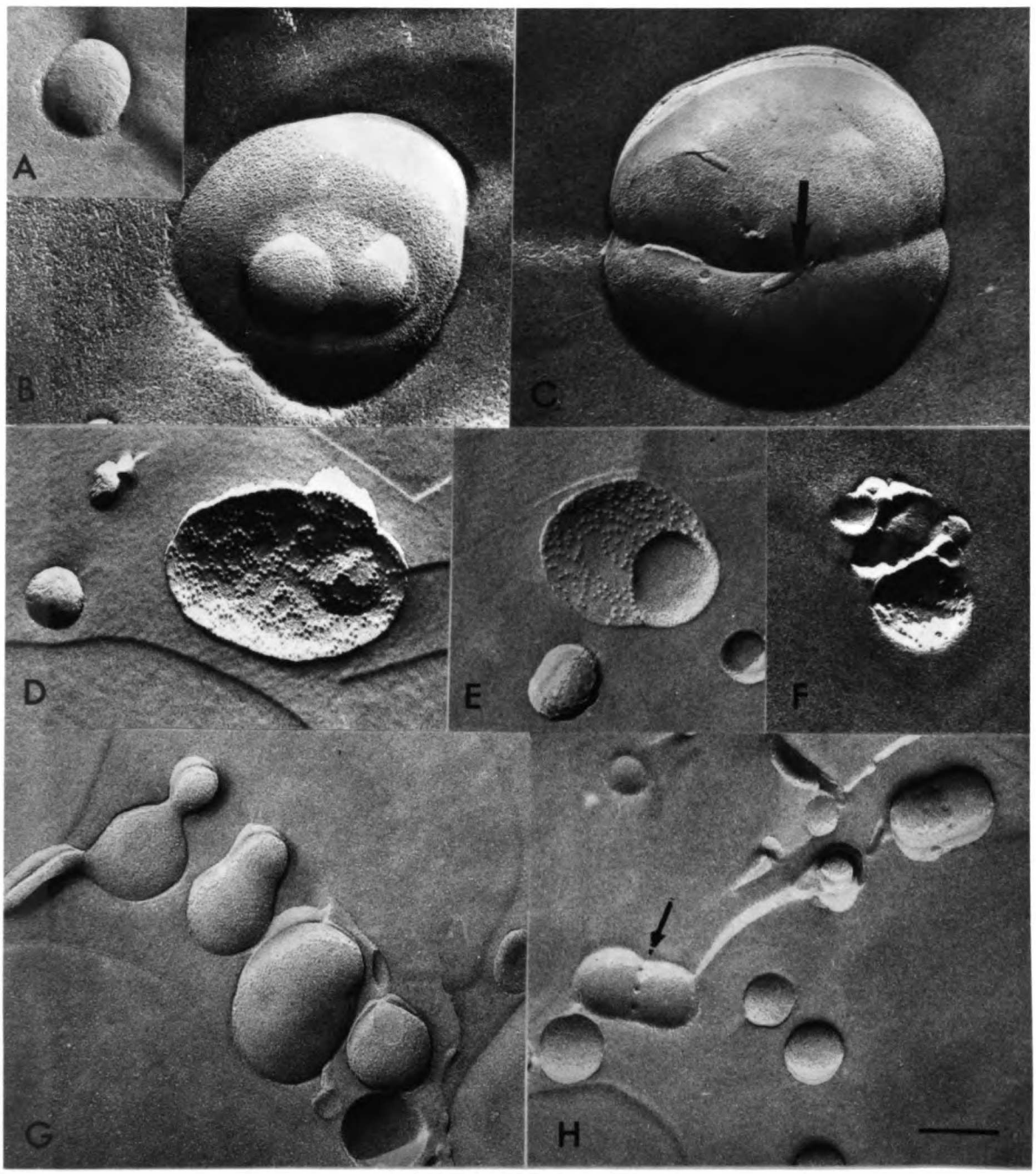

Fig. 1

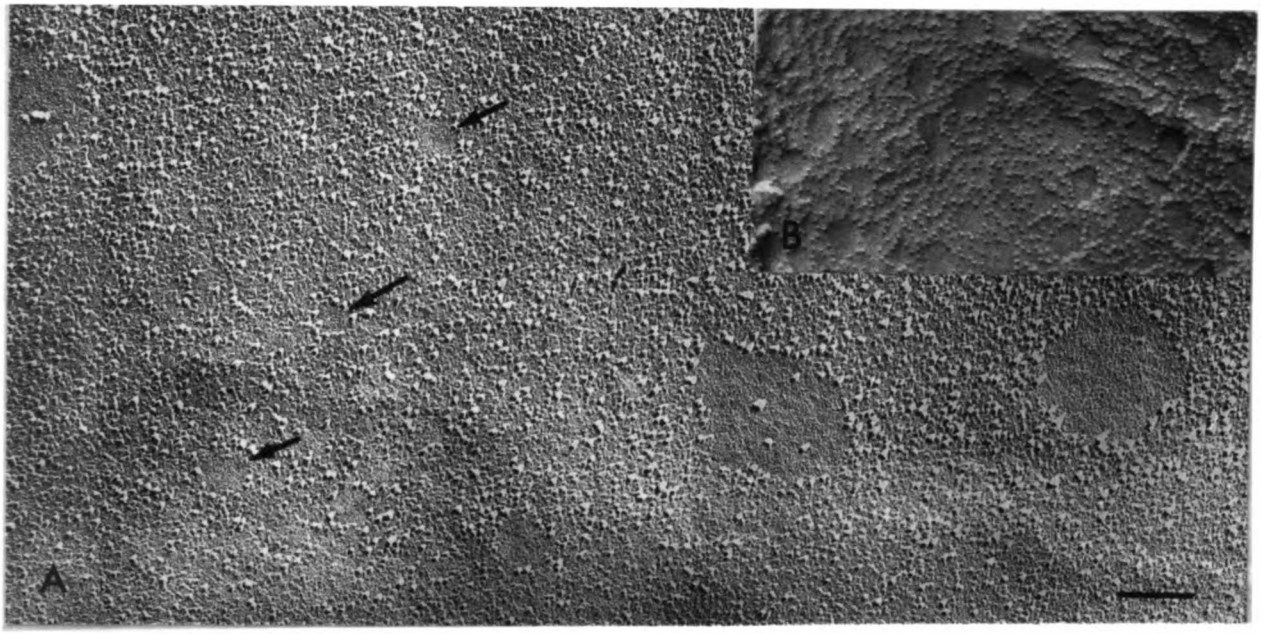

Fig. 2

Chapter 2

Anionic lipid domains: Correlation with functional topography in a mammalian cell membrane

ABSTRACT

Polymyxin B (PXB), a cyclic polypeptide antibiotic which specifically disturbs membranes containing anionic phospholipids, was used to explore their distribution in the plane of the spermatozoan plasma membrane by electronmicroscopy of freeze-fracture specimens. Exposed to HEPES-Tris-buffered PXB (4 mM), egg-lecithin liposomes showed no perturbations nor did they fluoresce with PXB dansyl derivative incubation. When phosphatidylethanolamine (PE), with or without cholesterol, was included in the liposomes, they became perturbed and fluoresced. Plasma membranes of Drosophila larval cells, whether containing or lacking the sterol, were also disrupted by PXB. Whereas the cell membranes of guinea-pig sperm were likewise disturbed, only specific-functional areas were affected. Fusional membrane domains showed crenulations and protrusions, while the stable membrane of the flagellar principal-piece revealed diffuse bubbling. Regions of well-defined particle arrays, as well as the post-acrosomal segment, maintained smooth contours. By fluorescence microscopy, we detected the same heterogeneous binding of the dansyl derivative. Specific properties of anionic lipids are primarily governed by their negative charge, allowing them to influence surface electrical potentials, buffer pH, and complex cations.

Examined by electronmicroscopy of freeze-fracture preparations, the cell membrane is a tapestry of different textural domains. Proteins, in the form of intramembranous particles such as those found in gap-junctional complexes, may be highly concentrated in one area of membrane and absent in others. In the guinea-pig sperm plasma membrane, particle arrays observed in freeze-fracture replicas exhibit characteristic patterns on particular surface-regions -- e.g., the "quilt" of the head, the zipper and annulus of the tail, and the midpiece strands (1). Recently, labeling sperm cells with filipin, a polyene antibiotic, has demonstrated the presence of cholesterol, deployed in an analogous patchwork fashion. Some membrane areas reveal considerable concentrations of the sterol, while other, neighboring zones contain only minute amounts (2, 3).

Although many transmembrane proteins are large enough for electronmicroscopic resolution, phospholipids, like sterols, are too small. Therefore, determining whether specific phospholipids are also heterogeneously dispersed would require a lipid-specific cytochemical reagent to render them visible by electronmicroscopy. Poly-myxin B (PXB) is such a tool.

After exposure to PXB, the outer membranes of gram-negative bacteria are known to erupt in protrusions (4-6). Protuberances, discernible by electronmicroscopy in thin-section, freeze-fracture, and scanning preparations (7, 8), correspond in number to the concentration of the agent applied to the cells (9). Moreover, PXB has a proven affinity for anionic lipids as follows: 1) Glucose leaks from liposomes composed of negatively-charged lipids when they are exposed to PXB (10, 11);

2) The radioactively-labeled antibiotic (PXB) adheres to monolayers of phosphatidylethanolamine (PE), phosphatidylglycerol (PG), and cardiolipin, as well as to the O-antigenic lipopolysaccharide of the gram-negative bacterial outer coat (12-19); 3) Phosphatidic-acid (PA) vesicles bind PXB in a ratio of 3:1 (14, 15), disclosing a cooperative binding curve identical to that for calcium dissociation and resulting in two new phase-transition temperatures -- one lower, the other higher, than that of untreated control vesicles; 4) Capacitance-conduction measurements of anionic lipid bilayers have established that PXB reduces capacitance and increases conduction (20), as well as decreasing surface potential (13); 5) Acholeplasma laidlawii becomes susceptible to PXB only when specific anionic lipids are incorporated into its membranes (17); and 6) Prokaryotes also display a punctate membrane-fluorescence when incubated with the dansyl derivative of PXB (5, 21).

In this report, we will demonstrate that PXB binds to eukaryotes, a mammalian spermatozoon, and insect larval cells, producing protrusions similar to those observed in prokaryotes. Unlike the uniformly disposed eruptions of bacterial membranes, however, a variety of membrane perturbations in sperm heterogeneously emboss the cell-surface.

MATERIALS AND METHODS

Liposomes. Unilamellar and multilamellar vesicles were prepared in Dr. Demetrios Papahadjopoulos' laboratory (Cancer Research Institute, University of California, San Francisco, CA) from egg phosphatidylcholine (PC) (Sigma Chemical Company, St. Louis, MO), PE formed from transesterification of egg PC, and cholesterol, as described by the above-mentioned investigator (22). Phospholipids (10 μmol), either PC alone or PC:PE (50% each), were formed and suspended in 1 ml of .1 M (N-2-hydroxyethylpiperazine-N'-2-ethane-sulfonic acid) (HEPES)-Tris buffer at pH 7.4. Cholesterol (5 μmol) was added to a 10-μmol aliquot of the PC:PE preparation, and the vesicles were stored under Argon^{R} at 4^{o}C until used. We incubated untreated vesicles in a final concentration of 25% glycerol for 1-2 hr before freezing, or processed them without glycerol for thin-sectioning as previously specified (2). Treated liposomes were incubated at 37^{o}C in 2 mM PXB (Sigma) in .1 M HEPES-Tris buffer (pH 7.4) and 25% glycerol for 15-45 min before freezing, or in 2 mM PXB in .1 M of the buffer without glycerol, and processed for thin-sectioning as above. Additionally, one group of PC: PE:cholesterol liposomes (1:1:1) was incubated for 1 hr in 1.25% glutaraldehyde (pH 7.4, 1% sucrose) in the same buffer and processed for freeze-fracture.

Cell Suspensions. Third-instar Drosophila melanogaster larval cells, provided by Christopher M. Havel in the laboratory of Brian McCarthy (Department of Biochemistry and Biophysics, University of California, San Francisco, CA), were grown in cholesterol-free media until depleted of the sterol (23) and the cells were subsequently

incubated with 4 mM PXB in .1 M HEPES-Tris buffer (pH 6.8) at 36°C for 10 min, or replenished with cholesterol and then incubated. Next, they were fixed for 1 hr in 1.25% glutaraldehyde in .1 M sodium cacodylate and 1% sucrose, and prepared for freeze-fracture as above. Control cells were fixed without PXB incubation. The lower pH may have influenced anionic charge of the lipids slightly, and also the cationic charge of the antibiotic. This could slightly change the kinetics of lipid-PXB association.

Guinea-pig spermatozoa from ether-anesthetized, mature (>500 g) male animals were obtained from the epididymal tails and vasa deferentia. The pooled sperm was incubated either in .1 M HEPES-Tris buffer for 10 min or in buffered 4-mM PXB for 10 min, at 37°C (pH 7.4). The preparations were then washed and fixed with 1.5-2.5% glutaraldehyde in .1 M cacodylate and 1% sucrose (pH 7.4) for 1-4 hr and processed for thin-sectioning or freeze-fracture. Incubation in PXB simultaneously with fixative or after fixation yielded essentially no protuberances up to a concentration of 50 mM; however, PXB incubation of washed, prefixed spermatozoa which were then resubjected to glutaraldehyde afforded results similar to those obtained using PXB treatment before fixation.

Fluorescence Microscopy. Polymyxin dansyl derivative was prepared as described (5), with dansyl chloride from Sigma. The eluate was tested chromatographically for purity as previously detailed (21). That conjugation had been achieved was confirmed by a shift of the absorption spectra to the red from 320 to 33 nm, as monitored by an Aminco SPF500 spectrophotometer (data not shown). Liposomes and sperm in buffered 5-

mM PXB dansyl derivative were monitored for 1 hr at 10-min intervals on a Zeiss fluorescence microscope equipped with a No. 45 barrier filter. Specimens were photographed with GAF 800A film, and exposures ranged from 20 sec to 5 min with the use of a Zeiss camera.

OBSERVATIONS

Liposomes. In the presence of PXB, multilamellar liposomes comprised of transesterified egg PE and egg PC in equal molar ratio, as well as liposomes with equimolar additions of cholesterol, developed protrusions on the outer lamellae at physiologic pH and temperature, in .1 M HEPES-Tris buffer (Figs. 1 and 4). Non-PXB-treated multilamellar vesicles of the same composition, and both treated and untreated egg-PC-containing vesicles, (Fig. 2) were smooth-surfaced, as were the inner layers of all liposomes (Fig. 2, 3, 4, and 5). The majority of outer lamellae of PE-inclusive liposomes was perturbed. Protrusions primarily embellished the outer membranes of larger vesicles, which is consistent with observations reported in regard to bacterial membranes -- i.e., that PXB fundamentally interacts with the outer membrane, not readily penetrating it.

In thin sections, the antibiotic disrupted the multilamellar structures (Fig. 4 as compared to Fig. 5). The outermost membrane formed protrusions of the same size as those seen in freeze-fracture replicas. When a dansyl-chloride fluorescent probe was conjugated to PXB, the PE-containing multilamellar vesicles fluoresced, demonstrating the binding of the antibiotic to model membranes. Liposomes harboring

cholesterol had slightly different emission-spectra than those lacking the sterol (data not shown).

Third-instar Drosophila larval cells, grown in cholesterol-deficient media, were exposed to PXB before and after incubation in a cholesterol-rich medium. Membranes known to contain no cholesterol (Fig. 6, PXB treated, as opposed to Fib. 7, non-treated) and cholesterol-saturated membranes were equally perturbed by the antibiotic (23).

Spermatozoa. The spermatozoon is an extensively specialized mammalian cell with three basic structural divisions: 1) the head (including the condensed nucleus and the acrosome), which in guinea-pig sperm is overlain by the crystalline pattern of the quilt. Here the plasma membrane covers three regions -- the acrosomal cap, the equatorial segment of the acrosome, and the post-acrosomal portion of the nucleus (Fig. 8); 2) the midpiece of the tail, arrayed with strands of particles, contains mitochondria, the flagellar root, centrioles, and the cytoplasmic droplet; and 3) the principal-piece, the continuation of the flagellum, which is separated from the midpiece by a densely particulate annulus, and embroidered down its length by two straight lines of transmembrane particles, the zipper.

Due to the clear functional and morphological delineation of each part, sperm cells are uniquely suitable for investigating the relationship of function to topographical differences in lipid concentrations.

Guinea-pig spermatozoa taken from the tails of the epididymides and

vasa deferentia were attacked by PXB, and sperm plasma membranes treated with the dansyl derivative of the antibiotic fluoresced vividly in the fusigenic acrosomal-cap region and faintly in the stable principal-piece of the tail (Fig. 9). The post-acrosomal region and mid-piece remained dark. Examined in freeze-fracture and thin section preparations, PXB-treated sperm revealed protrusions not seen in control cells (Fig. 10) but which are characteristically engendered by the agent (Figs. 11 and 12). Localization of perturbed areas correspond to those which fluoresced (Fig. 13).

Polymyxin B created several types of membrane-bilayer perturbations in different zones of the cell. Crenulations and small protrusions adorned 99% of the acrosomal caps when cells were incubated for 10 min in 4 mM PXB (Figs. 14 and 15), while blebs appeared less frequently (Figs. 13 and 15). Rivulets joined these when the cells were incubated in PXB for longer than 30 min or at concentrations higher than 4 mM. These harsher conditions did not affect localization of disturbed membrane, however. At first restricted to the tip of the acrosomal cap, the protrusions gradually descended toward the equatorial segment in the wake of the melting quilt pattern. Only small protrusions occurred in the midpiece, and these were only present over the cytoplasmic droplet. When sperm were incubated before fixation, principal-piece membrane, were occasionally bubbled down their length; whereas prefixed, incubated, and post-fixed principal-pieces were usually uniformly affected (Figs. 16-20). Conspicuously damaged principal-piece membrane, with clumped particles and irregularly-shaped, cleared patches, showed no increase in the density of surface bulges. Unperturbed areas of membrane consisted

of tracts covered with dense particle arrays -- e.g., the quilt (Figs. 14 and 15), the midpiece strands, the annulus (Fig. 20), and the zipper (Fig. 18). The portion which arches over the top of the nucleus, as well as the post-acrosomal segment, also remained untouched (Figs. 13 and 14). Neither the acrosomal outer membrane nor the nuclear envelope was altered by PXB treatment. Thin sections of the head and principal-piece revealed the same membrane perturbations observed in fracture replicas (Figs. 10, 17, and 19).

Barring the cytoplasmic droplet, the midpiece, too retained its smooth contours and typical protein arrays after incubation with PXB.

Sperm continued to swim for more than 1 hr in media containing the PXB dansyl derivative if not subjected to ultraviolet irradiation. This duration of incubation, however, proved to be unnecessary, since the distribution of fluorescence did not change or increase after the first 10 min in the media. Addition of 0.4 ml of 10 mM calcium chloride to 1 ml of sperm or liposome suspension inhibited the fluorescence of both liposomes and sperm.

DISCUSSION

Polymyxin B binds anionic phospholipids as well as the O-antigenic lipopolysaccharide of gram-negative bacteria (4). Exposed to the antibiotic, the entire outer membranes of these bacteria form protrusions, corresponding in number to the concentrations of PXB (5-9). Only in specific areas, however, are the plasma membranes of spermatozoa susceptible to the effects of PXB. In contrast, the whole membrane is

affected by this agent in Drosophila larval cells and liposome membranes containing anionic lipids. The heterogeneous distribution of PXB receptors on the surface of the highly specialized gamete implies that these lipids, deployed in a patchwork pattern within the plane of the bilayer, are not free to diffuse throughout the membrane. In addition, fluorescent-labeling techniques substantiate freeze-fracture testimony of the heterogeneity of binding availability, since fluorescence depends upon binding alone. Previously, investigations utilizing filipin proved that the plasmalemma is indeed capable of forming protrusions in membrane regions lacking susceptibility to PXB; for these regions lose their smooth contours on the occasion of polyene:sterol aggregation (3). Although it may be argued that inhibition of binding, rather than a paucity of anionic lipids, spares the membrane of the spermatozoan midpiece and post-acrosomal segment in the presence of PXB, most potential inhibitory effects can be excluded: 1) the membrane is available to filipin, and this polyene is capable of insertion; 2) neither cholesterol nor PC (both implicated as binding inhibitors) prevents membrane disruption in Drosophila cells or liposomes; 3) moreover, anionic sites remain unmasked in these presumed-insensitive areas, as evidenced by the binding of colloidal iron hydroxide (CIH), a much larger molecule than PXB (24). A less specific agent than PXB, CIH binds most negatively-charged molecules, including sialic acid moieties and acidic amino acid residues, as well as unidentified anionic sites insensitive to trypsin or neuraminidase. Its distribution on the plasma membrane overlaps that of PXB-induced disturbances. We therefore consider it highly probable that anionic lipids are heterogeneously dispersed in the plane of the bilayer, and that positive and neutral zwitterionic lipids may be present

in much greater proportions in non-PXB-perturbed membrane.

Polymyxin-B-induced membrane disruption is variable in terms of contour. The type of agitation is nonspecific, but disruption of any sort may indicate the presence of anionic lipids. Various forms of "blebbing" and wrinkling may be a result of the deletion of anionic lipids from the membrane, thereby destabilizing it. In high concentrations or with long incubation, PXB solubilizes the membrane, denuding the cell and casting vesicles into the surrounding media. Because of susceptible-membrane variance in form, it is impossible to pinpoint the precise whereabouts of the PXB-lipid complex. Even now, however, large areas of perturbed membrane can be seen neighboring other large, undisturbed portions of smooth membrane. These tracts, though appearing sizable in electronmicroscopic replicas, are still too small to be isolated by biochemical techniques.

All four of the phospholipid substrates for PXB -- PG, cardiolipin, PE, and PA -- are present in mammalian sperm, with PE the greatest in proportion. Porcine and ram sperm membranes have also been analyzed for phospholipid content. Ram membranes contain 9% PE, less than 1% PA and PG, and high levels of cardiolipin -- 6% (25). Procine membranes contain much more PE, 28%, 1-2% PA and PG, and 3.6% cardiolipin (26-28). Biochemical purification and lipid analysis of guinea-pig spermatozoan plasma membranes have not yet been achieved.

The three major functional regions of the spermatozoon respond quite differently to the antibiotic PXB: Specialized for fusion, the

head, where exocytosis of the acrosomal contents occurs over the cap, becomes crenulated as the quilt pattern vanishes. Meanwhile the post-acrosomal area of the membrane, the site of subsequent sperm:egg fusion, is seldom disrupted in epididymal, non-capacitated sperm. The midpiece, performing the remaining cellular functions, including energy transduction, is perturbed only over the cytoplasmic droplet and not over the mitochondria. Finally, the principal-piece, the terminus of the motile flagellum, is diffusely bubbled along its length. These differences in perturbation correlating with the three functional areas (fusional, energy-generating, and motile) suggest that differing amounts of anionic lipids participate in these membrane specializations, either in response to or in the pursuit of cellular activity.

Phase-separation of lipid bilayers (composed of either a single lipid or a combination of lipids) has been the focus of many studies, but other biophysical properties of lipids may result from or influence lipid heterogeneity. Cholesterol, for example, does have a dominant role in bilayer fluidity -- thus its unhomogeneous distribution regulates focal phase parameters. Anionic lipids, however, perform other, less well-established functions. As carriers of negative charge, they are uniquely able to modulate electrical fields, surface voltage potential, and other charge-dependent forces (13, 29-31). Polymyxin B, by binding anionic lipids, decreases membrane capacitance (20). It is probably that effects of negatively-charged lipids on bilayer fluidity are minimal, whereas the effect of fluidity of them -- i.e., their aggregation or separation -- could control the magnitude of their electrical, ionic, or neutrophilic influence on other molecules in their

vicinity. Phase-separations of these lipids are affected by pH as well as by ionic strength, temperature, and cholesterol (15, 32, 33). With high concentrations of cations, significantly Ca^{++}, tight aggregations of PA can form at physiologic pH and temperature (32). These aggregates squeeze out PC, thus enriching two adjacent areas of membrane in two different lipids. Binding of Ca^{++} also creates a point of high cationic concentration localized on the membrane.

Well-defined foci of high anionic charge such as that seen on the sperm head may serve a completely different purpose in membrane function than that of diffusely high levels of acidic lipids -- e.g., as found on the principal-piece. In all liklihood, the uniform bubbling on the spermatozoan principal-piece indicates a disseminated but high anionic lipid concentration; while the crenulations are distinct and protrusions on the head, poking through rifts in the crystalline quilt, may reflect focal sites of aggregations. As the acrosomal cap is preparing for fusion, the plasma membrane enclosing the tail must be non-fusigenic. Diffuse deployment of these lipids may then stabilize the membrane, and focusing of the lipids could help to unite apposing membranes by cationic cross-linking of negative charges. It is especially thought-provoking that either Ca^{++} or Mg^{++} can compete with PXB for the same binding sites (13, 14, 19, 34).

REFERENCES

1. Friend, D. S. & Fawcett, D. W. (1974) J. Cell Biol. 63, 641-664.
2. Elias, P., Friend, D. S., & Goerke, J. (1979) J. Histochem. Cytochem. 27, 1247-1262.
3. Friend, D. S. (1980 in Membrane-Membrane Interactions, ed. Gilula, N. B. (Raven Press, New York, NY), pp. 153-165.
4. Lounatmaa, K. & Nanninga, N. (1976) J. Bacteriol 128, 665-667.
5. Schindler, P. R. G. and Teuber, M. (1975) Antimicrob. Agents Chemother. 8, 95-104.
6. Storm, D. R., Rosenthal, K. S. & Swanson, P. E. (1977) Annu. Rev. Biochem. 46, 723-763.
7. Koike, M., Iida, K. & Matsuo, T. (1969) J. Bacteriol. 97, 448-452.
8. Lounatmaa, K., Makela, P. H. & Sarvas, M. (1976) J. Bacteriol. 127, 1400-1407.
9. Wahn, K., Lutsch, G., Rockstroh, T. & Zapf, K. (1968) Arch. Mikrobiol. 63, 103-116.
10. Feingold, D. S., Hsu Chen, C. C. & Sud, I. J. (1974) Ann. N. Y. Acad. Sci. 235, 480-492.
11. Imai, M., Inoue, K. & Nojima, S. (1975) Biochim. Biophys. Acta. 375, 130-137.
12. Bader. J. & Teuber, M. (1973) Z. Naturforsch. (B) 28C, 422-430.
13. El Mashak, E. M. & Tocanne, J. F. (1980) Biochim Biophys. Acta. 596, 165-179.
14. Hartmann, W., Galla, H. -J. & Sackmann, E. (1978) Biochim. Biophys. Acta. 510, 124-139.

15. Sixl, F. & Galla, J. -J. (1979) Biochim. Biophys. Acta. 557, 320-330.

16. Teuber, M. (1973) Z. Naturforsch. (B) 28C: 476-477.

17. Teuber, M. & Bader, J. (1976) Antimicrob. Agents Chemother. 9, 26-35.

18. Teuber, M. & Bader, J. (1976) Arch. Microbiol. 109, 51-58.

19. Teuber, M. & Miller, I. R. (1977) Biochim. Biophys. Acta. 467, 280-289.

20. Miller, I. R., Back, D. & Teuber, M. (1978) J. Membrane Biol. 39, 49-56.

21. Newton, B. A. (1955) J. Gen. Microbiol. 12, 226-236.

22. Szoka, F., Jr. & Papahadjopoulos, D. (1978) Proc. Natl. Acad. Sci. USA 74, 4194-4198.

23. Silberklang, M., Friend, D. S., McCarthy, B. J. & Watson, J. A. (1980) Fed. Proc. Am. Soc. Biol. Chemists Biophys. Soc., ASBC/BS Mt., in press (Abstr.).

24. Yanagimachi, R., Noda, Y. D., Fujimoto, M. & Nicolson, G. L. (1972) Am. J. Anat. 135, 497-520.

25. Scott, T. W., Voglmayr, J. K. & Setchell, B. P. (1967) Biochim. J. 102, 456-461.

26. Evans, R. W., Weaver, D. E. & Clegg, E. D. (1980) J. Lipid Res. 21, 223-228.

27. Snider, D. R. & Clegg, E. G. (1975) J. Animal Sci. 40, 269-274.

28. Weaver, D. E., Evans, R. W. & Clegg, E. D. (1978) Biol. Reprod. 18, 47A (Abstr.).

29. Benz, R., Frohlich, O., Lauger, P. & Montal, M. (1975) Biochim. Biophys. Acta. 394, 323-334.

30. Benz, R., Beckers, F. & Zimmerman, U. (1979) J. Membrane Biol. 48, 181-204.

31. Kolber, M. A. & Haynes, D. H. (1979) J. Membrane Biol. 48, 95-114.

32. Galla, H. -J. & Sackmann, E. (1975) Biochim. Biophys. Acta. 401, 509-529.

33. Sun, S. T., Hsang, C. C., Day, E. P. & Ho, J. T. (1979) Biochim. Biophys. Acta. 557, 45-52.

34. Klausner, R. D., Kleinfeld, A. M., Hoover, R. L., and Karnovsky, M. J. (1979) J. Biol. Chem. 225, 1286-1295.

35. Rosenthal, K. S., Swanson, P. E. & Storm, D. R. (1976) Biochemistry 15, 5783-5792.

FIGURE LEGENDS

Fig. 1. Freeze-fracture replica of a PC:PE:cholesterol liposome incubated in PXB, then fixed in glutarladehyde. Note the conspicuous antibiotic-induced bubbles (0.8 μ in diameter) which primarily decorate the outer membrane. (X 26,000).

Fig. 2. PC vesicles incubated in PXB and not showing protrusions. (X 21,000).

Fig. 3. Electronmicrograph of a fractured PC:PE:cholesterol non-PXB-treated liposome, its smooth lamellae contrasting with the liposome in Fig. 1. (X 29,000).

Fig. 4 and 5. Thin sections through the specimens depicted in Figs. 1 and 3, respectively. All the untreated bilayers and only the inner bilayers of PXB-treated vesicles show linearity, whereas the outer treated membranes form 0.8-μ-diameter blebs. (Figs. 4 and 5, X 70,000).

Fig. 6. Portion of a Drosophila larval cell, depleted of cholesterol, after PXB incubation. Multiple 0.8-μ protrusions cover the plasma membrane. (X 55,000).

Fig. 7. Untreated, cholesterol-depleted Drosophila larval cell, fractured through the plasma membrane and shadowed from above. A few truncated microvilli dot the otherwise smooth surface. (X 22,000).

Fig. 8. Plasma membrane of a control sperm head, exhibiting undisrupted contours. The regions illustrated are the acrosomal cap (a), the position corresponding to the tip of the nucleus (t), the equatorial segment (e), and the post-acrosomal segment (p). (X 6000).

Fig. 9. Fluorescent acrosomal cap (a) of a spermatozoon incubated in PXB dansyl derivative. Both the equatorial (e) and post-acrosomal (p) segments remain dark, while tail (t) faintly fluoresces. (X 1,000).

Fig. 10. Section through the acrosomal cap of a control spermatozoon. Plasma membrane (p), outer acrosomal membrane (a). (X 78,000).

Fig. 11. Section through the acrosomal cap of a sperm cell incubated in PXB. The plasma membrane (arrow) is crinkled, while the acrosomal membrane remains flat. (X 92,500).

Fig. 12. Freeze-fracture replica of a normal acrosomal cap (a) in a non-PXB-treated sperm cell. (X 14,500).

Fig. 13. An extensively perturbed plasma membrane of a PXB-treated sperm head, with acrosomal cap (a) studded with blebs (arrows). Overlying the tip of the nucleus (t) the membrane remains smooth, whereas the plasmalemma over the remainder of the acrosome (r) is lightly crenulated (X 6,000).

Fig. 14. Lightly crinkled plasma membrane over the acrosomal cap (a) and, proximally, an undisturbed quilted area (q). The degree of perturbation ranged from that shown here to the wide-spread wrinkles and blebs with loss of the quilt pattern illustrated in Fig. 13. (X 16,000.

Fig. 15. High magnification of the crenulation amidst the disintegrating quilt. Two round areas devoid of quilt, particles, or crinkles eventually become blebbed. These circular patches may have been free of anionic lipids, analogous to the particle-free circles observed in control and in filipin-treated sperm (3). Alternatively, they may result from PXB binding of anionic lipids and the consequent loss of anionic forces from the plane of the membrane. (X 85,000).

Fig. 16. Zipper (arrow) of a non-PXB-treated spermatozoan principal-piece with a taut membrane. (X 34,000).

Fig. 17. Thin section of the principal-piece, with a linear plasmalemmal bilayer. (X 60,000).

Fig. 18. PXB-treated principal-piece. An intact zipper runs between the bubbles of the plasma membrane. (X 25,000).

Fig. 19. Thin section of a PXB-treated principal-piece. Note that the plasma membrane is bubbled. (X 45,000).

Fig. 20. The intact annulus (arrow) encircles a greatly perturbed PXB-treated sperm tail. Grid patterns retain their normal organization, while the membrane they occupy bubbles. (X 27,000).

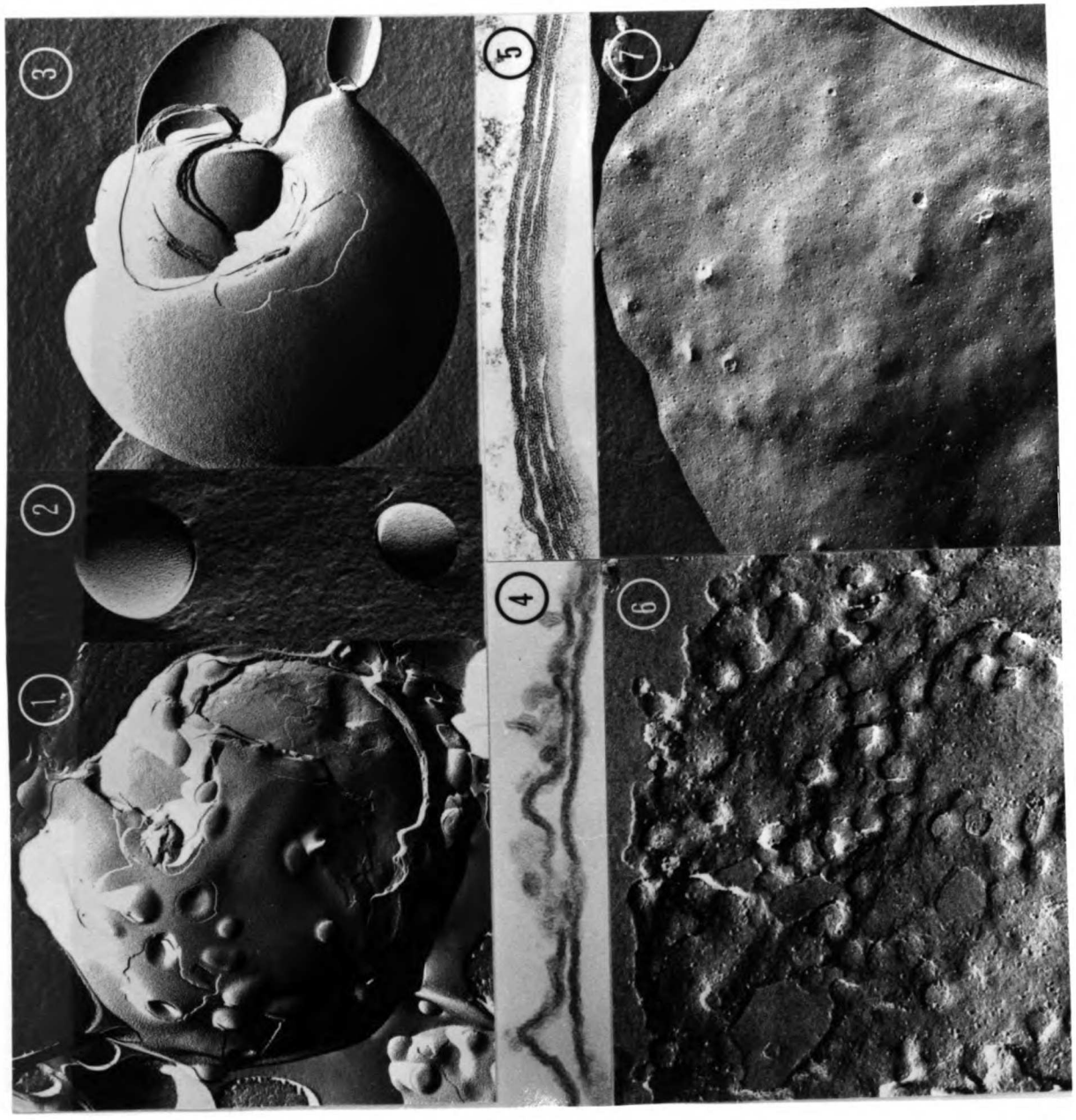
1
2
3
4
5
6
7

8
p
e
t
a
10
a
p
11
9
ta
p
e
a

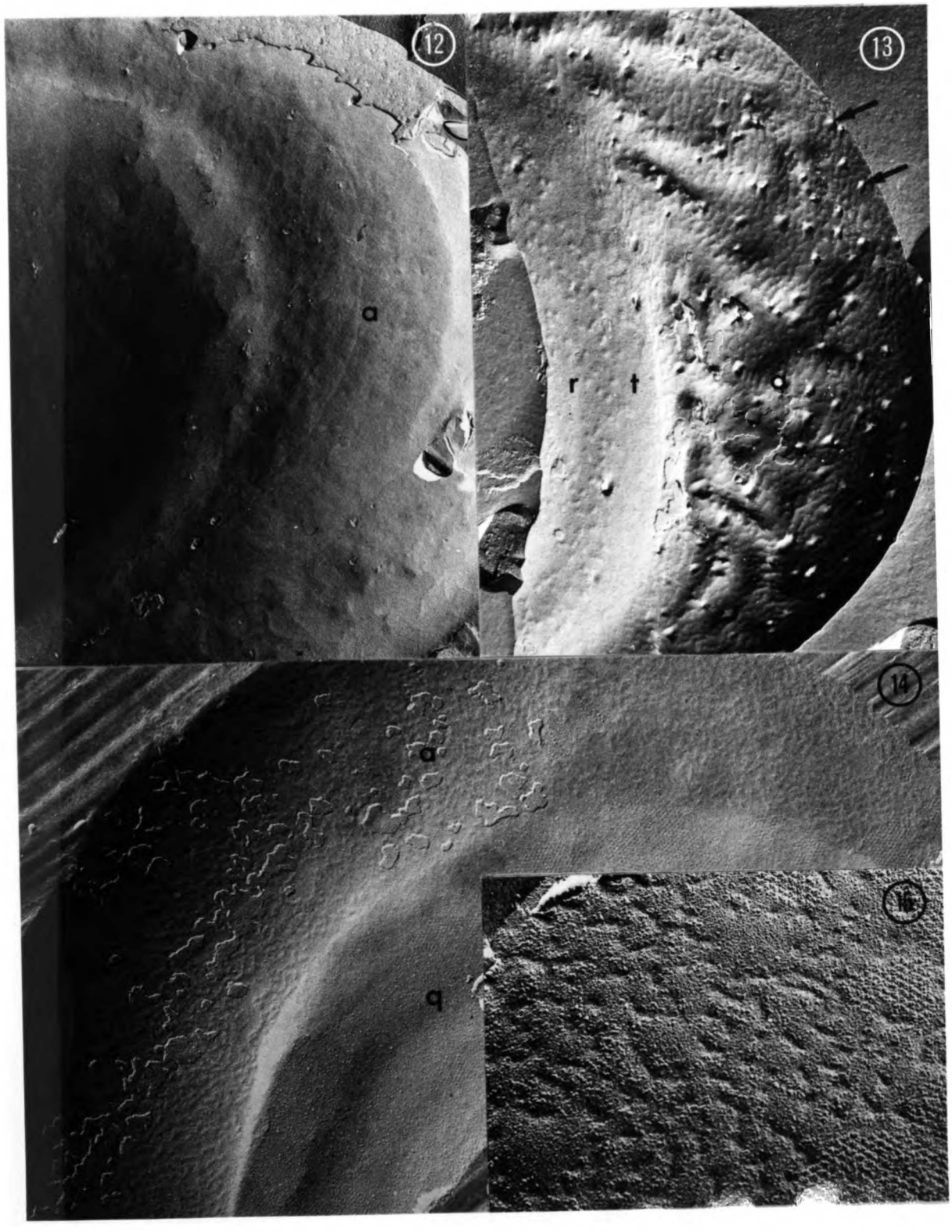
12
a
13
r
t
o
14
a
q
15

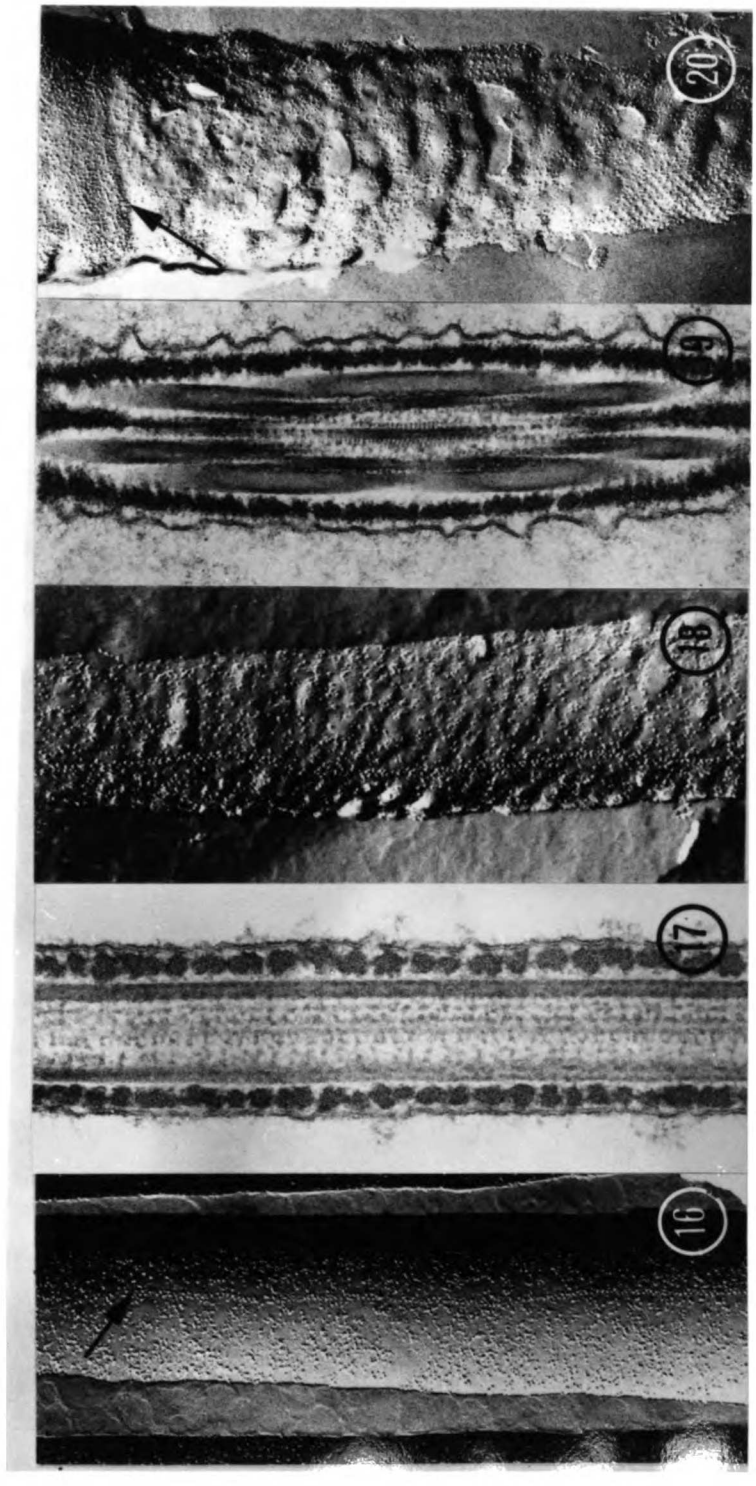
20
19
18
17
16

Chapter 3

Modifications of anionic lipid domains preceding membrane fusion in guinea-pig sperm

ABSTRACT

The relationship between anionic-lipid concentration and the functional properties of plasma-membrane domains was explored using the guinea-pig sperm membrane as a model, with polymyxin B (PXB) as a probe. Areas of plasmalemma specialized for fusion during the acrosome reaction had a higher affinity for the probe than adjacent non-fusigenic regions. In addition, capacitation -- a process preceding acrosome:plasma-membrane fusion -- markedly enlarged the area susceptible to PXB binding over the acrosomal cap. Protease treatment mimicked capacitation by increasing the acrosome-reaction incidence as well as PXB binding, at enzyme concentrations not affecting the surface coat nor altering filipin/sterol localization. Both proteolytic digestion and capacitation failed to augment PXB- or filipin-affinity in non-fusigenic zones, such as the post-acrosomal segment, including its particle-free maculae. Incubation of sperm in capacitating medium supplemented with ^{32}P-labeled phosphate, followed by lipid extraction, thin-layer chromatography, and autoradiography, revealed a radioactive band co-migrating with cardiolipin and phosphatidic acid. Vermiform protrusions elicited by PXB in the outer lamellae of cardiolipin-phosphatidylcholine liposomes resembled those seen in fusional regions of sperm membrane. We conclude that 1) differing concentrations of anionic lipids are found in adjacent domains of the sperm plasma membrane; 2) these domains mirror the functional

regions of the membrane, with higher anionic-lipid concentrations localized over fusional zones; 3) the surface coat does not participate in the maintenance of such domains; 4) anionic lipid synthesis may contribute to their formation; and 5) anionic-lipid concentrations increase as the membrane becomes fusionally competent, indicating that cellular modulation of lipid domains accompanies regulation of membrane function.

That phospholipids mediate fusion in diverse biological or model membrane-systems has been advocated by a number of investigators. Particularly, workers in reproductive biology have shown that fertilization is not prevented by the treatment of eggs with proteolytic or carbohydrate-hydrolyzing enzymes which leave phospholipids intact (26). Moreover, biophysicists have established that phospholipid vesicles can fuse, not only with each other (44) but with natural membranes (23, 55). Certain lipids have a greater potential for fusion than others. For example, liposomes composed solely of phosphatidylcholine (PC) resist merger for hours, yet vesicle membranes incorporating anionic lipids fuse readily upon the introduction of divalent cations (44).

The requirement for negatively-charged lipids in the event of membrane:membrane fusion has been demonstrated in various systems -- e.g., the entry of Semliki Forest virus into cells via the viral envelope-membrane union with the cell's lysosomal membrane (55), or the coalescence of lipids from two different model liposome populations (44).

Some acidic lipids are isothermically triggered by calcium (Ca^{2+}) to freeze from the liquid-crystalline to the gel state; while others partially melt, forming hexagonal arrays (14, 32). Accompanying the induction of a new phase, permeability, compressibility, and surface-potential become altered (43, 44). These phase transitions have been hypothesized to create disorganized lipid arrays necessary for the initiation of fusion (44). In cells as well as liposomes, Ca^{2+} triggers membrane fusion, suggesting that an analogous mechanism is active in

vesicle:vesicle coalescence and in cellular processes such as exocytosis and fertilization. Cholesterol also affects these phase transitions; thus its presence or absence as evidenced by filipin is a clue to the physical state of the membrane.

That a cell can concentrate anionic lipids in areas of the membrane bilayer where fusion occurs, and conversely, that these lipids can be excluded from stable regions of the membrane, is the subject of this paper. Other membrane components appear to have a differential topography in the plane of the membrane. Many integral membrane proteins (e.g., the acetylcholine receptor and ouabain-sensitive ion pumps) reside in preferential foci within the plane of the bilayer (17, 35). In addition, labeling of β-OH sterols with the polyene filipin has demonstrated the heterogeneity of these components in the plasmalemmae of various cell types (15, 36). This differential topography correlates with specific functional domains of the membrane. Furthermore, we propose that fusigenic domains, high in anionic-lipid concentration, form in dynamic response to the fusional activity of the cell rather than permanently occupying exact sites in the plane of the membrane, awaiting fusion activation.

The findings reported here primarily stem from the transmission electronmicroscopy of freeze-fracture replicas, which permits large vistas of membrane to be examined. We used the antibiotics polymyxin B (PXB) as a probe for anionic lipids, and filipin as a probe for β-OH sterols such as cholesterol. It has already been established that PXB binds to anionic lipids (52, 54), and through this binding, disrupts the

normally smooth contours of eukaryotic-cell membranes (1, 4). Filipin binding to sperm has been described (15, 19); thus we could use it as a tool to monitor the availability to deform in the presence of a lipid-binding agent. The model we have selected is the guinea-pig spermatozoon (Fig. 1). This highly polarized cell has the advantage of an extensive area of fusigenic plasma membrane -- the acrosomal cap, easily recognized in freeze-fractures. Contiguous with the fusigenic region lies the stable post-acrosomal membrane. Newly removed from the tail of the epididymis or from the vas deferens, sperm must be capacitated before the addition of Ca^{2+} kindles fusion between the plasmalemma and the outer portion of the acrosomal membrane -- the acrosome reaction (3). Capacitation, the process which readies these membrames for the reaction, can be achieved in vitro (58). The absence of calcium, however, can halt fusion, arresting the cells at the threshold of the acrosome reaction. In this paper, we have compared the binding of PXB to the head membranes of fresh spermatozoa with that of cells incubated in calcium-free capacitating media, in order to assess their relative distribution of anionic lipids. Thus, changes in distribution which accompany capacitation, but occur prior to the acrosome reaction, can be described.

MATERIALS AND METHODS

Fresh Sperm

Spermatozoa were removed from the vasa deferentes and epididymal tails of mature (500 g), ether-anesthetized guinea pigs. The pooled sperm at a concentration of 10^7 cells/cc were then mixed in Ca^{2+}-free Tyrode's solution (TS), pH 7.4, and treated as follows:

1) Control sperm were incubated in TS containing comparable (molar) sucrose concentrations to replace PXB.

2) For polymyxin-B (Sigma Chemical Co., St. Louis, Mo.) labeling, sperm were treated as previously reported (1), except that TS was substituted for HEPES-Tris.

3) Filipin labeling was accomplished according to the method used in earlier experiments (15), but with the omission of dimethylsulfoxide (DMSO).

4) Hemocyanin-PXB conjugation was achieved by using a modification of the method of Jan and Revel (28) wherein we substituted keyhole limpet hemocyanin (KLH) (Sigma) for that of Busycon canaliculatum, and 10 mg of PXB for IgG. After dialysis for 24 h at $4^{o}C$, a Bio Gel A 1.5-m column (2.5 x 20 cm) was used to separate nonreacted PXB from the conjugate. Hemocyanin-PXB was recovered by monitoring absorption spectra of the fractions at 280 nm, and subsequent ultrafiltration of the absorbing fractions. A final volume of 10 ml contained protein concentrations of 1.5-2.5 mg/ml, as measured by the Biorad protein-determination method (4).

5) Next, the sperm were incubated for 30 min at $37^{o}C$ in a phosphate buffered saline (PBS)/hemocyanine-PXB solution (pH 7.4).

Enzyme-treated Sperm

Sperm were incubated in TS supplemented with 1 mg/ml proteinase (crude trypsin extract, Sigma, Type II, pancreatic; trypsin activity 1050 U/mg; chymotrypsin activity 1040 U/mg) for 30 min at $37^{o}C$ (pH 7.2-7.4), followed by the addition of 1 mg/10 ml soybean trypsin inhibitor (Sigma; 0.9 mg inhibits 10,000 U trypsin). Subsequently the cells were

washed twice and labeled with PXB or filipin, or incubated with sucrose as described above. Comparable aliquots of sperm were incubated for 30 min without proteinase.

Capacitated Sperm

Sperm were incubated in Ca^{2+}-free TS, with 2% bovine serum albumin (BSA) and 1% glucose in 1ml aliquots at $37^{o}C$ under sterile mineral oil for 24-26 h according to the method of Yanagimachi and Usui (58). To some of these aliquots of sperm, we added .4 cc of a 10-mM $CaCl_2$ solution. Droplets of these sperm were taken at 10-min intervals, examined to establish motility and quantitate acrosome reactions, and then allowed to air-dry for subsequent staining (see below). The rest were washed once and treated with the lipid-binding agents as previously described here. Only dishes containing 90% motile sperm were retrieved for further processing.

Quantification of Acrosome Reactions

Ten aliquots from preparations of unfixed, fresh, protease-treated, TS-incubated, and capacitated sperm (with or without calcium) were first monitored at the light-microscopic level to determine motility and acrosome reactions, then permitted to air-dry on glass microscope-slides. They were subsequently stained with erythrosin B and naphthol yellow S (9).

Preferentially staining acrosomal contents bright red with these dyes greatly facilitates counting reacted vs. nonreacted sperm by light microscopy (Figs. 2 and 3). To eliminate the effect of air-drying and

staining on acrosomal patency, we substracted the fraction of acrosome-reacted cells in non-calcium-treated samples from those with calcium. The fraction of sperm which lost their acrosomal contents after incubation and subsequent addition of calcium was calculated according to the following formula:

$$\frac{\text{No. of acrosome-reacted sperm 20 min post-Ca}^{2+}}{\text{Total sperm 20 min post-Ca}^{2+}} \text{ minus } \frac{\text{No. of acrosome-reacted sperm pre-Ca}^{2+}}{\text{Total sperm pre-Ca}^{2+}}$$

We counted sperm at random by "blind" selection of a high-power field, followed by enumeration of all the sperm within that field. Ten fields were counted for each droplet.

Preparation of Sperm for Electronmicroscopy

All preparations were fixed in 1.25% glutaraldehyde buffered with .1 M sodium cacodylate, 1% sucrose (pH 7.4). Freeze-fractures were obtained as described (21); and surface replicas were processed by critical-point-drying (45), mounting in a Balzers apparatus, and shadowing with carbon-platinum at -2 X 10^{-6} torr. For surface replicas, samples were kept at room temperature, although the cutting arm was cooled to liquid nitrogen temperature. Thin sections of standard material were prepared with tannic acid according to the technique of Simionescu and Simionescu (50). Sections were post-stained with uranyl acetate (20 min) and lead citrate (2 min).

Radioactive Labeling

Sperm were incubated under sterile oil at 37°C in Ca^{2+}-free TS containing 1 mg/ml glucose and 2 mg/ml BSA and supplemented with 1 MCi/ml ^{32}P-labeled inorganic phosphate. Motile sperm were collected after 30 min and after 24 h, and lipid extraction was conducted as detailed below. Additionally, protease incubation was performed as above, but also in the presence of 1 mCi/ml $^{32}PO_4$ with subsequent lipid extraction.

Liposomes

Liposomes were prepared and treated as we have previously reported (1). These liposomes consisted of equimolar ratios of egg phosphatidyl choline and bovine heart cardiolipin (Avanti, Birmingham, Ala.).

Lipid Extraction and Separation

Lipids were extracted from sonicated sperm in TS with chloroform: methanol. After filtration of the lower phase through glass wool, the solvent was evaporated under nitrogen at 35°C. The yellowish deposit was resuspended in dichloromethane and applied to silica gel G250 (Merck AG, Darmstadt, West Germany), along with lipid standards supplied by Dr. Papahadjopoulos (Cancer Research Institute, University of California School of Medicine, San Francisco). The plate was developed in chloroform:acetone:methanol:acetic acid:water (6:8:2:2:1 v/v). Following determination of the presence of ninhydrin-stainable and sulfuric-acid-burnable material, plates of radioactively labeled sperm lipids were autoradiographed (12 h, 4°C).

OBSERVATIONS

Viewed under the light microscope, freshly removed epididymal or vasal sperm were freely motile; more than 90% retained the acrosome upon air-drying and staining for light microscopy. After 24-26 h of incubation at 37^{o}C in calcium-free Tyrode's solution, the acrosome reaction was triggered in 60-80% of the cells (Figs. 2 and 3) by the addition of calcium to motile sperm cultures.

Fresh guinea-pig sperm revealed smooth expanses of plasma membrane when examined in freeze-fracture replicas (Fig. 4). After treatment with the anionic-lipid-binding agent PXB, however, the distal acrosomal cap became crenulated; while the proximal cap membrane retained the flat aspect of untreated sperm (Figs. 5 and 7).

Keyhole limpet hemocyanin conjugated to PXB rendered the antibiotic visible in surface replicas (Fig. 6), disclosing PXB binding to the same regions of membrane which appeared crenulated or bubbled in fractured specimens.

Incubation of the sperm in capacitating media increased the extent of PXB disturbance (Fig. 8). Whereas the distal acrosomal cap was perturbed in both fresh and capacitated sperm, the proximal membrane, free of PXB damage before incubation, became susceptible to the antibiotic only after incubation in capacitating medium, thus making it competent to undergo fusion (cf. Figs. 7 and 8). Yet this enhancement in sensitivity did not encroach upon a band of membrane fronting the tip of the

nucleus, even when the bilayer on either side of the tract crenulated. In both fresh and capacitated sperm, round maculae barren of intramembranous particles (IMP) frequently punctuated this undisturbed band (19). These circles, too, remained unaffected by PXB (Fig. 8) or the sterol-binding agent filipin. In tannic-acid-stained thin sections, a density lay between this area of the outer leaflet of the granule membrane and the PXB-resistant plasma membrane (Fig. 9). Neither the equatorial segment nor the post-acrosomal region of the plasmalemma -- areas of non-fusigenic membrane uninvolved in acrosomal granule exocytosis -- had any PXB affinity, either before or after capacitation (Figs. 10 and 11). Again these PXB-resistant areas displayed a thick density beneath the post-acrosomal membrane in thin sections (Fig. 12). Intramembranous-particle-free maculae in front of the tip of the nucleus (Fig. 13), as well as those just subjacent to the equatorial zone, were undisturbed by filipin or PXB (Figs. 14 and 15).

Tannic-acid staining of sperm from the cauda of the epididymis or vas deferens revealed a dense extracellular material with a periodicity of 200 A lying over the acrosomal caps of fresh spermatozoa (Fig. 9) and diminishing after incubation in capacitating media (21). This "coat" was also visible in our surface replicas of unwashed sperm freshly removed from the cauda or vas (Fig. 16). Occupying large plaques on the membrane, the coat manifested the same 200 A periodicity as that of the quilt (22), embossed on the inner face of the bilayer in freeze-fracture preparations (Fig. 21 shows the quilt accentuated by filipin treatment). Neither corpus epididymal sperm nor any of the incubated sperm, exhibited

this structure (Figs. 17-20). Instead, incubation for 30 min in TS alone or in TS-protease produced a filigree design in the surface components which apparently lie beneath the quilt (Figs. 18 and 19). In contrast, fresh corpus epididymal sperm had rough yet regular surfaces but no quilt (Fig. 17). And capacitated sperm exposed surface designs ranging from rough, through filigreed, to smooth (Fig. 20). Sperm which remained in stacks throughout the 24 h incubation even retained vestiges of the quilt.

To determine the effect of these coats on PXB binding, we attempted to remove them with proteinase. However, the plaques of the quilt disappeared in 30 min without the enzyme, and the "subcoat" diminished in both treated and untreated sperm equally. But proteinase did accelerate functional capacitation, so that after a 30 min incubation with enzyme, 60% of the acrosomes were lost within 20 min subsequent to the addition of calcium. In comparison, less than 20% of the acrosomes reacted when calcium was added to sperm incubated without enzyme for 30 min.

Preincubation in the crude protease extract also influenced the binding of PXB, but not that of filipin. The binding of the latter antibiotic over the acrosomal caps of protease-treated sperm was identical to that of TS-incubated control preparations, but differed radically from the polyene/sterol distribution in unwashed sperm (Figs. 21 and 22). After 30 min, regardless of the presence of enzymes, spermatozoa resembled fully capacitated cells in respect to the loss of the quilt pattern and the increased number of sterol/filipin complexes in comparison

to those of fresh sperm: complexes now covered the entire acrosomal cap. That capacitation enhances filipin binding has already been reported (20).

Whereas filipin binding demonstrated no disparity between fusionally competent and fusionally incompetent cells, PXB was dramatically augmented in the fusionally competent cell, whether protease-treated or capacitated by standard incubation (Figs. 23 and 24). In contrast, 30 min incubation without enzymes produced no elevation in PXB binding.

Protease failed to enhance either PXB or filipin perturbations in areas of membrane normally unaffected by these agents (Fig. 24). The equatorial segment, the post-acrosomal membrane, and the band at the tip of the nucleus remained smooth after treatment. Circular clearings of IMP and filipin/sterol complexes were more prevalent in protease-treated sperm, but also appeared in the non-treated cells. Like the post-acrosomal segment, these barren maculae remained free from polyene or antibiotic assault, even after proteolysis. A summary comparing the effects of filipin and PXB on fresh, capacitated, protease-treated, and briefly TS-incubated sperm is given in Table I.

To identify the anionic phospholipid responsible for the increased binding of PXB during capacitation, we incubated sperm in TS containing ^{32}P-labeled phosphate. Thin-layer chromatographic (TLC) separation of the chloroform:methanol lipid extract and subsequent autoradiography of the TLC plate revealed a dark band comigrating with phosphatidic acid

(PA) and with cardiolipin, as well as some radioactivity over other lipid fractions (Fig. 25B). Sperm incubated for 30 min in $^{32}PO_4$-supplemented TS, with or without protease showed only one, slightly radioactive band again co-migrating with PA and cardiolipin (Fig. 25A). When liposomes composed of equimolar ratios of PC and cardio lipin were treated with PXB, they exhibited vermiform protrusions and rivulets (Figs. 26 and 27). Such protrusions were reminiscent of those mediated by PXB in the capacitated spermatozoan proximal acrosomal-cap membrane.

DISCUSSION

We interpret this diversity in PXB binding as indicative that anionic lipids in the external half of the plasma-membrane bilayer are restricted to the fusigenic acrosomal-cap region, since they are undetectible in the adjacent but stable post-acrosomal segment. Furthermore, the enhanced PXB binding over the fusigenic area following proteolysis or capacitation suggests that these procedures make more anionic lipid accessible to the probe. Internal organelle membranes do not crenulate when PXB is in the bathing media -- supporting the view that the antibiotic does not readily penetrate lipid bilayers. Anionic lipid, therefore, must be exposed on the outer leaflet to be attacked by PXB. "Flip-flop" of lipid from the cytoplasmic to the external leaflet could thus explain the enhanced labeling following capacitation or proteolysis. Very rarely is the principal piece perturbed by PXB (1). Again, the inability of PXB to pass through the bilayer may account for this, since only those tails with broken membranes would be affected if the anionic lipid resided primarily on the cytoplasmic leaflet, as has been

advocated for other cells (8).

In fresh or capacitated sperm, three foci within the plasmalemma of the head fail to crenulate in the presence of the probe: the band at the tip of the nucleus, the equatorial segment, and the near-by post-acrosomal segment. The distribution of hemocyanin-conjugated PXB in surface replicas parallels that of the protuberances in freeze-fractured preparations, supporting the conclusion that alterations in membrane contour correlate with binding. Hence this lack of crenulation indicates that decreased binding probably reflects a relative paucity of anionic lipids (although other explanations may also apply). The capacity of the probe to detect anionic lipids may be influenced by such factors as: (a) membrane lipids in the gel state may have a lower affinity for lipid-binding agents; (b) peripheral proteins, which can induce the gel state, (3) may also restrict the insertion of probes into the bilayer or prevent the probe from reaching the lipid; (c) positive surface charges may repulse cationic molecules such as PXB; and bound calcium, which competitively inhibits PXB binding (25, 33), may occupy binding sites.

Of the three foci that fail to bind PXB, the post-acrosomal segment is presumably less fluid than the acrosomal-cap region. When human spermatozoa are exposed to anilinonaphthalene sulfate (34), or guinea-pig sperm to merocyanine S 540 (2) -- agents known to partition into liquid crystalline but not gel lipid bilayers (48) -- fluorescence is observed in the acrosomal cap, yet is absent in the post-acrosomal membrane. However, a less fluid state of the lipid bilayer is not

likely to affect PXB binding, since protrusions have been reported in liposomes incubated with PXB below their transitional temperatures (1, 51). Moreover, decreased fluidity may contribute to the maintenance of these lipid domains by depressing the lateral diffusion rate of anionic lipids from adjacent areas. Conversely, the gel state could be a result of a peripheral-protein-mediated inhibition of lateral mobility. Structures suggestive of peripheral proteins or glycoconjugates appear on both sides of these membrane sites in thin sections: Cytoplasmic densities underlie the plasmalemma; and a thick extracellular coating can be discerned as well. That external peripheral proteins do not prohibit PXB from approaching the post-acrosomal membrane is demonstrated by the inability of protease to increase PXB binding in this segment. In view of the function of the post-acrosomal membrane at this stage of the spermatozoan life-span -- i.e., to remain stable during acrosomal exocytosis -- it would be expected to be less fluid and to contain little if any anionic lipid, as either condition would render it labile. It is not until after the acrosome reaction that this membrane acquires its ability to fuse with the egg (3, 4, 11).

Calcium may be culpable in the inhibition of binding at the tip of the nucleus. Puroantimonate, which precipitates where divalent cationic metals are present in high concentrations, is deposited in this band (20), and calmodulin is localized there, as demonstrated by antibody-specificity and Stalazine^{R} binding (30, 39). Because calcium competitively inhibits PXB binding (25, 33), its presence could readily explain the dearth of protuberances here. Finally, it is doubtful that charge-

charge repulsion plays a role in obstructing PXB, since it does not prevent colloidal iron hydroxide (18, 57) from attaching to these membrane regions.

IMP Clearings

Circular clearings of intramembranous particles have been described in various other fusional systems, such as frog neuromuscular junctions, pancreatic islet cells and Phytophthora p. zoospores (10, 42, 46). It has been argued that these maculae are artifactually produced by either glutaraldehyde or glycol, for they were not seen in freeze-fracture images of quick-frozen mast cells (12). Nevertheless, we have observed these clearings in the cytoplasmic droplet of quick-frozen sperm, neither fixed nor cryoprotected (22). In the present study, we report IMP clearings in traditionally fixed and cryoprotected sperm membranes. They appeared at two sites on the head: in the band fronting the tip of the nucleus, where (we presume) the acrosomal granule first begins to fuse with the plasma membrane; and in the post-acrosomal segment near the equatorial region, where sperm:egg fusion ultimately occurs (4, 11). While the latter clearings were present regardless of the capacitation status of the membrane, those near the tip of the nucleus became evident only after the quilt pattern melted -- that is, within half an hour of incubation in capacitating medium. Both areas of membrane manifested densities on the cytoplasmic surface, and neither group of maculae was susceptible to PXB or filipin attack. In addition, the clearings were still extant after protease digestion, indicating that polypeptide moieties exposed to the outer milieu were not involved in their maintenance. These clearings appeared in regions of membrane where fusion

takes place. However, since they were present in membrane before it attained fusional competence, they were therefore unable to induce such fusion by themselves.

Effects of Crude Trypsin Extract on the Incidence of the Acrosome Reaction, Surface Coat, and Lipid Topography

Protease incubation mimics capacitation by increasing both the incidence of the acrosome reaction and the anionic-lipid concentration in the fusional membrane, leaving surface appearance and sterol distribution unchanged. Neither trypsin nor chymotrypsin used separately can accelerate capacitation, although pronase can (56). A common component of the crude bovine pancreatic extract we used was β-amylase (13), which has been purported to facilitate capacitation (29, 31).

Although it could expedite functional capacitation, the crude extract was incapable of altering the normal morphological maturation of the spermatozoan surface. That the surface coat is modified both during transit through the epididymis and after *in vitro* or *in vivo* capacitation is demonstrable by differences in lectin agglutination (53) and binding (24, 49); in antigenic determinants (37); and in surface charge as measured by the electrophoretic mobility of whole sperm (38) or by surface affinity for charged colloidal iron (18, 57). In the course of passage through the cauda of the epididymis in the rat, a highly glycosylated secretory product adheres to the sperm and masks previously accessible surface components from radioiodination (41); while the heads of both rat and rabbit sperm increase in affinity for concanavalin A (24, 40). The coat probably corresponds to the quilted plaques described

here, since they, too, cannot be detected in earlier maturational stages and disappear rapidly upon incubation.

Antibody agglutination (53) and elegant fluorescence microscopy (49) have revealed that some lectin receptors increase in abundance following capacitation of guinea-pig sperm -- perhaps because they are unveiled by the loss of the coat (24); whereas others decrease. It is likely that the rough mat draping the acrosomal caps of all sperm shown here, although overlain by the quilted plaques in caudal specimens, represents an architectural counterpart to the lectin receptors and antigenic sites that are masked by the epididymal secretory product. The mat peels more slowly than the quilt and remains extant in a large proportion of sperm which have been incubated for 24 h in capacitating media, and thus are capable of granule exocytosis as well as PXB binding throughout the region covered by the mat. This attests to the mat's inability to prevent the acrosome reaction or to maintain lipid boundaries.

Like the quilt, the mat does not participate in restricting the access of either probe to the membrane. The quilt, however, may presumably inhibit filipin binding and contribute to patchy PXB binding over the distal acrosomal cap. But it has been lost long before PXB-induced crenulations invade the proximal acrosomal cap, strengthening the theory that the quilt is also incapable of maintaining lipid domains.

Enzyme treatment had no effect on the low binding-level of either probe to the post-acrosomal segment. This further validates the conclu-

sion that hydrolyzable surface components do not limit the entry of probes to the membrane or preserve lipid boundaries. Enzymatic extension of PXB binding could be due to the digestion of integral membrane components that control either lipid flow from the distal to the proximal acrosomal cap or the rate of flip-flop from the inner to the outer plasma-membrane leaflets.

Radioactive Phosphate Incorporation

Since the spermatozoon lacks rough endoplasmic reticulum (RER), it was surprising that our preparations could incorporate radioactive phosphate into phospholipids. A slight enhancement of cardiolipin has been reported during capacitation of porcine sperm (16); but this lipid may be synthesized in mitochondria, which contain the largest amounts (27). The synthesis of the other phospholipids has only been conclusively demonstrated in endoplasmic reticulum. However, the presence of just PA and cardiolipin in brief incubations suggests that the synthesis we observed was following the established pathway, which begins with PA.

Protease greatly enhanced PXB-susceptibility, but did not qualitatively change the synthesis of PA or cardiolipin. Because our methods of extraction removed lipid from all of the sperm membranes, it was impossible to ascertain the source of these lipids. Both PA and cardiolipin have been isolated as a small percentage of plasma-membrane lipid in diverse cells (27), although cardiolipin primarily inhabits mitochondrial membranes. Polymyxin B, however, forms volcanic lesions in liposomes composed of PA (25), while cardiolipin vesicles respond to PXB with vermiform protrusions -- also common in capacitated sperm membranes.

Cardiolipin synthesis occurs in 30-min TS-incubated sperm without the addition of protease and without elevation of PXB binding. Thus, an increased rate of anionic-lipid flip-flop outward across the bilayer could account for the enhanced PXB-binding following protease digestion. The inner leaflet, though, may replace its anionic lipid via the synthesis noted here.

Yet is is not unexpected that cardiolipin should contribute to cellular fusional events. Using model lipid systems (14), biophysicists have proposed a possible function for this lipid in fusion. By ^{32}P nuclear magnetic resonance, X-ray diffraction, and freeze-fracture electronmicroscopy, cardiolipin has been observed to form hexagonal arrays at high temperatures or upon the addition of calcium to the suspension (14). These arrays seem particularly attractive in the role of bilayer "destabilizing centers" for the initiation of membrane:membrane fusion. The tiny pores encountered in quick-frozen mast cells during exocytosis correlate with a theoretical model of one small, perpendicularly oriented, rod-like, lipid channel.

CONCLUSIONS

1) Polymyxin B, a cytochemical probe of anionic phospholipids, revealed a concentration of these lipids in fusigenic parts of the spermatozoan plasma membrane, and a paucity in neighboring but stable domains.

2) As the membrane prepares for the actual fusional event -- i.e., the acrosome reaction -- anionic-lipid concentration increases in fusional areas of the membrane. These lipid domains, therefore, are dynamic and

form in response to cellular activity.

3) Crude trypsin extract can augment anionic-lipid concentrations in fusional membrane domains, but not in other regions. Nor does the protease affect β-OH sterol distribution as determined by filipin.

4) Cell-surface structures do not maintain these lipid domains. The disappearance of the quilt is not sufficient to promote fusion, while the underlying mat remains throughout capacitation.

5) During incubation in capacitating media, spermatozoa incorporate radioactive phosphate into cardiolipin, PA, and other phospholipids.

6) Protease does not qualitatively affect the early stages of $^{32}PO_4$ incorporation into PA and/or cardiolipin.

7) Hence both the synthesis of anionic lipids and their "flip-flop" from interior to exterior plasma-membrane leaflets may be participants in the sequential events leading to capacitation.

This study was supported by U. S. Public Health Service Grants GM 07618-Martin to Ms. Bearer, a Medical Scientist Training Program student, and HD 10445 to Dr. Friend. We thank Irene Rudolf, Chris Havel, and Yvonne Jacques for superb technical assistance, and Rosamond Michael for her invaluable editing.

REFERENCES

1. Bearer, E. L., and D. S. Friend. 1980. Anionic lipid domains: correlation with functional topography in a mammalian cell membrane. Proc. Natl. Acad. Sci. U.S.A. 77:6601-6605.
2. Bearer, E. L., and D. S. Friend. 1981. Maintenance of lipid domains in the guinea-pig sperm membrane. J. Cell Biol. 91: 266a (Abstr).
3. Bedford, J. M., and G. W. Cooper. 1978. Membrane fusion events in the fertilization of vertebrate eggs. In: Membrane Fusion. G. Poste and G. L. Nicolson, editors. Elsevier North-Holland Biochemical Press. 65-125.
4. Bedford, J. M., H. D. M. Moore, and L. E. Franklin. 1979. Significance of the equatorial segment of the acrosome of the spermatozoon in euthenium mammals. Exp. Cell Res. 119:119-126.
5. Birrell, B. G., and O. H. Griffith. 1976. Cytochrome C induced lateral phase separation in a diphosphatidylglycerol-steroid spin-label model membrane. Biochemistry 15:2925-2929.
6. Bradford, M. M. 1976. A rapid and sensitive method for the quantitation of microgram quantities of protein utilizing the principle of protein-dye binding. Anal. Biochem 72:248-254.
7. Bradley, M. P., D. G. Ryans, and I. T. Forrester. 1980. Effects of filipin, digitonin, and polymyxin B on plasma membrane of ram spermatozoa -- an em study. Arch. Androl. 4:195-204.
8. Bretscher, M. S. 1973. Membrane structure: some general principles. Science (Wash. D. C.) 181:622-629.

9. Bryan, J. H. D., and S. R. Akruk. 1977. A naphthol yellow S and erythrosin B staining procedure for use in studies of the acrosome reaction of rabbit spermatozoa. Stain Technol. 52:47-51.

10. Ceccarelli, B., F. Grohavez, and W. P. Hurlbut. 1979. Freeze-fracture studies of frog neuromuscular junctions during intense release of neurotransmitter. I. Effects of black widow spider venom and Ca^{++}-free solutions on the structure of active zones. J. Cell Biol. 81:163-177.

11. Chacon, R. S., and P. Talbot. 1980. Early stages in mammalian sperm-oocyte plasma membrane fusion. J. Cell Biol. 87:131a (Abstr).

12. Chandler, D. E., and J. E. Heuser. 1980. Arrest of membrane fusion events in mast cells by quick freezing. J. Cell Biol. 86: 666-674.

13. "Chymotrypsin"; protease. 1972. In: Worthington Enzyme Manual. Worthington Biochemical Corp., Freehold, N. J. pp. 128-130.

14. Cullis, P. R., and B. DeKruijff. 1979. Lipid polymorphism and the functional roles of lipids in biological membranes. Biochim. Biophys. Acta. 559:399-420.

15. Elias, P. M., D. S. Friend, and J. Goerke. 1979. Membrane sterol heterogeneity. Freeze-fracture detection with saponins and filipin. J. Histochem. Cytochem. 27:1247-1260.

16. Evans, R. W., D. E. Weaver, and E. D. Clegg. 1980. Diacyl, alkenyl, and alkyl ether phospholipids in ejaculated, in utero-, and in vitro incubated porcine spermatozoa. J. Lipid Res. 21: 223-228.

17. Fambrough, D. M. 1979. Control of acetylcholine receptor in skeletal muscle. Physiol. Rev. 59 (1):165-227.

18. Flechon, J. E., and J. Morstin. 1975. Localisation des glycoproteines et des charges negatives et positives dans le revetement de surface des spermatozoides ejacules de lapin et de taureau. Ann. Histochim. 20:291-300.

19. Friend, D. S. 1980. Freeze-fracture alterations in guinea-pig sperm membranes preceding gamete fusion. In: Membrane-Membrane Interactions. N. B. Gilula, editor. Raven Press, New York. pp. 153-165.

20. Friend, D. S., and E. L. Bearer. 1981. β-hydroxysterol distribution as determined by freeze-fracture cytochemistry. Histochem. J. 13:535-546.

21. Friend, D. S., and D. W. Fawcett. 1974. Membrane differentiations in freeze-fractured mammalian sperm. J. Cell Biol. 63: 641-664.

22. Friend, D. S., and J. E. Heuser. 1981. Orderly particle arrays on the mitochondrial outer membrane in rapidly-frozen sperm. Anat. Rec. 199:159-175.

23. Friend, D. S., L. Orci, A. Perrelet, and R. Yanagimachi. 1977. Membrane particle changes attending the acrosome reaction in guinea-pig spermatozoa. J. Cell Biol. 74:561-577.

24. Gordon, M., P. V. Dandekar, and W. Bartoszewicz. 1975. The surface coat of epididymal, ejaculated and capacitated sperm. J. Ultrastruct. Res. 50:199-207.

25. Hartmann, W., H. -J. Galla, and E. Sackmann. 1978. Polymyxin binding to charged lipid membranes -- an example of cooperative lipid-protein interaction. Biochim. Biophys. Acta. 510:124-139.

26. Hirao, Y., and R. Yanagimachi. 1978. Effects of various enzymes on the ability of hamster egg plasma membranes to fuse with spermatozoa. Gamete Res. 1:3-12.

27. Ioannou, P. V., and B. T. Golding. 1979. Cardiolipins: their chemistry and biochemistry. Progr. Lipid Res. 17:279-318.

28. Jan, L. Y., and J. -P. Revel. 1975. Hemocyanin-antibody labeling of rhodopsin in mouse retina for a scanning electron microscope study. J. Supramol. Struct. 3:61-66.

29. Johnson, W. L., and A. G. Hunter. 1972. Seminal antigens: Their alteration in the genital tract of female rabbits and partial in vitro capacitation with β-amylase and β-glucuronidase. Biol. Reprod. 7:332-340.

30. Jones, H. P., R. W. Lenz, B. A Palevitz, and M. J. Cormier. 1980. Calmodulin localization in mammalian spermatozoa. Proc. Natl. Acad. Sci. U.S.A. 77:2772-2776.

31. Kirton, K. T., and H. D. Hafs. 1965. Sperm capacitation by a uterine fluid or β-amylase in vitro Science (Wash., D. C.) 150: 618-619.

32. Lee, A. G. 1977. Lipid phase transitions and phase diagrams. I. Lipid phase transitions. Biochim. Biophys. Acta. 472:237-281.

33. Mashak, El E. M., and J. F. Tocanne. 1980. Polymyxin B phosphatidylglycerol interactions -- a monolayer $\pi,\Delta\nu$ study. Biochim. Biophys. Acta. 596:164-179.

34. Mercado, E., and A. Rosado. 1972. Structural properties of the membrane of intact human spermatozoa. Biochim. Biophys. Acta. 298:639-652.

35. Mills, J. W., A. D. C. MacKnight, J. A. Jarrell, J. M. Dayer, and D. A. Ausiello. 1981. Interaction of oubain with the Na^+ pump in intact epithelial cells. J. Cell Biol. 88:637-643.

36. Montesano, R., P. Vassalli, A. Perrelet, and L. Orci. 1980. Distribution of filipin-cholesterol complexes at sites of exocytosis -- a freeze-fracture study of degranulating mast cells. Cell Biol. Int. Reports 4:975-984.

37. Myles, D. G., P. Primakoff, and A. R. Bellve. 1981. Surface domains of the guinea-pig sperm defined with monoclonal antibodies. Cell 23:433-439.

38. Nevo, A. C., I Michaeli, and H. Schindler. 1961. Electrophoretic properties of bull and rabbit spermatozoa. Exp. Cell Res. 23:69-83.

39. O'Kane, D. J., R. W. Lenz, F. W. Schmidt, B. A. Palevitz, and M. J. Cormier. 1980. Binding of photooxidized stelazine derivatives to calmodulin. J. Cell Biol. 87:199a (Abstr.).

40. Olson, G. E., and G. J. Danzo. 1981. Surface changes in rat spermatozoa during epididymal transit. Biol. Reprod. 24:431-443.

41. Olson, G. W., and D. W. Hamilton. 1978. Characterization of the surface glycoproteins of rat spermatozoa. Biol. Reprod. 19: 26-35.

42. Orci, L., A. Perrelet, and D. S. Friend. 1977. Freeze-fracture of membrane fusions during exocytosis in pancreatic islet cells. J. Cell Biol. 75:23-30.

43. Papahadjopoulos, D. 1968. Surface properties of acidic phospholipids: interactions of monolayers and hydrated liquid crystals with uni- and bi-valent metal ions. Biochim. Biophys. Acta. 163: 240-254.

44. Papahadjopoulos, D. 1978. Calcium-induced phase changes and fusion in natural and model membranes. In: Membrane Fusion. G. Poste and G. L. Nicolson, editors, Elsevier/North-Holland Biomedical Press. pp. 765-790.

45. Phillips, D.M. 1977. Surface of the equatorial segment of the mammalian acrosome. Biol. Reprod. 16:128-137.

46. Pinto da Silva, P., and M. L. Nogueira. 1977. Membrane fusion during secretion. A hypothesis based on electron microscope observations of Phytophthora palmivora zoospores during encystment. J. Cell Biol. 73:161-181.

47. Robinson, J. M., and M. J. Karnovsky. 1980. Specializations in filopodial membranes at points of attachment to the substrate. J. Cell Biol. 87:562-568.

48. Schlegel, R. A., B. M. Phelps, A. Waggoner, L. Terada, and P. Williamson. 1980. Binding of merocyanine 540 to normal and leukemic erythroid cells. Cell 20:321-328.

49. Schwarz, M. A., and J. K. Koehler. 1979. Alterations in lectin binding to guinea-pig spermatozoa accompanying in vitro capacitation and the acrosome reaction. Biol. Reprod. 21:1295-1307.

50. Simionescu, N., and M. Simionescu. 1976. Galloyl-glucoses of low molecular weight as mordents in electron microscopy. I. J. Cell Biol. 70:608-621.

51. Sixl, F., and J. -J. Galla. 1979. Cooperative lipid protein interaction. Effect of pH and ionic strength on polymyxin binding to phosphatidic acid membranes. Biochim. Biophys. Acta. 557: 320-330.

52. Storm, D. R., K. S. Rosenthal, and P. E. Swanson. 1977. Polymyxin and related peptide antibiotics. Annu. Rev. Biochim. 46: 723-763.

53. Talbot, P., and L. E. Franklin. 1978. Surface modification of guinea-pig sperm during in vitro capacitation: An assessment using lectin-induced agglutination of living sperm. J. Exp. Zool. 203:1-13.

54. Teuber, M., and I. R. Miller. 1977. Selective binding of polymyxin B to negatively charged lipid monolayers. Biochim. Biophys. Acta 467:280-289.

55. White, J., and A. Helenius. 1980. pH-dependent fusion between the Semliki forest virus membrane and liposomes. Proc. Natl. Acad. Sci. U.S.A. 77:3273-3277.

56. Yanagimachi, R. 1975. Acceleration of the acrosome reaction and activation of guinea-pig spermatozoa by detergents and other reagents. Biol. Reprod. 13:519-526.

57. Yanagimachi, R., Y. D. Noda, M. Fujimoto, and G. I. Nicolson. 1972. The distribution of negative surface charges on mammalian spermatozoa. Am. J. Anat. 135:497-520.

58. Yanagimachi, R., and N. Usui. 1974. Calcium dependence of the acrosome reaction and activation of guinea-pig spermatozoa. Exp. Cell Res. 89:161-174.

FIGURE LEGENDS

Figure 1 (a) Diagram of the surface of a guinea-pig sperm; (b) cross-section of the head only, as it appears in thin section.

Figures 2 and 3 Light micrographs of fresh and capacitated sperm.

Figure 2 The acrosomal granules in these fresh sperm were deeply stained. After washing and treatment with Ca^{2+}, they were allowed to dry on the slide and stained with naphthol yellow S and erythro-sin B. X 1,000.

Figure 3 Acrosome-reacted sperm. Capacitated sperm, in contrast, lose the brightly stained granule upon the addition of Ca^{2+}. X 1000.

Figure 4 The smooth contours of a fresh, untreated sperm as observed in conventional freeze-fracture replicas. Note the circular clearing of IMP (arrows) at the tip of the nucleus (t) which delineates the proximal (p) and distal (d) cap. X 36,000.

Figure 5 PXB treatment of fresh sperm creates crenulations in the distal cap. X 24,000.

Figure 6 Hemocyanin-conjugated PXB, as seen in critical-point-dried surface replicas, deposits large globules (arrows) on the distal cap; while the tip of the nucleus and proximal cap are left clean. X 16,000.

Figure 7 A fresh sperm treated with PXB exhibits only a slight dimpling of the proximal cap. The tip of the nucleus is undisturbed. X 24,000.

Figure 8 Drastic perturbations of the membrane cover the acrosomal cap of this capacitated sperm, except for the persistently smooth membrane arching the tip of the nucleus. Unaffected maculae are visible in this smooth band of membrane (arrows). X 45,000.

Figure 9 In a thin section of a fresh sperm, a density (arrow) lines the granule's outer leaflet at the tip of the nucleus (n). Notice the surface coat (arrowhead). X 70,000.

Figures 10, 11, and 12 The equatorial region as a boundary between acrosomal cap and post-acrosomal membrane.

Figure 10 A few protrusions poke through the quilt over the proximal acrosomal-cap (p) membrane of a fresh sperm, but do not penetrate beyond the equatorial segment. X 50,000. Proliferation of disturbance (Figure 11) in this same region of capacitated sperm is also arrested at the end of the equatorial segment. The post-acrosomal (pa) membrane is undisturbed by PXB in both specimens. X 38,000 (shadowed from above).

Figure 12 A density (arrowhead) underlines the cytoplasmic surface of the post-acrosomal plasma membrane of a non-capacitated sperm. X 60,000.

Figure 13 Circular clearings of IMP (arrow), unaffected by PXB, punctuate the also-undisturbed band at the tip of the nucleus (t) in this capacitated PXB-treated sperm. X 54,000.

Figure 14 A capacitated sperm, with macular clearings (arrows) in the post-acrosomal segment, remains unaffected by PXB, which induced perturbations of the adjacent proximal cap. X 36,000.

Figure 15 Filipin attacks the proximal cap of a capacitated sperm heavily, and more lightly affects the post-acrosomal segment; but, like PXB, the polyene leaves the particle-free clearings barren. X 45,000.

SURFACE REPLICAS

Figure 16 Plaques of extracellular material coat the acrosomal cap (a) of unwashed epididymal or vasal sperm, while finger-like projections demarcate the equatorial segment (e). The post-acrosomal surface exhibits no plaques. X 32,000.

Figure 17 Unwashed sperm from the body of the epididymis lack a quilt, but a rough mat drapes the surface of the acrosomal cap (a). X 30,000.

Figure 18 After 30-min TS-incubation, the quilt vanishes and a filigree design appears in the underlying coarse mat covering the cap (a). X 36,000.

Figure 19 Sperm incubated in crude trypsin extract display the same filigreed surfaces as their non-treated counterparts. X 36,000.

Figure 20 After incubation in capacitating media, the spermatozoan surface is polymorphic. Some cells, however, lose the rough mat as well as the quilt, exposing the membrane surface. X 36,000.

Figures 21-24 The effects of trypsinization on filipin and PXB distribution.

Figure 21 Filipin intensifies the quilt design in fresh sperm. X 24,000.

Figure 22 After 30-min trypsinization, filipin/sterol complexes are diffusely dispersed over the whole cap, although the IMP clearings above the tip of the nucleus remain bare (arrows). X 25,000.

Figure 23 Sperm incubated for 30 min in TS have lost the quilt, but the proximal cap membrane (p) is still unaffected by PXB. X 34,000.

Figure 24. Trypsinization produces enhanced susceptibility to PXB over the entire acrosomal cap, particularly in the proximal portion (p), but does not influence the susceptibility of the post-acrosomal membrane (pa). X 50,000.

Figure 25 (A) Autoradiograph of a thin-layer chromatogram of chloroform:methanol lipid extracts of sperm incubated for 30 min in $^{32}PO_4$-supplemented TS containing crude trypsin extract. (B) Autoradiograph of a thin-layer chromatogram of chloroform:methanol lipid extracts from sperm capacitated in a ^{32}P-supplemented medium. The arrowheads indicate co-migration of lipid standards: PC, phosphatidylcholine; PS, phosphatidylserine, PE, phosphatidylethanolamine; PG, phosphatidylglycerol; CL, cardiolipin; PI, phosphatidylinositol; PA, phosphatidic acid.

Figure 26 Phosphatidylcholine-cardiolipin multilamellar vesicles, fixed, glycerinated, and frozen from room temperature. X 34,000.

Figure 27 The same vesicle preparation pre-incubated in PXB. X 25,000.

	Fresh	24-h Incub*	30-min Incub	Protease
% Acro reaction post-Ca^{2+}	10%	60-80%	20%	50-60%
		PXB distribution/filipin distribution		
Distal acro cap	+/+ clustered	++/++	+/++	++/++
Tip of nucleus	-/+	-/++	-/++	-/++
Prox acro cap	-/+ clustered	++/++	-/++	++/++
Pa including ES	-/+	-/+	-/+	-/+
		Presence of surface coat/presence of quilt		
Acro cap	+/+	-/-	peeling/-	peeling/-

TABLE I

* Abbreviations: Incub, Incubation; Acro, Acrosome reaction 20 min post-calcium, acrosomal; Acro cap, acrosomal cap membrane; Prox, proximal; Pa, post-acrosomal region; Es, equatorial segment; +, present; -, absent.

Average of 10 high-power fields (40 X), from 3-5 different experiments.

Intramembranous particle clearings in these regions do not bind either PXB or filipin.

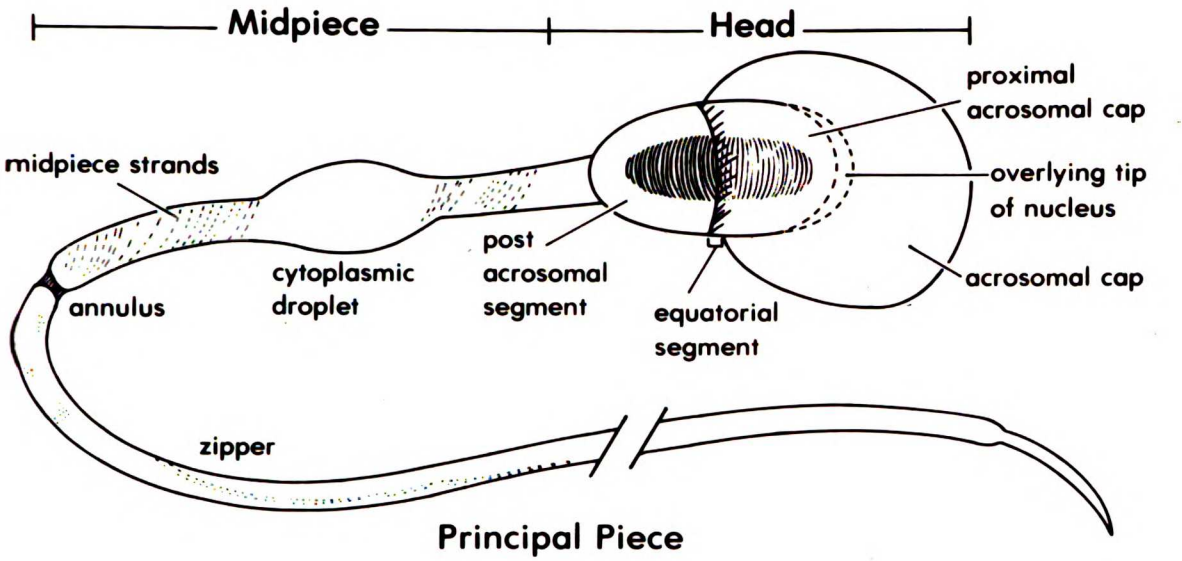

Principal Piece

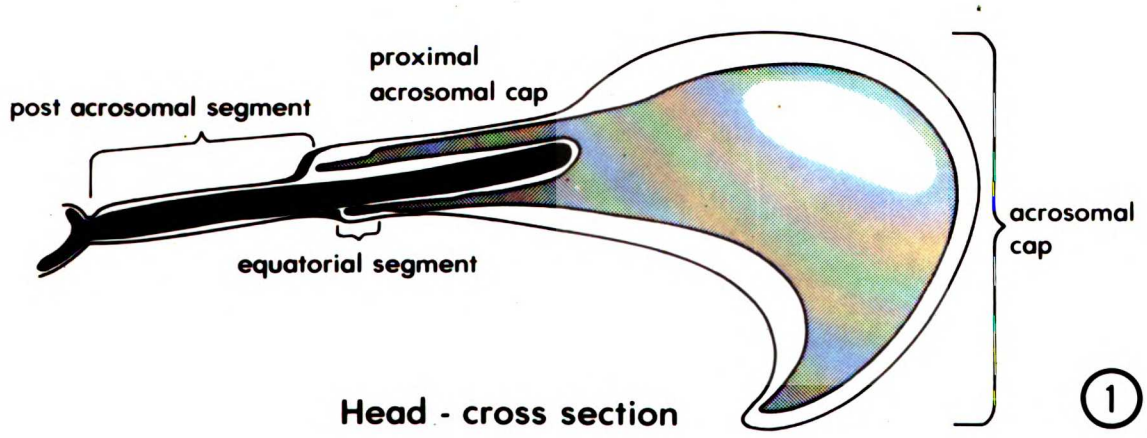

Head - cross section

(1)

(2)

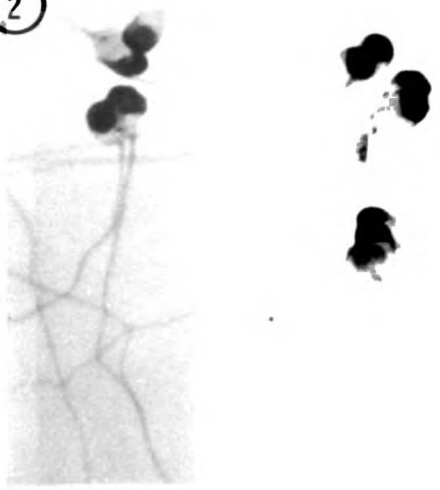

(3)

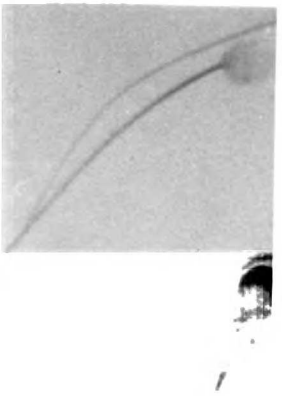

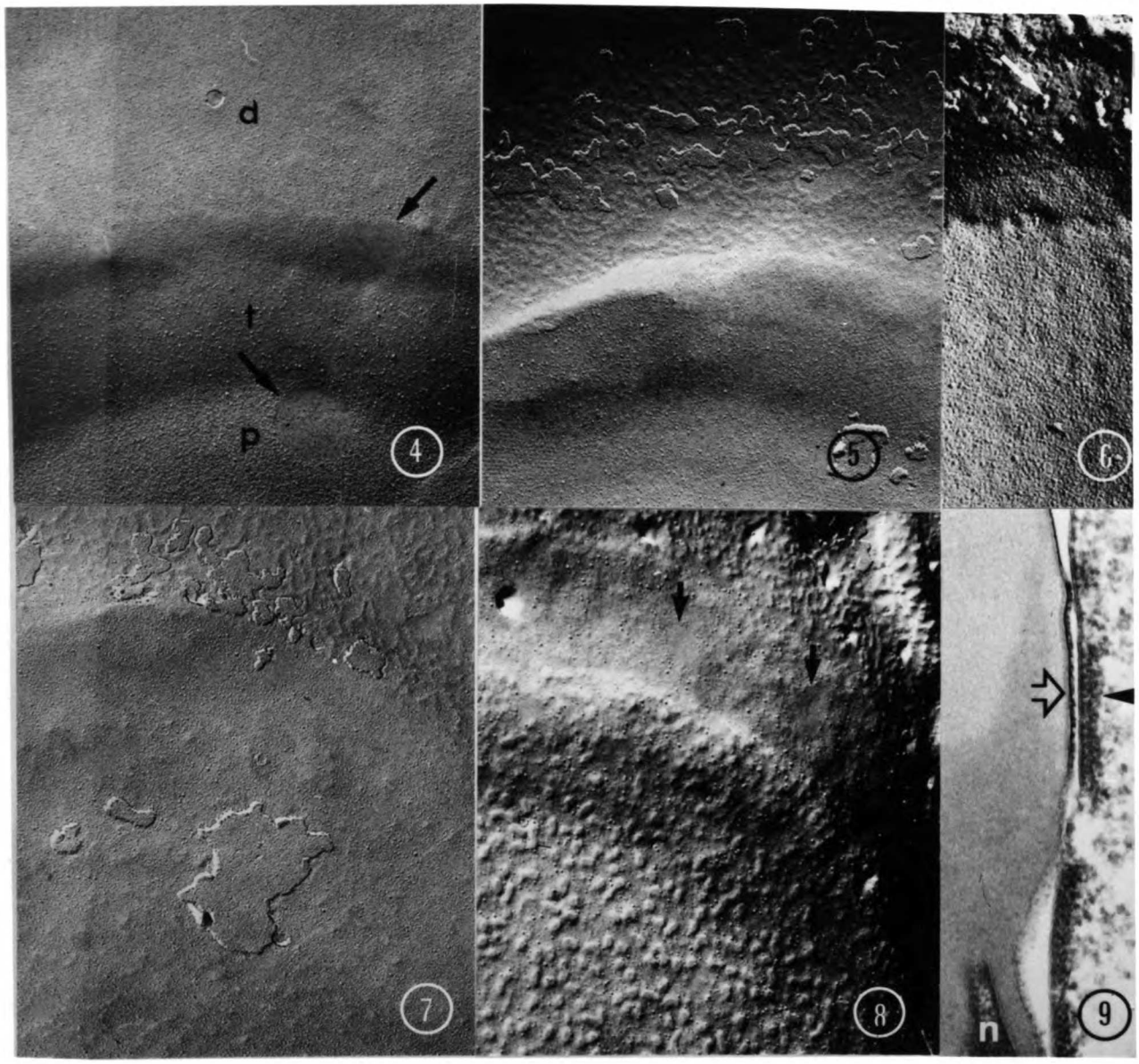
d
t
p
4
5
C
7
8
n
9

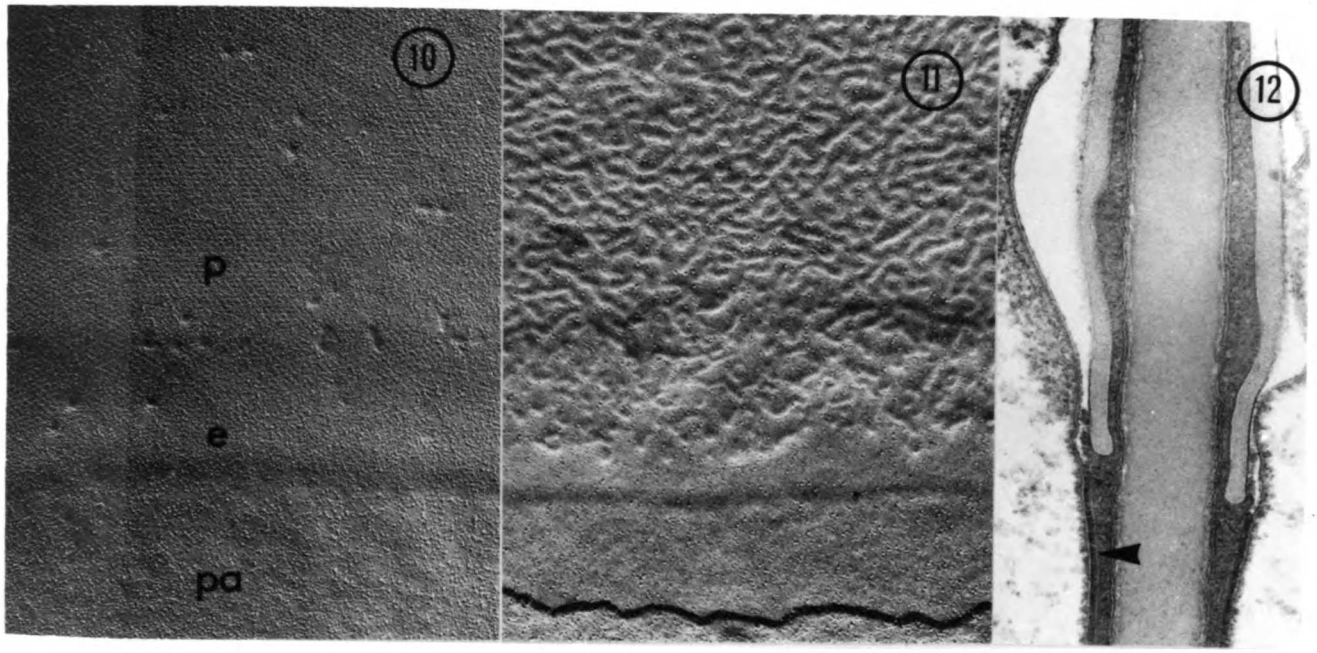
10
p
e
pa
11
12

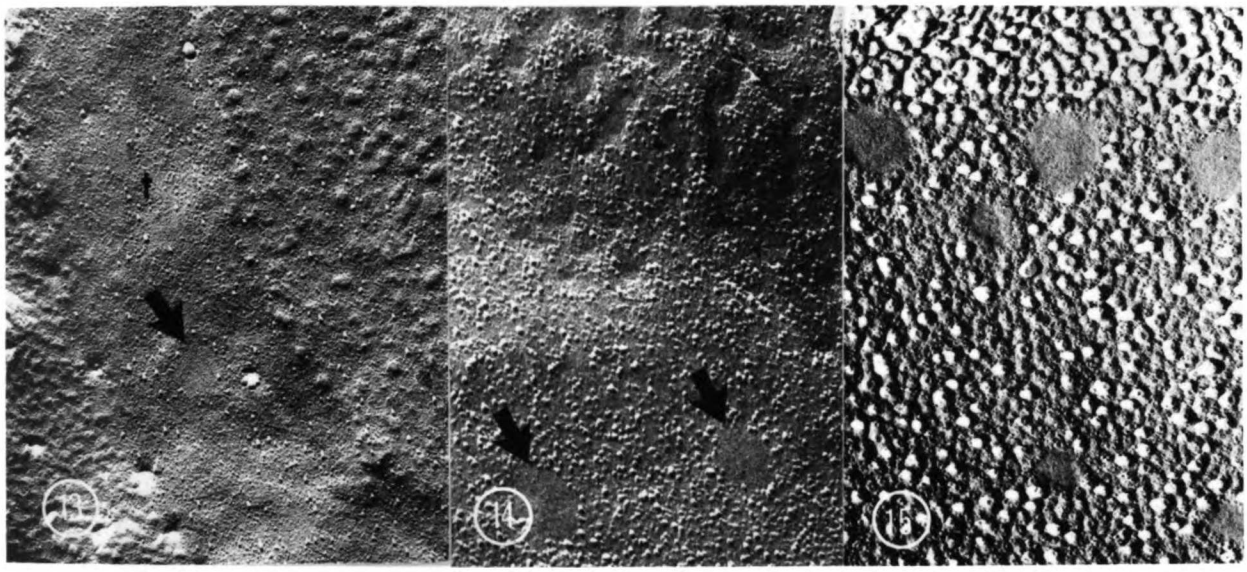
13
14
15

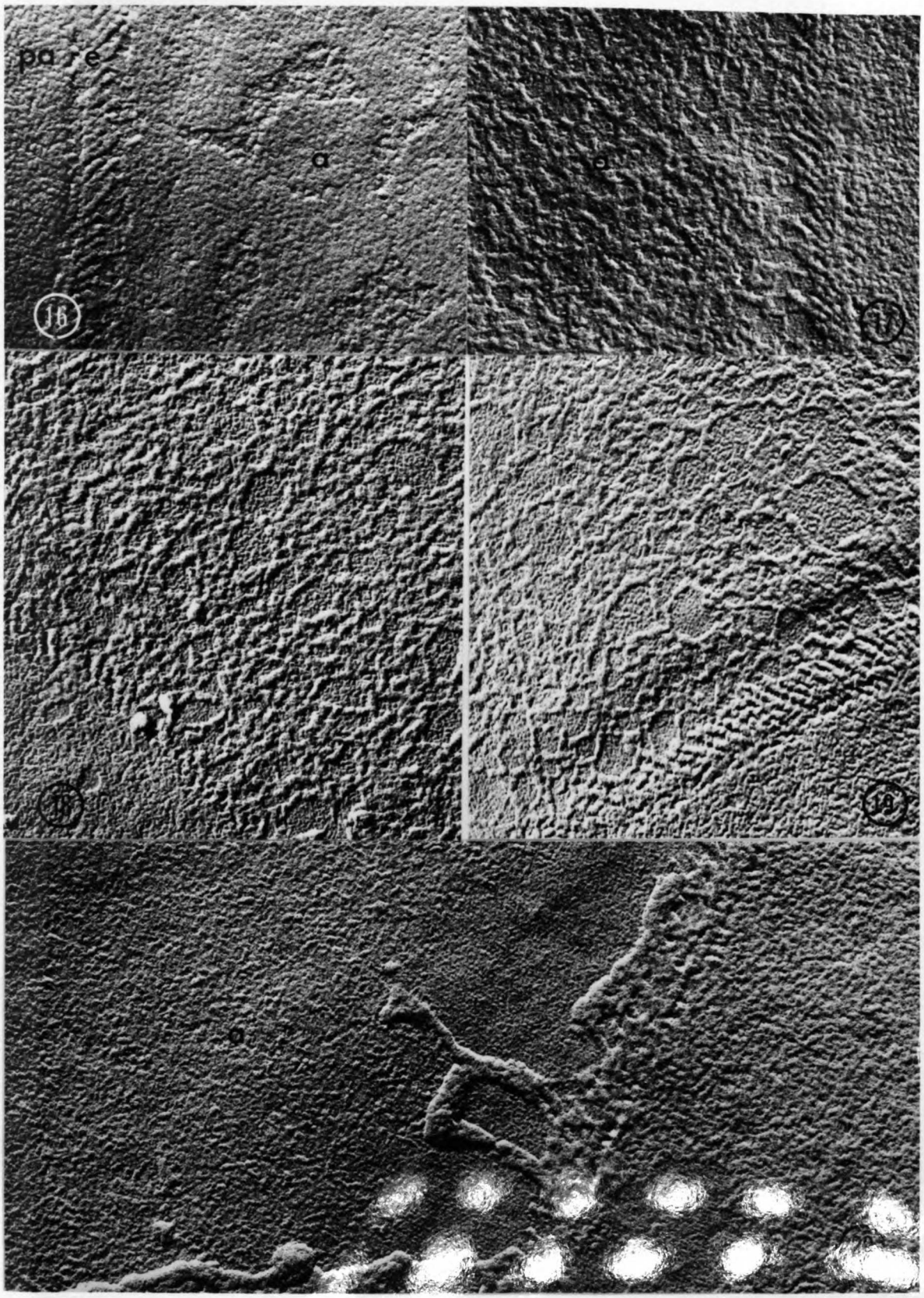
pa
e
a
16
17
18
19
o

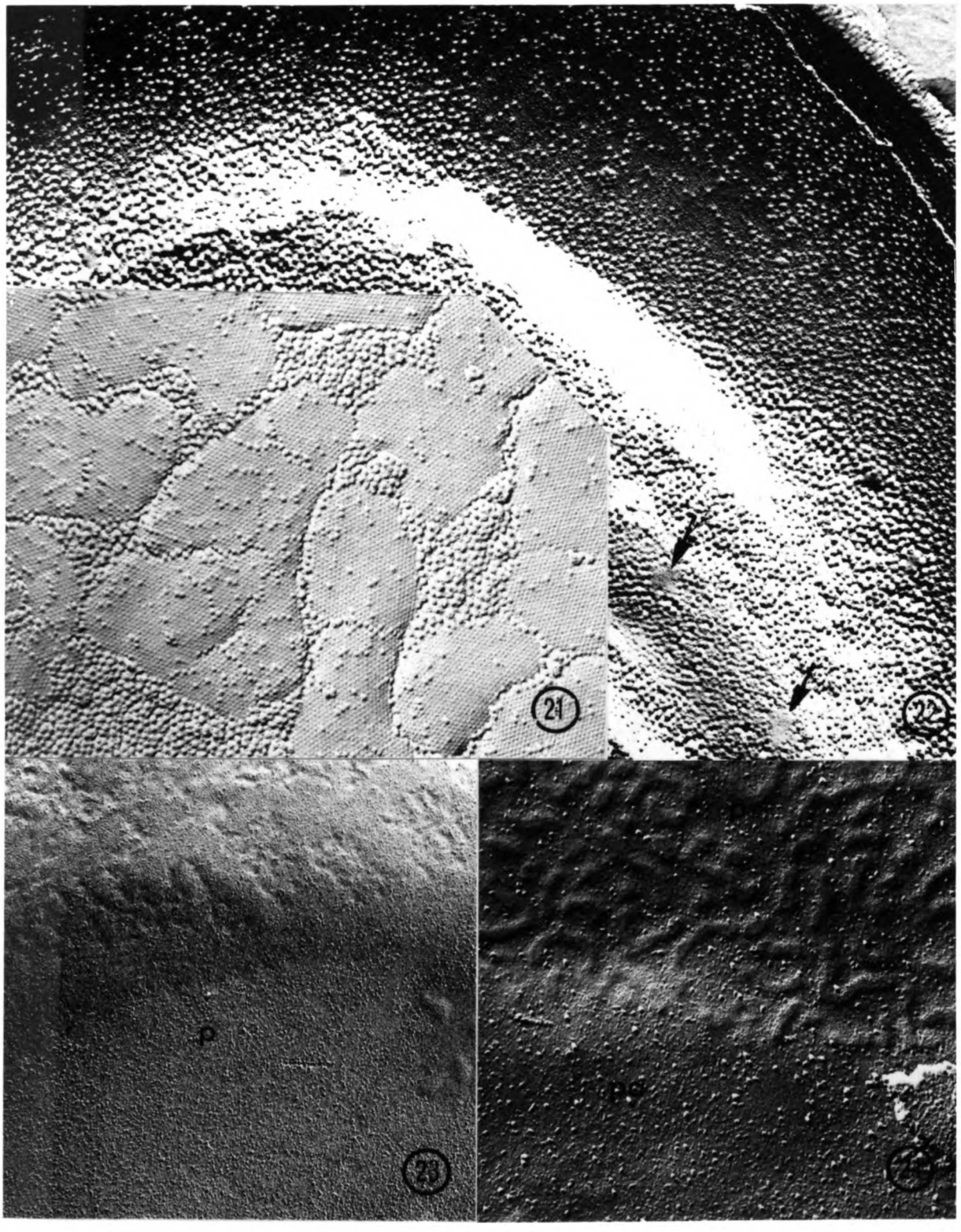
21
22
P
23
P
24

-CL, PA

-PG

-PE

-PI

-PS

-PC

origin

25 A B

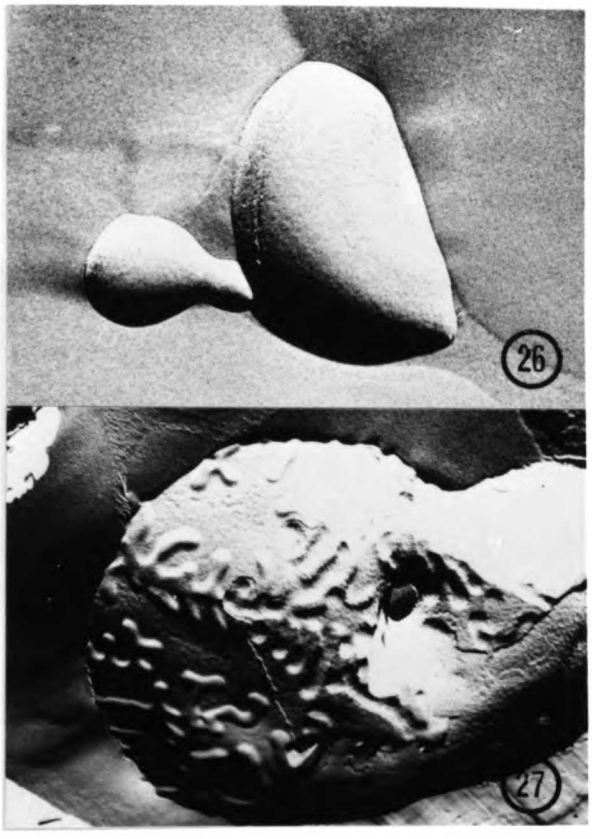
26
27

Chapter 4

Maintenance of Anionic Lipid Distribution

ABSTRACT

Asymmetric transmembrane lipid distribution in mammalian cells has been detected cytochemically through the comparison of the distribution of labeling of either of two anionic-lipid-binding antibiotics: one, adriamycin, membrane permeant, and the other, polymyxin B, not. In addition, a topographical relationship existed between membrane asymmetry and a cytoplasmic infrastructure observable in thin sections of tannic-acid-stained platelet ghosts and rotary-shadowed replicas of quick-frozen deep-etched cells. To test the specificity and permeability of the probes, polymyxin B (PXB) and adriamycin (ADR), we treated liposomes, composed of various lipid mixtures, as well as red blood cells. Polymyxin B induced crenulations in the plasma membranes only when acidic lipids were present in the external leaflet; but ADR, detectable both by fluorescence and by osmium precipitation, penetrated cells and bound acidic lipids on both sides of the bilayer. Thus, asymmetric membrane with acidic lipids primarily concentrated on the internal leaflet bound ADR but was PXB-resistant. We then used these methods to explore asymmetry in two other cells with secretory activity -- the guinea-pig spermatozoan and the human blood platelet. Sperm revealed domains of asymmetry complementary to those of externally deployed anionic lipids already described, while accumulation of acidic lipids in the outer lamellae of fusional regions demonstrated by the loss of differential binding by the two probes accompanied preparation

for acrosome granule exocytosis. By the same criterion, the whole membrane of the platelet was asymmetric until stimulated by thrombin to secrete at which time acidic-lipids became accessible to PXB. Hence, secretory activity in both cell types was accompanied by PXB susceptibility, suggesting a loss of asymmetry. Comparison of the cytoplasmic surface, revealed by deep-etching or tannic-acid-staining of asymmetric and symmetric membrane in each of these cells afforded the observation of a distinct structure in sperm which lined the membrane only in ADR-sensitive, PXB-resistant domains. In platelets, these techniques revealed a cytoplasmic membrane-associated structure which underwent a metamorphosis simultaneously with the appearance of outer lamellar anionic lipids. These comparisons provide circumstantial evidence for cytoplasmic elements maintaining membrane lipid asymmetry as well as regulating anionic lipid domains in the outer leaflet of the plasma membrane.

INTRODUCTION

Asymmetry of membrane lipids has long been known to exist in relatively simple systems such as erythrocytes, bacteria, and viruses (1), which lack internal membranous organelles which complicate biochemical approaches to the study of this phenomenon. Recently, a novel technique which analyzes the membranes of enveloped viruses grown on various cell-lines has also indirectly demonstrated lipid asymmetry in nucleated cells (2). Also, in the resting platelet, the inability of non-penetrating reagents and phospholipases to attack amino-phospholipids has been proposed to indicate asymmetry, although the location of these inaccessible lipids cannot be clearly shown to be the inner plasma-membrane leaflet by the techniques employed (2,4,5). The amino-lipids become available to the reagents following stimulation by thrombin (4), which intimates that the platelet is capable of modulating plasmalemmal asymmetric distribution of acidic lipids, possibly either through membrane fusion with granules or through donation by flip-flop from the inner leaflet. Here, we report that ultrastructural investigation of asymmetry in more complex cells can be conducted with cytochemical probes. The advantage of in situ labeling and fine-structural localization is the higher resolution obtained which allow discrimination of different lipid concentrations in membrane compartments and microdomains too small for biochemical dissection.

Our probes, polymyxin B (PXB) and adriamycin (ADR), have been shown to bind specifically to anionic lipids in various biophysical and biochemical studies (6,7,8,9). Adriamycin also binds DNA and perhaps other negatively-charged molecules, and this may be true of PXB as well.

However, digestion by either neuraminidase nor protease which should remove any other PXB-binding external membrane components did not alter the sperm-membrane affinity for PXB (10). Both probes can be observed ultrastructurally. The inability of PXB to attack anionic lipids on the inner leaflet of the plasma membrane allows its use as a probe for the detection of anionic lipid domains only in the outer leaflet. In addition, this inability has clinical consequences as selective toxicity for bacteria probably depends on the abundance of acidic lipid in the outer leaflet of their membranes. The side-effects of PXB therapy offer clues as to the cell systems where asymmetry of these lipids is less conserved.

Maintenance of asymmetry in the erythrocyte at least is attributable to a cytoskeletal protein, spectrin, which contributes to membrane contours (11), fluidity (12), and protein mobility (13). Descriptions of the structure, morphology, and membrane-binding characteristics of spectrin provide a basis with which to compare it to membrane-associated cytoskeletal structures appearing to perform some of these functions in other cells. Such cytoskeletal elements are reported here in platelets and sperm. Although we cannot yet offer biochemical evidence relating these structures to spectrin, certain analogies can be drawn with respect to <u>in situ</u> morphology. Additionally, the structures in both cells appeared to perform some of the same functions as the red cell protein: they were in close apposition to lipid-asymmetric regions of the membrane, and either changed their morphology or were absent from membrane when acidic lipids resided in the outer lamella. In conclusion, these results imply a mechanism by which cells could maintain domains of acidic lipids on the outer leaflet of the plasma membrane, as well as maintain or modulate asymmetry in response to function.

MATERIALS AND METHODS

Excitation/Emission Spectra of Adriamycin

Colloidal suspension of 0.1 M ADR in Tyrode's solution (TS) were put in 2-cc aliquots into cuvettes for examination in an Aminco spectrofluorometer no. SPF 500 and excited with a 468-nm wavelength beam, with 2-nm band passes. Emission spectra were monitored at a 300-nm/sec scanning rate, a 1.0-sec damping and a 1.0-intensity off-set range. Spectra of three samples were obtained: 0.1 M ADR in TS; 0.1 M ADR mixed in equal volume-ratio with a 0.2 μmol/cc lipid suspension in the form of PC:CL equimolar-ratio vesicles; and the same ADR-vesicle suspension to which a final concentration of 2% OsO_4 was added just before scanning.

Liposomes

Sonicated vesicles were prepared according to the reverse-phase evaporation (REV) technique of Szoka and Papahadjopoulos (14). Vesicles composed of bovine heart cardiolipin (CL) (Avanti, Birmingham, Ala) and egg phosphatidylcholine (PC) in equimolar ratio; soya phosphatidylethanolamine (PE); bovine brain phosphatidylserine (PS); and pure egg phosphatidylcholine (all lipids except PS and CL prepared according to the method of Papahadjopoulos and Miller (15) were used in this study.

Cell Suspensions

Blood from healthy human volunteers was drawn through a 19-gauge needle into either a 1.0% EDTA/3.8% sodium citrate solution or 3.8% sodium citrate alone, with a dilution of 10cc blood to 1cc anticoagulant. After centrifugation in plastic tubes at 150-200 g at room temperature for 10 min, the red cell pellet was separated from the platelet-

rich plasma (PRP). The red cells were either fixed directly in 1.5% glutaraldehyde or processed for ADR- or PXB-labeling as detailed below. Some of the PRP was slowly dripped into 1/5 PRP/1.5% glutaraldehyde fixative in 0.1 M sodium cacodylate and 1% sucrose (pH 7.4). Other preparations were also processed for ADR- or PXB-labeling, with and without stimulation by thrombin (see below).

Sperm were obtained from the vasa deferentes and caude epididymides of ether-anesthetized mature guinea pigs. The spermatozoa were plunged directly into the 1.5% glutaraldehyde fixative described above, or treated with PXB (16) or ADR (see below). Capacitation was achieved by overnight incubations in Ca^{2+} free TS as previously described (10).

ADR Labeling

Adriamycin (Sigma, doxorubicin hydrochloride) was suspended at a concentration of 0.1 mM in 1.5% glutaraldehyde fixative buffered by 0.1 M sodium cacodylate, 1% sucrose at pH 7.4. Liposomes and cells were incubated in this ADR-fixative combination for 1 h at room temperature, after which the cells were washed several times in 0.1 M sodium cacodylate, 7% sucrose (pH 7.4). Some of the red ADR could be seen to pellet with the cells. Liposomes were not washed. Aliquots of the ADR-fixed specimens were allowed to air-dry on glass microscope slides. The remaining suspensions were then pelleted, cut into blocks 1-mm square and incubated in 2% unbuffered OsO_4 at $40^{o}C$ for 48 h. Liposomes were incubated in osmium in suspension and pelleted during ethanol dehydration. Without any further staining, the blocks were dehydrated and embedded in Epon. Separate cell or vesicle suspensions were processed exactly as above except for the omission of ADR in the fixative.

Thin sections of osmium-incubated cells or liposomes were post-stained with alkaline lead citrate for 2 min before viewing at 60 KV on a Siemens 101 electron microscope.

PXB Labeling

Red blood cells were treated for 10 min at 37°C with 4.0 mM polymyxin B (Sigma) in phosphate-buffered saline (PBS). Sperm PXB-labeling was achieved according to the technique of Bearer and Friend (16). Platelets were treated as follows: 6- droplets of PRP anticoagulated by 0.1% EDTA or 0.38% sodium citrate were applied to a small piece of Whatman filter paper no. 42 which was glued to an aluminum specimen platform. After cooling a copper block to liquid-helium temperatures by the method of Heuser, Reese, and Landis (17), we injected the platelet suspension with a 6- solution of either 4.0 mM PXB alone, or 5-10 U/cc of thrombin alone, or PXB and thrombin together. Additionally, to obtain quiescent, unlabeled cells, PRP was similarly quick-frozen without any injections.

Merocyanine S 540

Merocyanine S 540 (Eastman Kodak, Rochester, N.Y.) was used according to the method of Schlegel, et al. (18). Motile sperm, suspended in TS were treated with 10 ug/cc merocyanine, for 10 min, then washed twice in TS supplemented with 2% bovine serum albumin and 1% sucrose. Droplets on glass microscope slides were allowed to spread under a vaseline-coated coverslip, sealed around the edges with finger nail polish. The vaseline reduced the movement so that the sperm could be photographed. They were examined and photographed with rhodamine filter combinations on a Zeiss fluorescence microscope. Trypsinized sperm were prepared as described previously (10).

Fluorescence Microscopy of ADR-treated Samples

Adriamycin-fixed liposomes, platelets, and sperm were observed in a Zeiss fluorescence microscope with transmitted light excitation and BG 38 and KP 500 filters and emission barrier filters 53 and 44. Photomicrographs were taken with 5, 10, and 20 sec exposures on Kodak ASA 400 color-film for slides, or Kodak Tri X film for black-and-white prints. Non-ADR-treated specimens were observed and photographed under the same conditions.

Quick-frozen Sperm

Guinea-pig sperm freshly removed from the cauda epididymis or vas deferens were mounted in 12- droplets directly onto filter paper glued to the aluminum specimen platform. They were then quick-frozen as described above for PRP.

Platelets in Thin Sections

Platelet-rich plasma was dripped gently into 1.5% glutaraldehyde buffered by 0.1 M sodium cacodylate, containing 1% sucrose (pH 7.4). To obtain stimulated platelets, we centrifuged the PRP for 3 min at 1000 g, then resuspended them in PBS anticoagulated with .38% Sodium Citrate. The suspension was then injected with 5-10 U/cc thrombin (gift of Mark Shuman, Dept. of Hematology, UCSF), allowed to respond for 1 min, and dripped into fixative in a ratio of 1cc cells to 5cc fixative. After fixation for 1 h, the cells were washed and prepared for thin sectioning. Pellets cut into 1-mm square blocks were incubated at $4^{o}C$ in Palade's OsO_4, supplemented with 5% sucrose then stained *en bloc* for 1 h in 1% digallic tannic acid (pH 7.0) and finally incubated in 0.5% uranyl acetate buffered by Veronal acetate (pH 6.0), 4% sucrose, at

37°C for 1 h. Subsequently, they were dehydrated in graded ethanol. To create "ghosts", we permitted the blocks to sit for 24 h at room temp in Epon-propylene oxide in a ratio of 2:1. Less than 10% of the platelets lost their densely staining cytoplasm with this technique.

Deep-Etching and Rotary-Shadowing

Quick-frozen platelets treated with PXB or PXB-thrombin were shadowed after fracturing without deep-etching on a Balzers 360M freeze-fracture device. Other samples of platelets as well as sperm suspension fractured at -115°C, were allowed to warm for 5 min to between -95° and -80°C, then shadowed with platinum and carbon. Replicas were cleaned with swimming pool hypochlorite (Georgia-Pacific), washed in distilled water, and mounted on Formvar-coated copper grids.

OBSERVATIONS

Differential labeling of cell membranes by two cytochemical probes, PXB and ADR, reveals the "membrane-sidedness" of anionic lipids. We first established our ability to observe ADR, not hitherto used as a cytochemical tool, via fluorescence microscopy by analyzing its emission spectra, and via electronmicroscopy by its precipitation of osmium. Further, we tested the specificity of ADR for anionic lipids and its lack of effect on phosphatidylcholine (PC), by employing model membrane systems -- reverse-phase evaporation vesicles composed of PC alone or in combination with acidic lipids, and prepared for both light-and electron-microscopy. Finally, to explore the potential of ADR as a probe for both inner and outer membrane acidic lipids, we examined multilamellar vesicles and red blood cells. Polymyxin B has already proven to be a useful agent for studying anionic-lipid distribution (10). In this investigation, we have attempted to define more precisely its capacity to bind lipids on the inner leaflet of the plasma membrane by treating erythrocytes as well as non-stimulated platelets, since these cell-systems are known to concentrate acidic lipids on the inner leaflet (1,3,4,5).

Spectroscopy

When adriamycin (10^{-4}Mol) was suspended in Tyrode's solution (TS) and examined in the Aminco spectrofluorometer No. SPF 500, maximal emission was obtained from an excitation (EX) wavelength of 468 nm. At this wavelength, EX produced an emission spectrum showing peaks at 560 nm (yellow) and 590 nm (red) (Fig. 1). Although the addition of 0.2 μmol of cardiolipin (CL):PC vesicles decreased the overall intensity of

emission, both the position of the peaks and their intensity relative to each other remained unchanged. Adding 2% osmium tetroxide (OsO_4) to the mixture, however, abolished the signal. Therefore, fluorescence microscopy was performed using fluorescein excitation filters (KP 500 and BG 38) as well as barrier filters (Nos. 44 and 53), which excite in the 400-500-nm wavelengths and permit observation of emissions above 500-nm wavelengths.

Liposomes

With these filters, neither PS:PE nor CL:PC vesicles glowed brightly enough to be detectable. But after the addition of 0.1 mM ADR to the liposome suspension, both types of vesicle fluoresced yellow; while red clumps of unbound ADR stayed in the media. PC vesicles failed to respond to the antibiotic -- i.e., there was no discernible fluorescence.

Osmium-tetroxide Labeling of Adriamycin

Since OsO_4 abolished ADR emission, we used it to localize the antibiotic by electronmicroscopy of thin sections. Colloidal suspensions of adriamycin alone incubated in OsO_4 exposed a black precipitate surrounding less compact, grey clumps. Liposomes treated with the agent were subsequently incubated in OsO_4 at $40^{o}C$; those consisting of anionic lipids such as CL or PS were speckled with osmium precipitate (Fig. 2a). In contrast, vesicles either composed of PC or not treated with ADR showed no such speckling (Fig. 2b). The internal membranes of multilamellar acidic-lipid vesicles treated with ADR were heavily speckled, indicating that adriamycin had crossed the bilayers (Fig. 2a).

Erythrocyte and Platelet Labeling

Since we entertained the suspicion that PXB did not cross the

bilayer nor label anionic lipids located on the inner leaflet of the plasma membrane, and that, in fact, ADR and PXB differences in membrane penetration accounted for their disparity in labeling, we applied the same techniques to red blood cells to test the theory. Adriamycin induced both the appropriate fluorescence and osmium disposition in these cells (Fig. 3a,b), but PXB failed to crenulate the membrane (Fig. 3c).

We then treated another cell, in which anionic lipids are exposed on the surface of the outer leaflet only after stimulation -- the human blood platelet (4,5). Adriamycin produced fluorescence in platelets before and after stimulation by factor IIa (thrombin, a powerful secretogogue) (Fig. 4, a-c). Unfortunately, long-term incubation in OsO_4 created so much osmium reduction in platelets that ADR had no additional effect. In contrast to ADR-labeling, which was independent of stimulation, quick-frozen platelets were unaffected by PXB unless stimulated by thrombin. Unfixed platelets can be stimulated by injection of microliter thrombin solutions to the mounted platelet droplet one sec prior to quick freezing. Unstimulated platelets maintained smooth membranes whether PXB was present or not, even though filopodial projection had begun (Fig. 5a). Stimulation for 1 sec with thrombin elicited more of these projections, while granules could still be seen in the cytoplasm (Fig. 5b). The membrane remained smooth during stimulation. If the droplet containing the platelet suspension was injected with a thrombin-PXB solution, one sec before quick freezing, then the plasma membranes crenulated extensively (Fig. 5c & d). Again, granule secretion was not complete.

Spermatozoa

When fresh guinea-pig sperm, model cells for juxtaposed fusional and non-fusional membrane domains, were inspected with fluorescein filters, they were barely visible (Fig. 5a). Adriamycin treatment, however, elicited luminosity of the fusional membrane -- the apical acrosomal cap, a region also attacked by polymyxin B. Proximally, the cap remained dark in both PXB- and ADR-treated specimens; but unlike PXB, the latter agent also evoked a slight luminosity in the non-fusional post-acrosomal segment (Fig. 5b). Following incubation in capacitating media, the process which readies this membrane for fusion with the underlying acrosomal granule, the fluorescence induced by ADR in the apical cap descended through the proximal cap to the equatorial segment, which demarcates fusional and stable regions (Fig. 5c). When the cells were incubated in a combination of ADR and fixative, the antibiotic did not cause the nucleus to fluoresce. Conversely, cells allowed to air-dry on glass slides before adriamycin fixation displayed a red nuclear fluorescence.

Whereas untreated, osmium-incubated sperm revealed only a few black splotches (Fig. 7a & b), cells treated with ADR and OsO_4 disclosed intense precipitates resembling those seen in liposomes and red blood cells along the plasma membrane, as well as some speckling of internal structures (Fig. 7c). Acrosomal-cap plasma membranes labeled most heavily, but some osmium precipitate also lined the post-acrosomal membrane.

The preparation of PXB-treated sperm for freeze-fracture electron-microscopy resulted in crenulations that initially perturbed only the apical acrosomal cap, but subsequently progressed throughout the entire

cap after capacitation (Fig. 8a & b). However, unlike the osmium speckling induced by ADR, never were these crenulations encountered in the membranes of organelles such as the nuclear envelope, even when the plasma membrane had been severely perturbed (Fig. 8a & b). Nor were they seen in the post-acrosomal membrane (Fig. 8b).

Cytoplasmic Structures

Both platelets and spermatozoa disclosed membrane which bound ADR but was inaccessible to PXB. This membrane is the non-fusional post-acrosomal segment in sperm and the plasma membrane of non-stimulated platelets. Sperm demonstrated neighboring regions susceptible to both antibiotics. In order to explore the mechanisms by which sperm could maintain such adjacent domains, we used merocyanine to identify domains of fluidity in the outer leaflet of the sperm plasma membrane (Fig. 9a & b). While these domains correlated with PXB topography, the time-course of merocyanine progression during incubation in capacitating media from apical to proximal acrosomal cap was much more rapid (in the order of 30 min) than that of PXB or ADR, which took 3 h or longer.

The role of cytoplasmic peripheral membrane elements was next explored by examination of tannic-acid-stained thin sections and quick-frozen deep-etched replicas of sperm and platelets. The former specimens reveal a density lining the cytoplasmic surface of the post-acrosomal segment of the plasma membrane, and no such densities in the other, PXB- sensitive fusional regions of the head ( ). The latter procedure permitted a more detailed view of this structure through vents in the overlying membrane. Such deep-etching displayed a tightly packed series of rods made up of 5-7 nm globules with a 15 nm center-to-center spacing (Fig. 10a). In higher magnifications (Fig. 10b)

these rods could be seen to be composed of two subunits which twisted around each other, perhaps in a helical conformation. Correlative to the densities observed in thin section, rods could only be found in the PXB-resistant post-acrosomal segment.

A density demonstrable in tannic-acid-stained thin sections lined the platelets plasma membrane, too. Normally obscured by the easily-stained cytoplasmic matrix, this lining became clear when platelets were partially leached of cytoplasm (Fig. 11a & b). After factor-IIa stimulation, the lining changed, becoming punctate in some regions at center-to-center spacing of 15 nm, and linear in others, and was no longer distinctly attached to the membrane (Fig. 11c). Obviously, however, adherence to the membrane continued, since the structures retained this relationship even when there was considerable loss of cytoplasmic substance. Barren in unstimulated platelets, the external surface acquired a dark tannic-acid-stainable coating after thrombin stimulation. Deep-etching of platelets quick-frozen within 1 sec of thrombin stimulation displayed 15-nm thick rod-like struts paralleling the membrane and so close as to appear draped by it (Fig. 12a & c). In contrast, unstimulated platelets (Fig. 12b) had no such organization of the dense periplasmic matrix in the space between the microtubule circlet and the membrane. Elongating actin filaments were present in these labile cells even in the absence of any additional stimulation by thrombin, and in the absence of membrane associated struts (Fig. 12d). In the stimulated cells, these struts traversed the body of the platelet just beneath the membrane and outside the remaining microtubule circlet (Fig. 12e). In both tannic-acid-stained thin sections (Fig. 12a) and deep-etched replicas (Fig. 13b), an intimate association between these peripheral

plasma membrane-components and an intracellular membrane system was evident. Relationship of the struts to other cytoplasmic components was less clear. Cytoplasmic ground substance (Fig. 13c) occupied a deeper level in the cell, shared by persisting microtubules (Fig. 13d).

Thus, the fact tht ADR-sensitive, PXB-resistant membrane overlies a dense, closely apposed structure on the cytoplasmic surface suggested a correspondence between the concentration of anionic-lipid on the internal leaflet and periplasmic-structure: membrane association. Loss of anionic lipid asymmetry concommitant with morphological changes in these cytoplasmic supports was further evidence of such a correspondence.

DISCUSSION

By means of two different probes -- one membrane-permeant, the other not -- and two model cell-types, the platelet and the spermatozoan, we investigated the relationship between anionic-lipid domains in the external leaflet of the plasma membrane and the asymmetrical distribution of these lipids across the bilayer. Additionally, we explored the association and contribution to the maintenance of asymmetry of membrane lipids by cytoplasmic structures with electron microscopy of tannic-acid-stained thin sections and quick-frozen, deep-etched replicas, and by membrane phase state with a fluorescence dye.

Our results lead us to conclude that transbilayer asymmetry of acidic phospholipids can be determined by adriamycin-labeling of polymyxin-B-resistant membrane; therefore, the spermatozoan post-acrosomal membrane and the entire plasma membrane in non-stimulated platelets are asymmetrical in acidic-lipid distribution with their anionic lipids deployed in the membrane's inner leaflet. Moreover, the loss of acidic-lipidic asymmetry which occurred during stimulation of platelets corresponded to their appearance on the outer leaflet -- thus the cytoplasmic leaflet probably provides the source for some of these lipids. We also suggest that the asymmetry is sustained by cytoplasmic structures, similar to erythrocyte spectrin, which lie beneath the membrane and act as a sink for anionic lipids, attracting them to the cytoplasmic membrane-face, away from the external leaflet and adjacent regions. Detachment of these structures from the membrane would then permit the free diffusion of acidic lipids back to neighboring regions or accelerated

"flip-flop" to the outer lamella. In the platelet, stimulation triggers this detachment, perhaps through calcium influx. Indeed, calcium may participate in separating lipids from peripheral proteins -- that is, should it have a higher binding coefficient for these lipids or for the protein than that of the protein for the lipid. The above concept is portrayed in the diagram, Fig. 14. Finally, we propose that a loss of asymmetry, with the concomitant emergence of anionic lipids on the outer leaflet, represents one necessary step in initiating the fusion of intracellular granules with the plasma membrane. That our observations give credence to these proposals follows.

Demonstration of Asymmetry

Though the two probes, polymyxin B and adriamycin, differ in chemical parameters, they probably interact with negatively-charged lipids on the same ionic basis, since both are positively charged. PXB has previously been demonstrated to be an effective cytochemical tool for the detection of anionic lipid domains (10, 16).

Adriamycin is also known to have an affinity for acidic lipids (7, 8) --the attraction perhaps attributable to the antibiotic's positive charge at neutral pH and its hydrophobicity. The liposome experiments described here support this, since vesicles composed of PC neither fluoresced nor precipitated osmium in the presence of ADR; while vesicles which incorporated either PS or CL responded in both respects. Because OsO_4 resulted in the loss of emission spectra, we assume that osmium oxidized the resonant double bonds of the agent's anthracene moeity. A potential artefact in this system would be ADR-mediated peroxidation of unsaturated acyl chains -- an occurence which has been postulated as one mechanism of ADR toxicity (7) and could account for

osmium reduction in ADR-treated systems. Such peroxidation would not be specific for acidic lipids, however. Yet egg PC, with approximately one to two double bonds for each molecule, did not appreciably precipitate osmium in the presence of ADR, and osmium reduction took place around clumps of ADR in the absence of lipids. On the basis of these two facts, therefore, we conclude that lipid peroxidation was not the mechanism by which ADR-treated membranes gained their osmium granularity.

Adriamycin penetrates cells, as evidenced by its use as a cancer chemotherapeutic agent and substantiated by the presence of cytoplasmic granularity in ADR/osmium-treated cells and multilamellar vesicles reported here. Thus it detects lipid on both sides of the membrane as well as negatively-charged lipid in organelles. This is most conclusively shown in the erythrocyte, in which membrane asymmetry is well-known (1), and which deposited osmium along its membrane following ADR-fixation. Polymyxin B was unable to crenulate erythrocyte membranes, indicating that it does not attack inner-lamellar lipids, nor did it attack organelle membranes normally high in anionic lipids such as those of the sperm nuclear envelope. Hence anionic lipids could exist on either side of the bilayer in ADR-sensitive membranes, whereas PXB-resistant membrane would harbor them only on the inner lamella or have none at all. By using both probes, we were able to demonstrate either membrane with internally deployed anionic lipids or membrane with lipids on both sides of the bilayer. Obviously it was impossible to distinguish between membrane with all its acidic lipids on the external leaflet from membrane with these lipids in both halves of the bilayer.

It is conceivable that PXB cannot bind to acidic lipids even when

they are in the external leaflet when cytoplasmic elements maintain strict control of membrane contour. However, filipin, which also causes deformations of membrane contour, attacks the PXB-resistant sperm membrane, the post-acrosomal semgent, although in diminished intensity over the neighboring acrosomal cap. Binding by filipin in the PXB-resistant segment elicits 20 nm invaginations (20) which demonstrates that the membrane has the freedom to allow filipin penetration and to deform upon antibiotic attack.

Asymmetry and Domains

Platelets demonstrated an all-or-none response to PXB, dependent on stimulation but fluoresced in the presence of ADR independent of stimulation. This implies that, like the red cell, the nonstimulated platelets maintains an asymmetrical unit-membrane. Asymmetry of lipid classes in plasma membranes is not unusual (1). Although well-established for the red cell, such asymmetry has recently been reported to occur in nucleated cells as well. Enveloped viruses wherein membrane constitution reflects the cell from which it buds, show asymmetrical lipid distribution when grown from a variety of cell-culture lines (2). Moreover, phagolysosomes formed by plasma-membrane invagination of a murine fibroblast cell-line around a latex bead also conform to this pattern of asymmetry (21). In the nonstimulated platelet plasma membrane, a paucity of anionic lipids such as PS and PE in the outer lamella has been defined both by fluorinated nitrobenzene labeling and by phospholipase digestion (4, 5). However, these studies only differentiate between accessible and inaccessible phospholipids by the use of nonpenetrating reagents. Thus they cannot tell whether inaccessible

lipid are in organelles or in the plasma-membrane's cytoplasmic leaflet. Adriamycin cytochemistry provides a better resolution of these internally oriented lipids, revealing that some of them are deployed on the inner half of the plasmalemma, as we would expect for an asymmetric membrane.

Asymmetry could also be discerned in specific functional regions of guinea-pig sperm. Domains of acidic lipid mapped by PXB in this cell correlated with intense ADR fluorescence and dense ADR-induced osmium precipitation. Since no portions of the sperm membrane were totally free of ADR, however, lack of PXB mediated perturbation was not representative of transbilayer anionic lipid distribution, but rather only reflected a paucity in the outer leaflet. Thus in the post-acrosomal segment, not crenulated by PXB, anionic lipids are concentrated on the inner leaflet i.e., asymmetrically. Clearly, domains of acidic lipids in the outer lamella constitute a mirror-image of domains of asymmetric/symmetric membrane. The correlation of greater ADR intensity with PXB-binding over the acrosomal cap suggests that not only do anionic lipids reside in the outer leaflet of the fusional membrane, but that more of these lipids dwell in that region of the bilayer as a whole. This argues against flip-flop being the sole mechanism for producing PXB-susceptibility in this area during capacitation, for such a mechanism would predict that total lipid concentration remain the same. Therefore, some additional mechanism, e.g., loss of acidic lipids from the inner leaflet creating a vacuum attracting more lipid to flow from adjacent regions, or stimulating lipid synthesis, must account for overall increase in concentrations.

A wealth of data supports the existence of lipid asymmetry in plasma membranes (1). In view of this corroboration, it is all the more surprising to discover acidic lipids on the outer leaflet. In platelets, however, using the same non-penetrating reagents as were used to describe the asymmetry of the resting cell, acidic-lipid emergence following stimulation is again well-documented (4, 5). Thus, PXB-labeling of the stimulated cell simply confirms the results of biochemical experiments. In fact, the appearance of negatively charged phospholipids is essential to platelet function in initiating a clot. The other cells in which asymmetry has been described were studied in their resting state. Whether or not stimulation of other secretory cells produces an increase in outer-leaflet anionic lipids has yet to be determined.

Maintenance and Modification of Asymmetric Domains: Fluidity and Cytoplasmic Supports

Our results afford circumstantial evidence to support the proposal that cytoplasmic structures participate in the maintenance of asymmetric lipid distribution. In sperm, the segment of non-PXB-sensitive asymmetric membrane lay tightly against a cytoplasmic structure, while PXB-susceptible membrane regions demonstrated no such supports. In addition, the time-course of fluidity changes in the acrosomal cap fusional membrane was much faster than that of the emergence of outer leaflet acidic lipids. In platelets, a morphological change in the cytoplasmic membrane structure accompanied exposure of anionic lipids on the outer leaflet. Recent studies in which disturbance of platelet membrane-fluidity was accomplished by treatment with fatty acids, have shown that such disturbance blocks platelet function (22). Increased fluidity,

therefore, may be one step toward modification of asymmetry in response to cellular function -- yet the time-course of phase changes in sperm reveals that is not the controlling one.

It has long been suspected that cytoplasmically-oriented peripheral membrane-proteins contribute to the maintenance of various attributes of the cell membrane. Morphologically, spectrin, the membrane-associated protein of the erythrocyte, in some respects resembles the structures described here. In low-angle rotary shadowing, spectrin is a flexible rod composed of globular subunits which forms tetrameters 200 μm in length (23, 24). In thin sections of RBC ghosts, spectrin's width appears to be 9 nm (25, 26). The width of these sub-structures, twice that of spectrin, would also correspond should the dimeric subunits, barely discernible in the rods of the sperm, denote two tightly associated components. Length cannot be determined in these in situ observations. Membrane linings of red-cell ghosts, examined in tannic-acid-stained sections (27), as well as views of this structure recreated by the addition of spectrin to inside-out despectrinated red-cell ghosts in the presence of actin (25, 26), are analogous to the lining of thin-sectioned platelet ghosts reported here. These rods have been described previously in osmotically shocked platelets, another procedure which produces rarification of the cytoplasm. ADP, a stimulant of platelet activation, enhanced the presence of these "fibrils" (28).

That a cytoplasmically-oriented molecule can influence both the fluidity (29) and phospholipid asymmetry (12) of overlying membrane has been established by investigation of spectrin's function. These same functions, particularly the production and maintenance of asymmetry,

appear to be fulfilled by similar, rod-shaped cytoplasmic elements in sperm and platelets.

Some morphological aspects of the two periplasmic structures of sperm and platelets are dissimilar to spectrin. Unlike the 100 nm meshwork spectrin produces, the sperm structure is rods which traverse the whole post-acrosomal segment, in the order of 2 μm. Anti-actin antibodies preferentially bind this segment in bovine sperm of other species (30); thus, cross-linking by actin may be responsible for this tight packing as spectrin meshwork can be tightened by actin also (26). Spectrin is in turn capable of polymerizing actin (31, 32). Should the rods act as spectrin does and bind acidic lipids (29), they could be responsible for the paucity of these lipids evident in the external leaflet of the overlying membrane as well as in neighboring domains -- e.g., the proximal portion of the acrosomal cap. This attraction would create an anionic-lipid sink from which lipids could emerge as needed. In such a manner, the cell could regulate relative concentrations of negatively-charged lipid on the outer leaflet, as well as responses to divalent cations of the phase transitions of the membrane as a whole, reactions which depend upon the ratios of head groups and fatty-acid tails.

Further clues that a spectrin-like molecule exists in platelets is the presence of a high molecular doublet (250,000/230,000 daltons in comparison to spectrin and myosin) in platelet extracts (32). This protein is absent from platelets that have been treated with tetracaine, an irreversible inhibitor of filopodial projection activation. The molecule is released from platelet membranes by the same processes that release spectrin from erythrocytes (36). Recent evidence shows the 250,000 D band has actin-binding properties (34).

If one of the physiological roles of this periodic infrastructure is to maintain an anionic-lipid sink in the form of an asymmetric membrane and to release the lipids upon demand, then both the type of stimulation recognized by the cell as well as the effect of these lipids on its ability to perform various functions should provide clues to the molecular mechanism of the binding and detachment of the joists from the membrane. Platelets, which require the exposure of acidic lipids for the activation of clotting factor, need a structure which releases these lipids readily; whereas red blood cells require a more secure lipid-binding protein to conserve asymmetry and prevent the inappropriate triggering of clotting by the appearance of the wrong lipid on the external leaflet. Guinea-pig sperm, on the contrary, would prefer a protein with even higher affinity for acidic lipids than spectrin, and less actin-polymerizing ability, since the post-acrosomal segment must store the acidic lipids which appear during capacitation and which probably are necessary for fusion of the plasma membrane with the acrosomal granule membrane, a prerequisite for fertilization.

Acknowledgements

We would like to express our appreciation to Ivy Hsieh and Jrene Rudolf for their technical assistance, to Nejat Duzgunes and Demetrios Papahadjopoulos for their advice in the preparation of liposomes, and to Pat Calarco for the use of the fluorescence microscope.

1. Op den Kamp, Jos., A. F. 1979. Lipid asymmetry in membranes. Ann. Rev. of Biochem. 48: 47-71.

2. van Meer, G., K. Simons, J. A. F. Op den Kamp, and L. L. M. van Deenen. 1981. Phospholipid asymmetry in Semliki Forest virus grown on baby hamster kidney (BHK-21) cells. Biochem. 20: 1974-1981.

3. Morin, R. J. 1980. The role of phospholipids in platelet function. Ann. of Clin. and Lab. Sci. 10: 463-473.

4. Schick, P. K. 1977. The organization of aminophospholipids in human platelet membranes: selective changes induced by thrombin. J. Lab. Clin. Med. 91: 802-809.

5. Chap, H. J., R. F. A. Zwall, and L. L. M. van Deenen. 1977. Action of highly purified phospholipases on blood platelets: evidence for an asymmetrical distribution of phospholipids in the surface membrane. Biochim. Biophys. Acta. 467: 146-164.

6. Storm, D. R., K. S. Rosenthal, and P. E. Swanson. 1977. Polymyxin and related peptide antibiotics. Ann. Rev. Biochem. 46: 723-763.

7. Duarte-Karim, M., J. M. Ruysschaert, and J. Hildebrand. 1976. Affinity of adriamycin to phospholipids - a possible explanation for cardiac mitochondrial lesions. Biochim. Biophys. Acta. 71: 658-663.

8. Goormaghtigh, E., P. Chatelain, J. Caspers, and J. M. Ruysschaert. 1980. Evidence of a specific complex between adriamycin and negatively-charged phospholipids. Biochim. Biophys. Acta. 597: 1-14.

9. Murphree, V. A., T. R. Tritton, P. L. Smith, A. C. Sartorelli. 1981. Adriamycin-induced changes in the surface membrane of sarcoma 180 ascites cells. Biochim. Biophys. Acta. 649: 317-324.

10. Bearer, E. L.,and D. S. Friend. 1981. Modifications of anionic-lipid domains preceding membrane fusion in guinea-pig sperm. J. Cell Biol. (in press).

11. Lux, S. K. K. M. John, and M. J. Karnovsky. 1976. Irreversible deformation of the spectrin-actin lattice in irreversibly sickled cells. J. Clin. Invest. 58: 955-963.

12. Haest, C. W. M., G. Plasa, D. Kamp, and B. Deuticke. 1978. Spectrin as a stabilizer of the phospholipid asymmetry in the human erythrocyte membrane. Biochim. Biophys. Acta. 509: 21-32.

13. Marchesi, V. T. 1979. Spectrin: Present status of a putative cytoskeletal protein of the red cell membrane. J. Membrane Biol. 51: 101-131.

14. Szoka, F. Jr. and D. Papahadjopoulos. 1978. Procedure for preparation of lysosomes with large internal aqueous space and high capture by reverse-phase evaporation. PNAS 75: 4194-4198.

15. Papahadjopoulos, D. and N. Miller. 1967. I. Structural characteristics of hydrated liquid crystals. Biochim. Biophys. Acta. 135: 624-638.

16. Bearer, E. L. and D. S. Friend. 1980. Anionic lipid domains: Correlation with functional topography in a mammalian cell membrane. PNAS 77: 6601-6605.

17. Heuser, J. E., T. S. Reese, and D. M. Landis. 1972. Preservation of synaptic structures by rapid freezing. Cold Spring Harbor Symp. Quant. Biol. 40: 17-24.

18. Schlegel, R. A. and B. M. Phelps. 1980. Binding of merocyanine 540 to normal and leukemic erythroid cells. Cell 20: 321-328.

19. Friend, D. S. and J. E. Heuser. 1980. Orderly particle arrays on the mitochondrial outer membrane in rapidly-frozen sperm. Anat. Rec. 199: 159-175.

20. Friend, D. S., and E. L. Bearer. 1981. β-hydroxysterol distribution as determined by freeze-fracture cytochemistry. Histochem. J. 13: 535-546.

21. Sandra, A. and R. E. Pagano. 1978. Phospholipid asymmetry in L. M. Cell plasma membrane derivatives: polar head group and acyl chain distributions. Biochem. 17: 332-338.

22. MacIntyre, D. E., R. L. Hoover, M. J. Karnovsky, and E. W. Salzman. 1980. Inhibition of platelet aggregation by unsaturated fatty acids. Abs. of the 53rd Scien. Sessions 63: 191, abstr. no. 726.

23. Tyler, J. M., J. M. Anderson, and D. Branton. 1980. Structural comparisons of several actin-binding macromolecules. J. Cell Biol. 85: 489-495.

24. Shotton, D. M., B. E. Burke, and D. Branton. 1978. The molecular structure of human erythrocyte spectrin. Biophysical and electron microscopic studies. J. Mol. Biol. 131: 303-329.

25. Tsukita, S., S. Tsukita, and H. Ishikawa. 1980. Cytoskeletal network underlying the human erythrocyte membrane. Thin-section electron microscopy. J. Cell Biol. 85: 567-576.

26. Tsukita, S., S. Tsukita, H. Ishikawa, S. Sato, and M. Nakao. 1981. Electronmicroscopic study of reassociation of spectrin and actin with the human erythrocyte membrane. J. Cell Biol. 90: 70-77.

27. Tilney, L. G. and P. Detmers. 1975. Actin in erythrocyte ghosts and its association with spectrin. J. Cell Biol. 66: 508-520.

28. Zucker-Franklin, D. 1970. The submembranous fibrils of human blood platelets. J. Cell Biol. 47: 293-299.

29. Mombers, C., P. W. M., L. L. M. van Deenin, J. DeGier, and A. J. Verleij. 1977. The interactions of spectrin, actin, and synthetic phospholipids. Biochim. Biophys. Acta. 470: 152-160.

30. Greenberg, B. J., and T. M. Tamblyn. 1980. Actin from mature bovine spermatozoa. J. Cell Biol. abstract.

31. Cohen, C. M., and S. F. Foley. 1980. Spectrin-dependent and -independent association of F-actin with the erythrocyte membrane. J. Cell Biol. 86: 694-698.

32. Fowler, V. M., E. J. Luna, W. R. Hargreaves, D. L. Taylor, and D. Branton. 1981. Spectrin promotes the association of F-actin with the cytoplasmic surface of the human erythrocyte membrane. J. Cell Biol. 88: 388-395.

33. Nachmias, V. T., J. Sullender, J. Fallon, and A. Asch. 1979. Observations on the "Cytoskeleton" of human platelets. Thrombos. Haemostas. 42: 1661-1666.

34. Rosenberg, S., A. Stracher, and R. C. Lucas. 1981. Isolation and characterization of actin and actin-binding protein from human platelets. J. Cell Biol. 91: 201-211.

Figure Legends

Figure 1 Excitation with 268-nm-wavelength light produced these emission spectra for 1) 0.1 mM ADR suspended in Tyrpde's solution (---); 2) 0.1 mM ADR plus 0.2 μmol/cc lipid in the form of CL:PC vesicles (···); and 3) 2% OsO_4, the concentration used in cells, added to the same ADR/lipid suspension (——). All spectra were obtained with 2 nm band passes, and 1.0 gain.

Figure 2 Liposomes incubated in 0.1 mM ADR, then resuspended in 2% unbuffered OsO_4. (a): A multilamellar vesicle containing CL exhibits a granular heavy-metal precipitate on inner and outer membranes. X 42,000. (b): A phosphatidylcholine multilamellar vesicle shows minimal osmium speckling. X 42,000.

Figure 3 Human red blood cells (a): Lack of staining of the plasma membrane makes resolution difficult in this osmium-incubated erythrocyte. X 90,000. (b): Following ADR/fixative treatment, a dark granularity lines the membrane. X 72,000. (c): Polymyxin B has no effect on this red-cell membrane, as evidenced by the smooth P-face of the freeze-fracture replica. X 54,000.

Figure 4 Fluorescence of platelets exposed to ADR, examined with fluorescein filters, and photographed with a 10-sec exposure. (a): Untreated with ADR, platelets refract the light and are faintly discernible. (b): Adriamycin enhances the visibility of nonstimulated platelets. (c): Following thrombin stimulation, platelet fluorescence elicited by ADR parallels that of the non-stimulated cells. Fig. 4, a-c, X 1000.

Figure 5 Quick-frozen platelets. (a): An unfixed platelet reveals a smooth membrane except for numerous intramembranous particles and a few canalicular openings. X 29,000. (b): Injection of thrombin 1 sec before freezing induced the extension of filopodia and the opening of canaliculi (arrows). Cross-fracture exposes granules in the cytoplasm; the fine contours of the membrane remain unperturbed. X 29,000. (c): The inclusion of PXB in the stimulatory injection results in crenulated membranes, even in platelets arrested during activation by being quick-frozen within 1 sec of injection. X 49,000. (d): Granules still occupy the cytoplasm, while the plasma membrane crenulates extensively in this thrombin/PXB stimulated platelet. X 30,000.

Figure 6 Fluorescence of sperm exposed to ADR, examined with fluorescein filters, and photographed with a 20 sec exposrue. (a): In the absence of ADR, only ephemoral, greenish outlines can be discerned. X 1,2000. (b): After the addition of ADR to the fixative, the apical cap (small arrow) fluoresces. There is some fluorescence of the rest of the head, including the proximal cap (large arrow) and post-acrosomal segment (arrowhead), as well as luminosity of the cytoplasmic droplet. X 1,2000. (c): The entire acrosomal cap (arrow) of a capacitated sperm treated with ADR glows brightly. The post-acrosomal segment (arrowhead) is also slightly luminous. X 1,000.

Figure 7 Two-day incubations of sperm in OsO_4. (a): Thin section of sperm thus incubated. Acrosomal cap membrane (arrow) shows a very few nonspecific splotches. X 25,000. (b): Treatment with ADR results in granularity lining the plasma membrane over the acrosomal cap. X 25,000. (c): The equatorial

junction between the acrosomal cap (a) and post-acrosomal segment (pa) is free of granularity, although again a large nonspecific blotch is present. X 39,600. (d): This ADR-induced granular lining is less intense in the post-acrosomal segment (arrow). X 40,000.

Figure 8 Sites of PXB perturbation in freeze-fracture replicas of guinea-pig sperm. (a): In fresh sperm, PXB crenulates only the apical acrosomal cap (a). Inner membranes retain their smoothness (arrow). X 30,000. (b): Capacitation increases PXB-susceptibility of the proximal acrosomal cap (p), but the post-acrosomal segment of the membrane (pa) remains unperturbed. A small portion of the nuclear envelope (arrow) maintains undisturbed contours. X 36,000.

Figure 9 Merocyanine fluorescence of guinea-pig sperm, rhodamine filters, 20 sec exposures. (a): Fresh sperm fluoresce over the apical acrosomal cap. (b): Fluorescence descends through the equatorial segment within 30 min, or following trypsinization. Fig. 9a & b X 750 .

Figure 10 Quick-frozen, deep-etched sperm. (a): a row of equally-spaced doublet rods underlies the plasma membrane in the post-acrosomal segment. X 100,000. (b): These rods measure 15 nm in center-to-center spacing, with a periodicity of 7-8 nm. Each rod is composed of two similar components which twine about each other. X 112,500.

Figure 11 Platelet ghosts in tannic-acid-stained thin sections. (a and b): Loss of cytoplasmic density discloses a fuzzy coating still adhering to the inner surface of the plasma membrane (arrows). a, X 108,000, b, X 90,000.

(c): Thrombin stimulation for 1 min preceding fixation induces a metamorphosis of the cytoplasmic-membrane coating from indistinct fuzziness into rods, which, when transected, resemble dots (arrows) just inside the plasma membrane and about 15 nm apart. X 72,000.

Figure 12 Quick-frozen, deep-etched platelets. (a): Thrombin stimulation 1 sec before smashing the cells on a helium-cooled copper block captures submembranous struts 15 nm in width. X 69,000. (b): Prior to thrombin injection, no orderly array lies between the nonstimulated platelet membrane and the microtubule circlet (arrow). X 69,000. (c): A window fractured through the external surface (ES) reveals two deeper levels of specialization: the particulate fracture-face (P) (arrow) and linear ribs just below. X 69,000. (d): Slender filaments (9 nm in width) materialize beneath forming filopodia (arrow), even in nonstimulated platelets; but no submembranous differentiation is evident. X 69,000. (e): The microtubule circlet (arrow), still extant in cross-fractures of the cell body even after stimulation by thrombin for 1 sec, lies beneath the submembranous struts which traverse the platelet. X 38,000.

Figure 13 Relationship of stimulated-platelet infrastructure to other cytoplasmic components. (a): In thin section, struts connect an intracytoplasmic membrane system with the plasma membrane (arrows) in this partially leached, stimulated platelet. X 90,000. (b): Another stimulated platelet explored by deep-etching, displays struts also extending to internal organelles -- here, probably a granule or dense body. X 82,500. (d): Microtubules (arrow) lie between the infrastructure and the cytoplasmic matrix. The particulate fracture-face (PF) contrasts with the external surface (ES). X 82,500.

Figure 14 A diagram representing the hypothesis presented in the discussion. Submembranous structural elements bound to both lipid and protein membrane constituents create an anionic lipid sink by attracting these lipids laterally from adjacent membrane and from the outer leaflet opposite their attachment sites. Regions of membrane lacking these structures have random transbilayer lipid distribution, while bound regions are asymmetric. Thus domains poor in acidic lipid in the outer leaflet reflect regions of attachment sites on the inner leaflet. A stimulus for secretion, such as thrombin and/or calcium, mediates the release of the submembranous structure from its attachments to anionic lipid, which allows the lipids to diffuse across the bilayer and into neighboring regions. Free diffusion obliterates domains in the outer leaflet. Asymmetry is lost as the entire membrane acquires a random lipid distribution. Release from membrane lipids of the cytoskeletal elements could open sites for their binding to other cytoskeletal proteins.

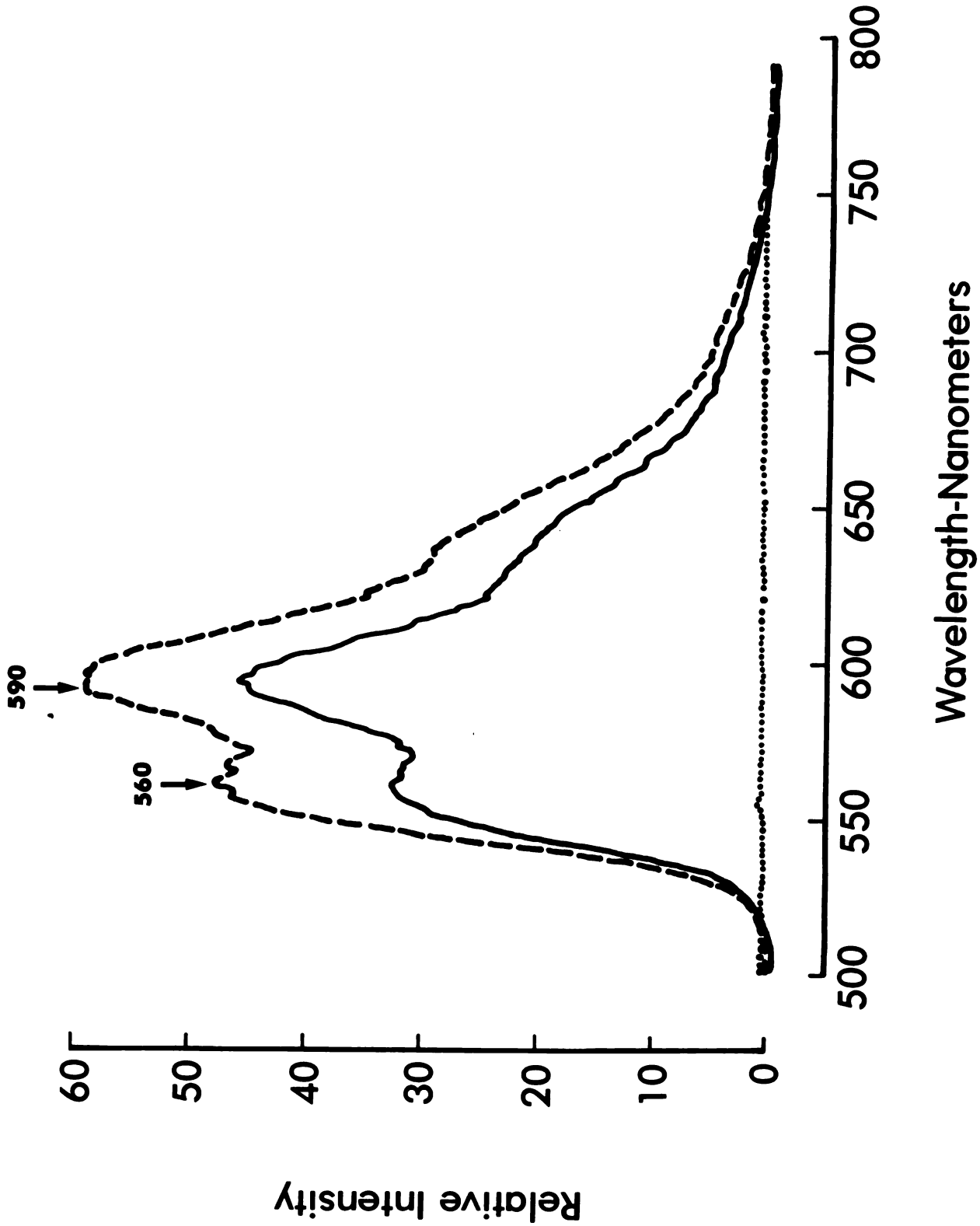
590
560
60
50
40
30
20
10
0
500
550
600
650
700
750
800
Relative Intensity
Wavelength-Nanometers

Fig 1

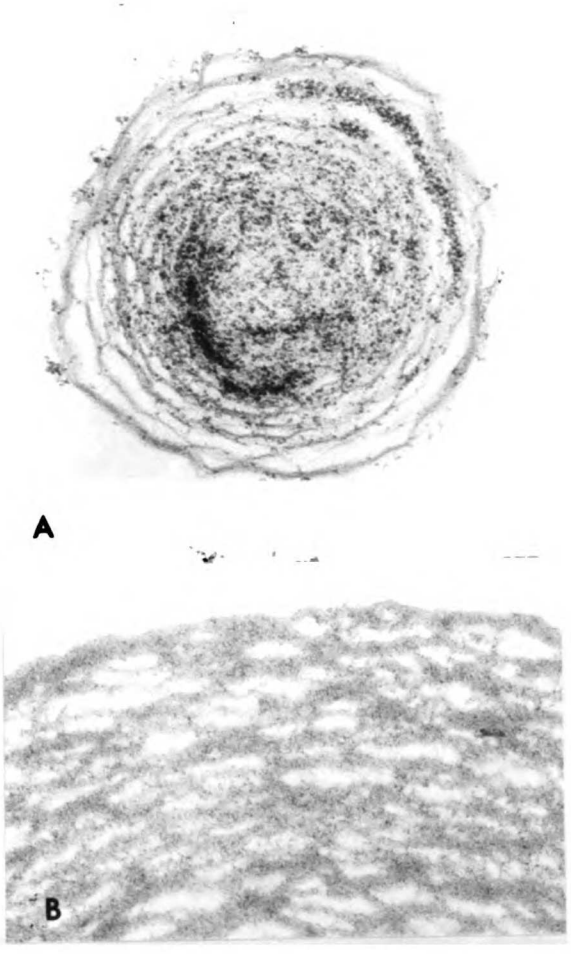

Fig. 2

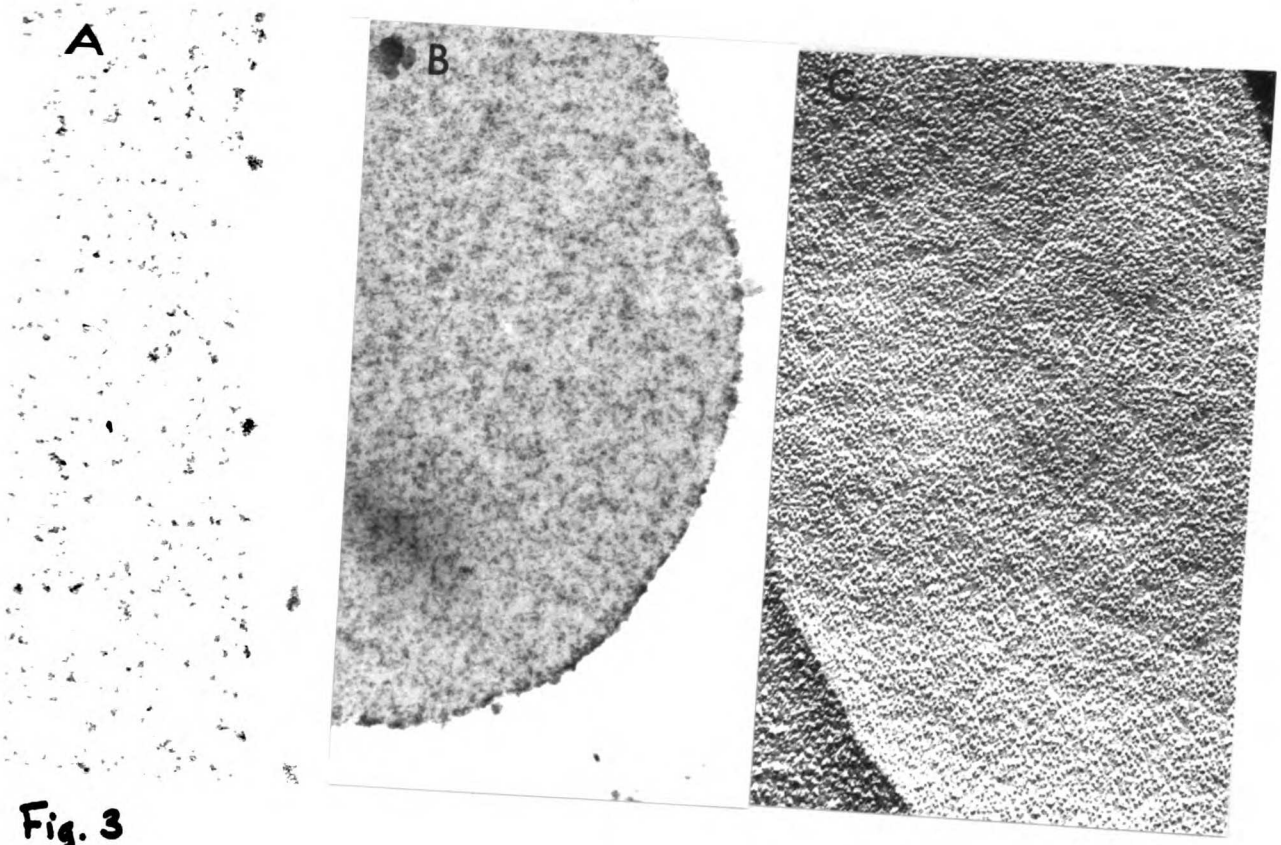

Fig. 3

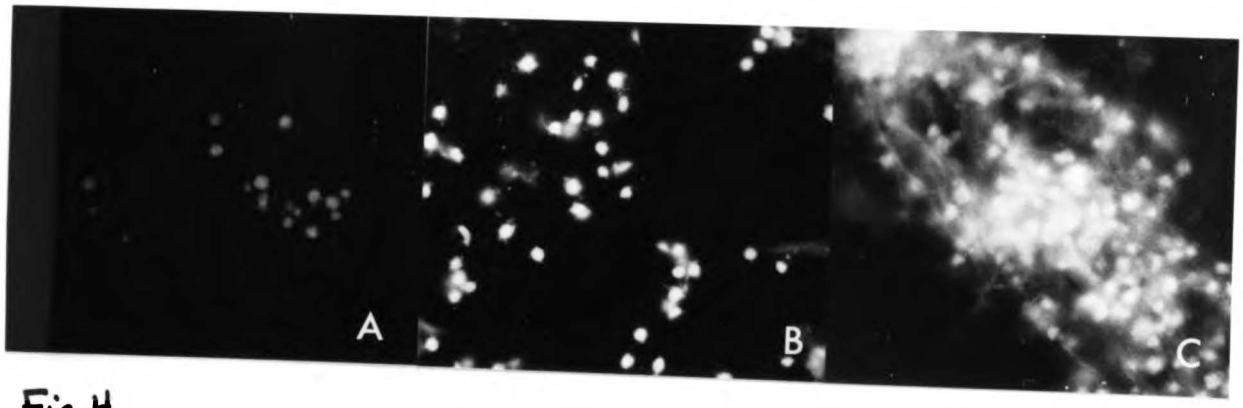

Fig 4

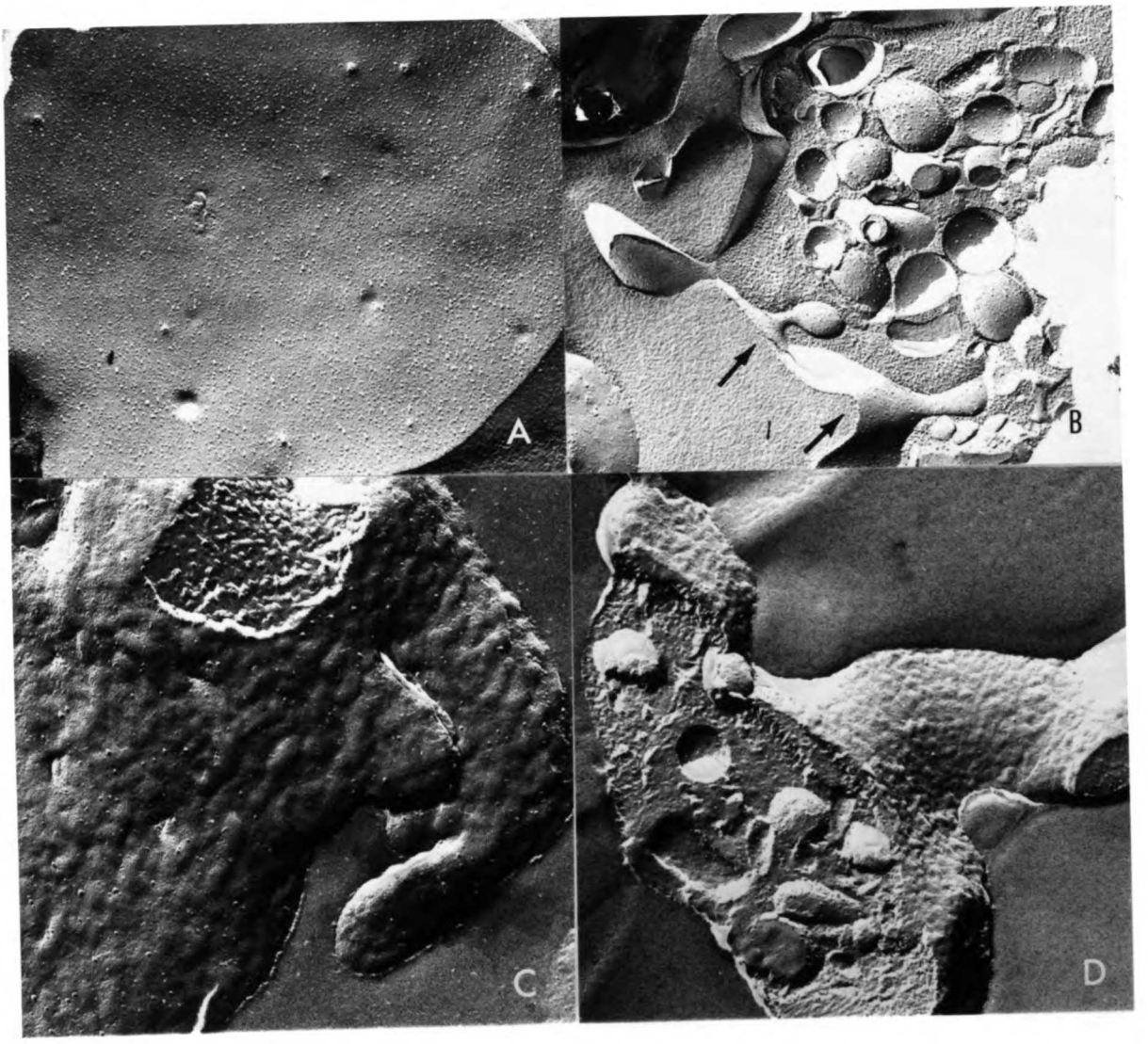

Fig. 5

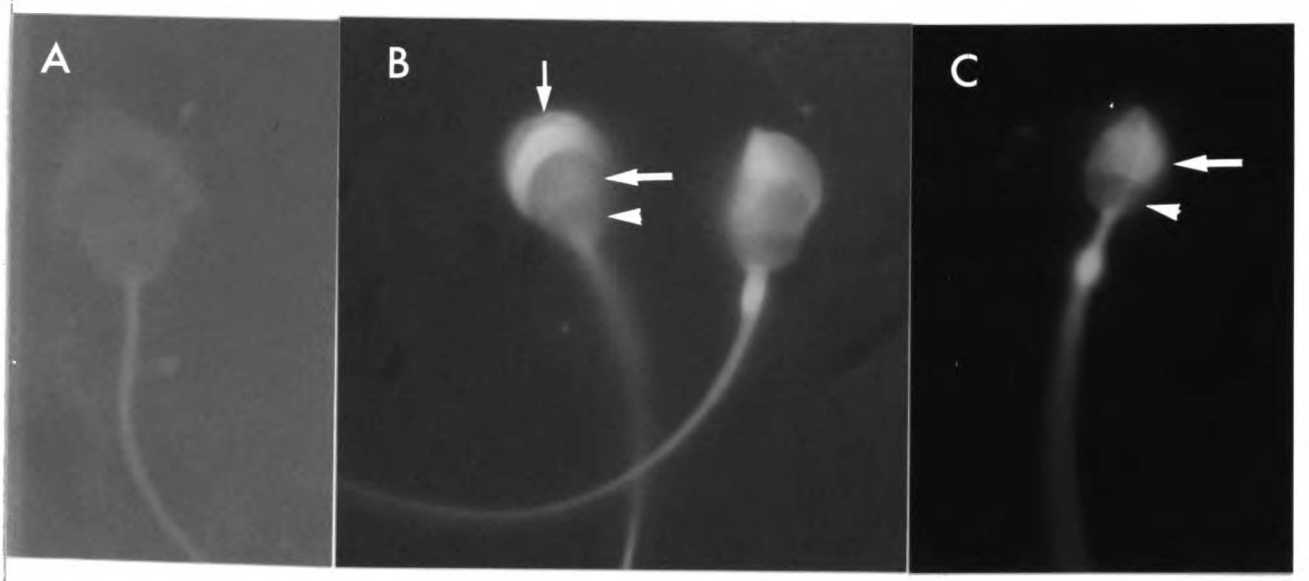

Fig. 6

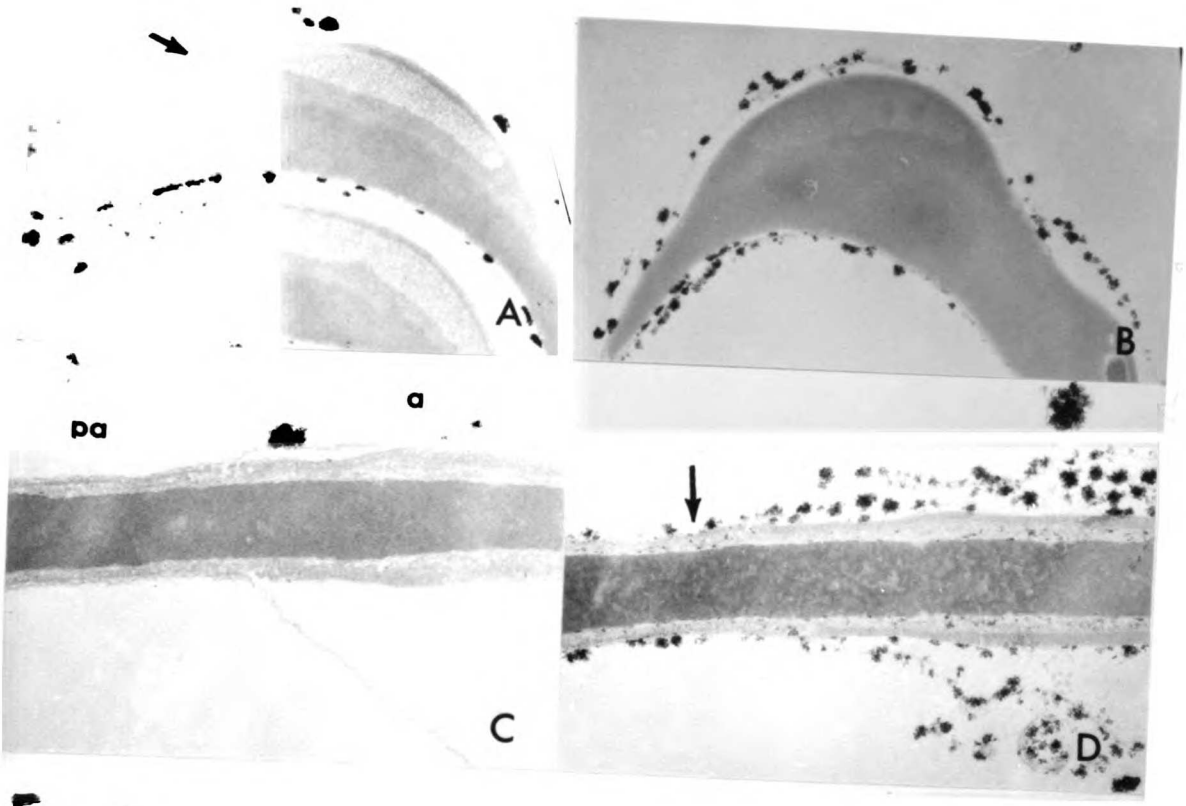

Fig. 7

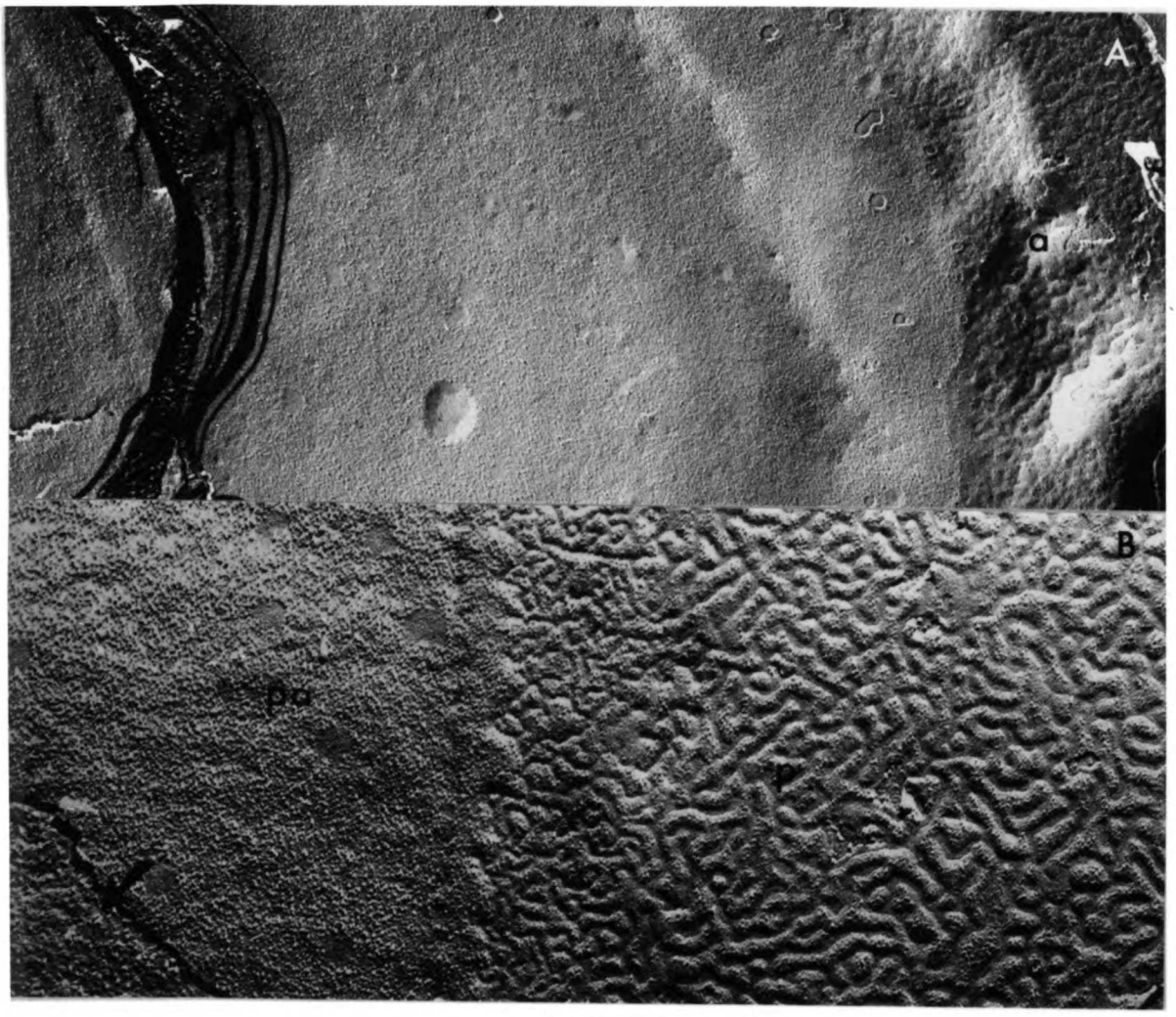

Fig. 8

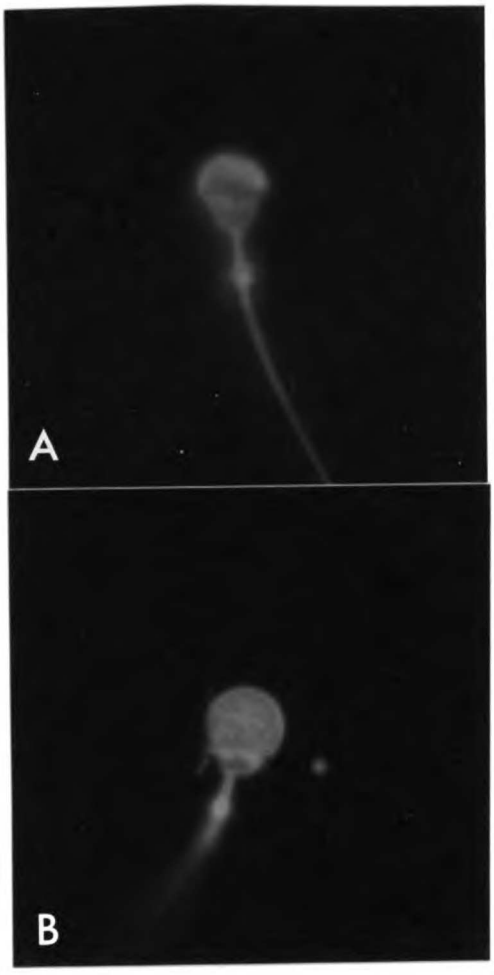

Fig. 9

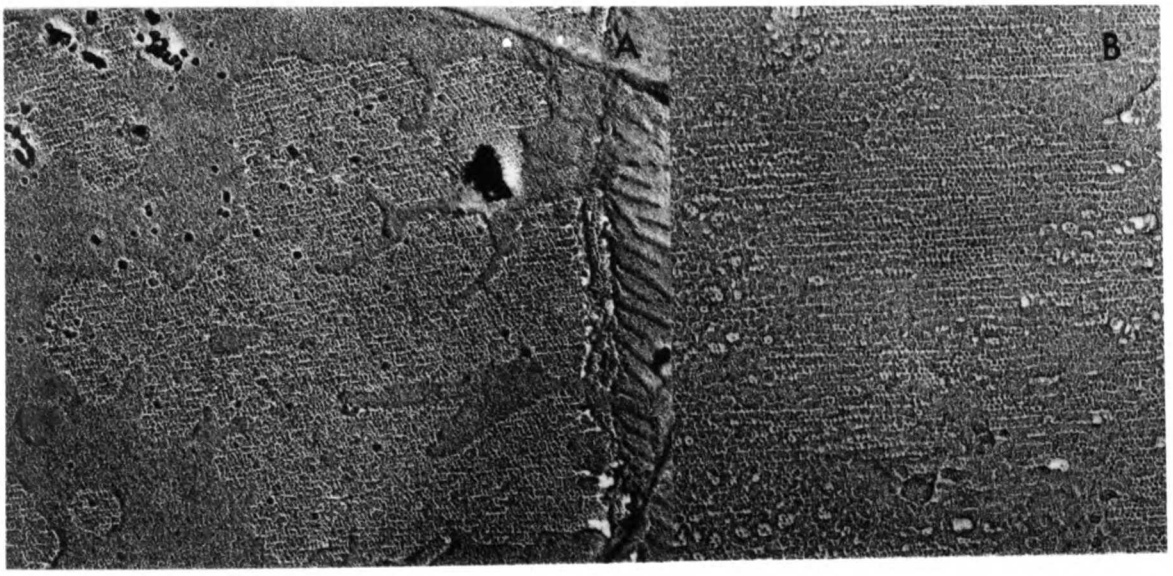

Fig. 10

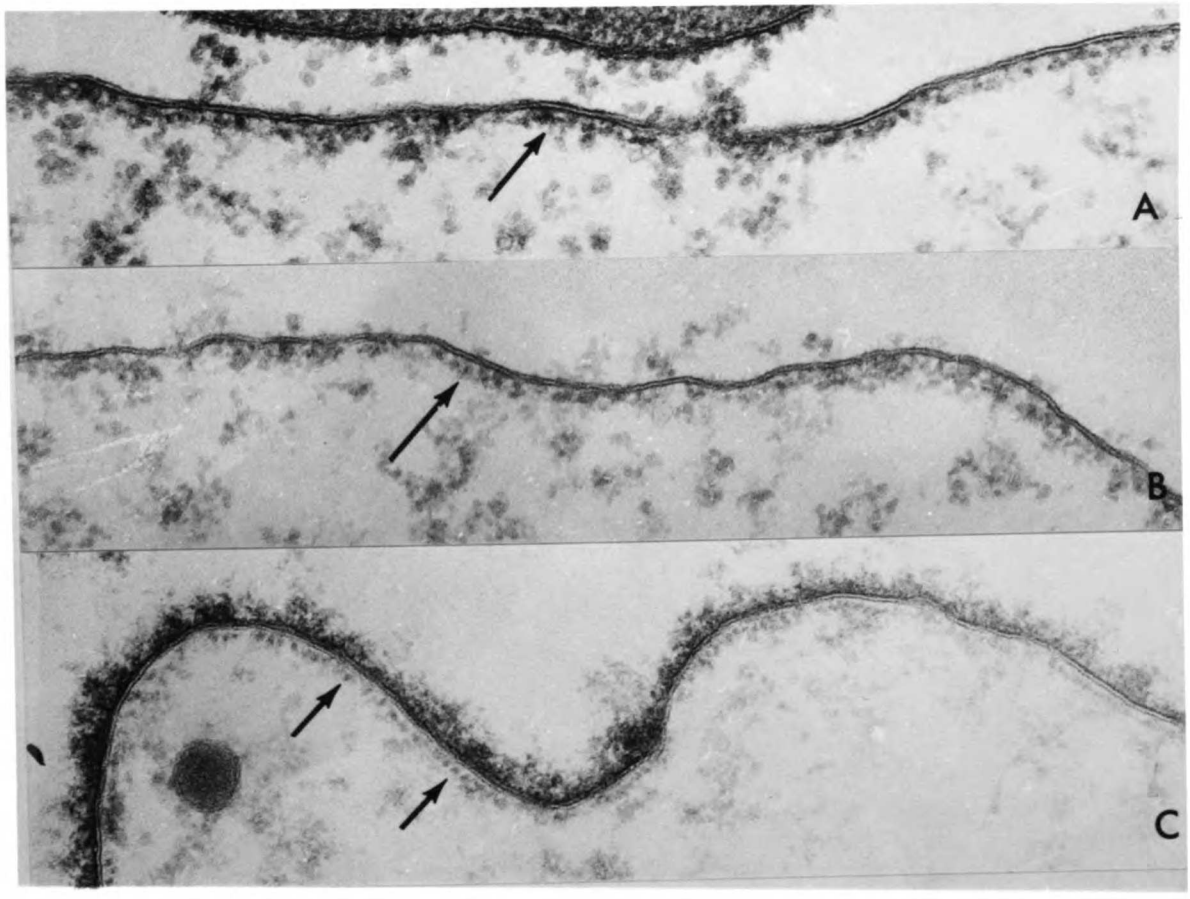

Fig. 11

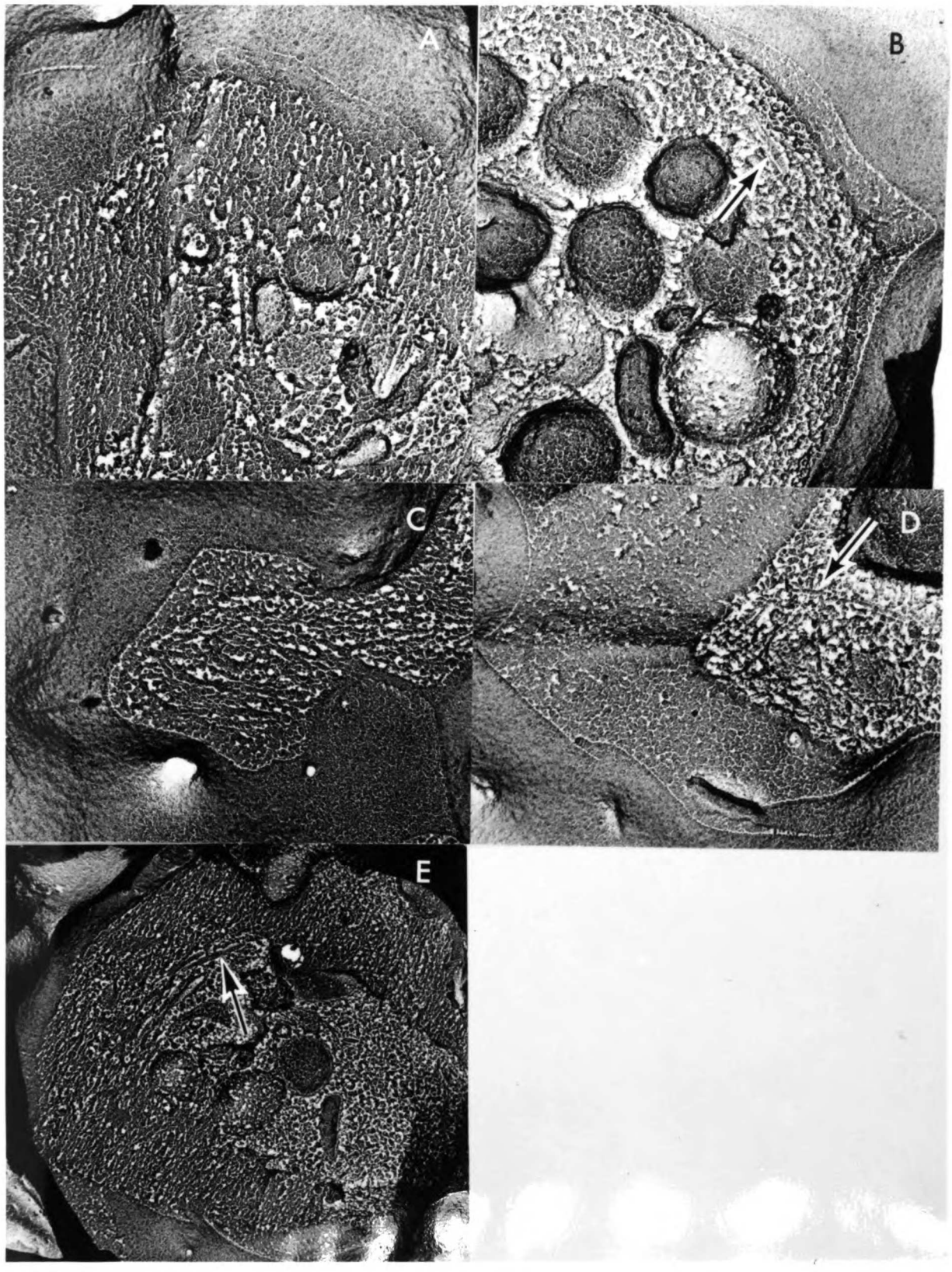

Fig. 12

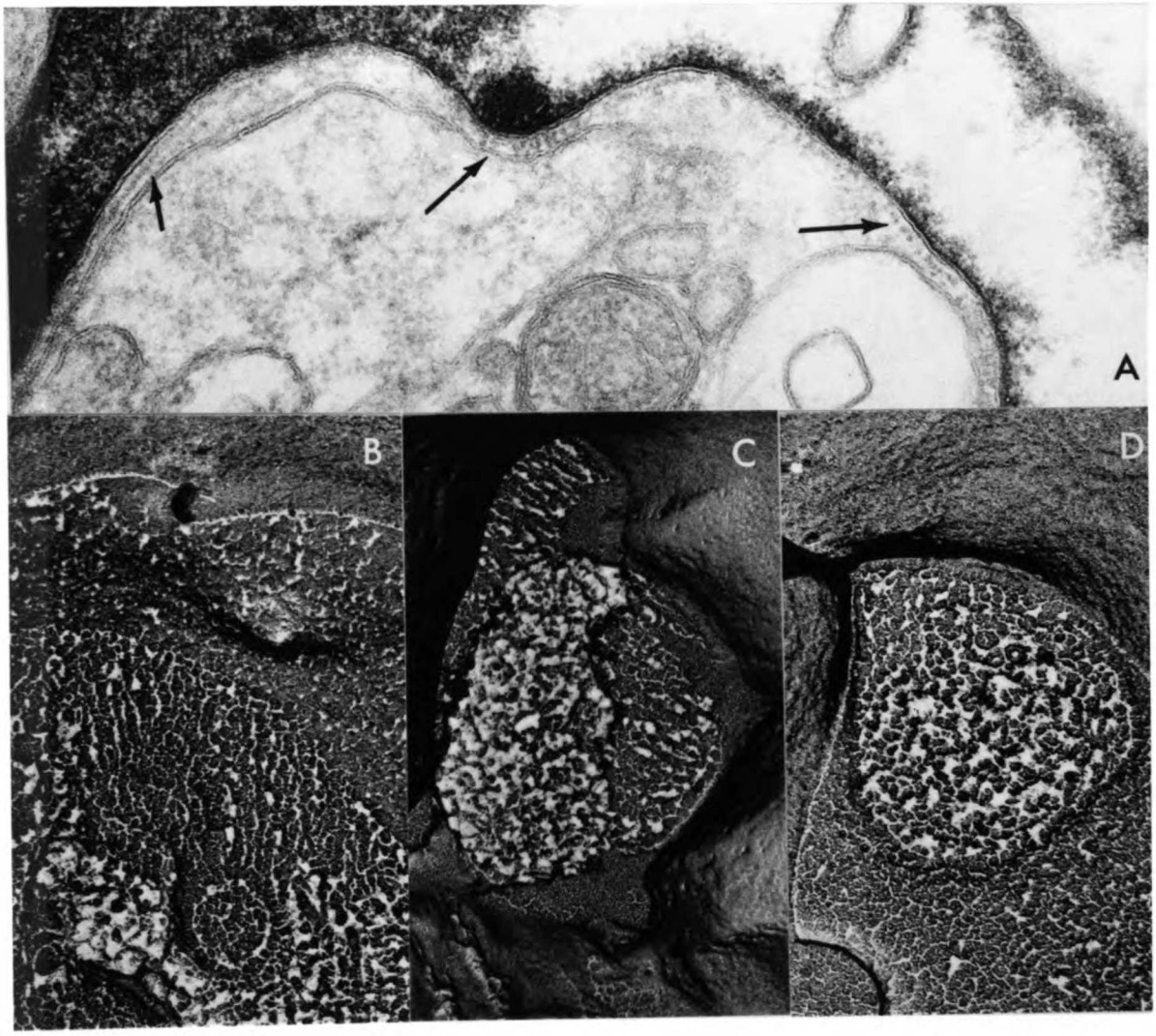

Fig. 13

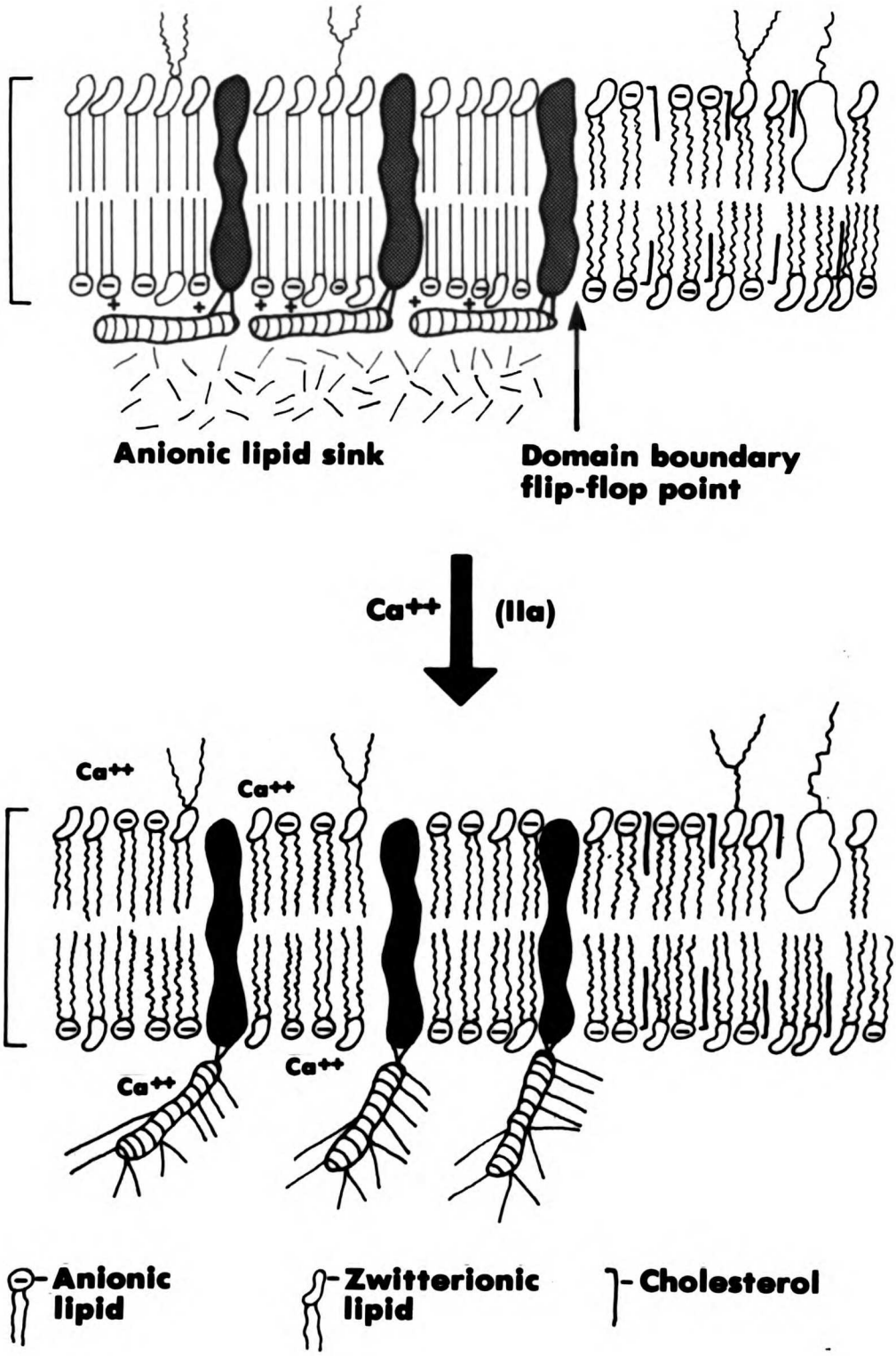
Anionic lipid sink
Domain boundary flip-flop point
Ca++
(IIa)
Ca++
Ca++
Ca++
Ca++
Anionic lipid
Zwitterionic lipid
Cholesterol

Fig. 14


UC
San Francisco
LIBRARY
UNIVERSITY OF CALIFORNIA